Testing for Jumps in a Discretely Observed Price Process with Endogenous Sampling Times

Qiyuan Li* Yifan Li† Ingmar Nolte‡ Sandra Nolte§ Shifan Yu¶

This Version: September 10, 2025

Abstract

This paper introduces a novel nonparametric high-frequency jump test for discretely observed Itô semimartingales. Based on observations sampled recursively at first exit times from a symmetric double barrier, our method distinguishes between threshold exceedances caused by the Brownian component and jumps, which enables the construction of a feasible, noise-robust statistical test. Simulation results demonstrate superior finite-sample performance of our test compared to existing methods. An empirical analysis of NYSE-traded stocks provides clear statistical evidence for jumps, with the results highly robust to spurious detections.

JEL Classifications: C12, C14, C22, C58

Keywords: High-Frequency Data, Jump Test, Market Microstructure Noise, Stochastic Sampling Scheme, First Exit Time

*Faculty of Business and Economics, University of Hong Kong; Email: qiyuanli@hku.hk.

†Alliance Manchester Business School, University of Manchester; Email: yifan.li@manchester.ac.uk.

‡Lancaster University Management School; Email: i.nolte@lancaster.ac.uk.

§Lancaster University Management School; Email: s.nolte@lancaster.ac.uk.

¶Corresponding author, Oxford-Man Institute of Quantitative Finance, University of Oxford; Email: shifan.yu@eng.ox.ac.uk.

1 Introduction

There exists a consensus in the financial literature that modeling asset price dynamics requires the specification of different components. In addition to the stochastic volatility component, which accounts for the persistence of volatility, "jumps" in asset prices serve as an explanation for abnormally large variations that play an important role for the tail behavior of return distributions. Jumps are believed to contain predictive information, so correctly identifying them often leads to improved price or volatility forecasts and better portfolio outcomes (see, e.g., Yan, 2011, Jiang and Yao, 2013, Cremers et al., 2015, for empirical applications using daily or monthly financial data, and Andersen et al., 2007a, Corsi et al., 2010, Nolte and Xu, 2015, Bollerslev et al., 2015, 2020, Pelger, 2020, for those using high-frequency intraday data). The increased availability of high-frequency financial data has further motivated the development of methodologies designed to test the model specification based on a discretely observed semimartingale.

Over the past two decades, a number of nonparametric jump tests have been developed. Starting from the seminal work of Barndorff-Nielsen and Shephard (2004), most of these tests are constructed on jump-robust measures of returns or their variations, see, e.g., Huang and Tauchen (2005), Barndorff-Nielsen and Shephard (2006), Andersen et al. (2007b), Jiang and Oomen (2008), Lee and Mykland (2008), Aït-Sahalia and Jacod (2009b), Corsi et al. (2010), Podolskij and Ziggel (2010), Andersen et al. (2012), Lee and Mykland (2012), and Aït-Sahalia et al. (2012), among others. Some recent works focus on modified versions of these tests when conventional assumptions are violated, see, e.g., Laurent and Shi (2020) and Kolokolov and Renò (2024), and tests for co-jumps in a collection of assets, see, e.g., Bibinger and Winkelmann (2015) and Caporin et al. (2017).

Despite the theoretical developments in the literature, these jump tests can sometimes deliver inconsistent results in practice. Unlike the noiseless theoretical framework, the presence of market microstructure noise in real-world high-frequency data requires practitioners to either sample sparsely or pre-average the tick-level data. Although the literature establishes asymptotic consistency of calendar-grid tests under both the null and alternative hypotheses, their finite-sample performance deteriorates markedly at commonly used sampling frequencies in practice (Dumitru and Urga, 2012; Maneesoonthorn et al., 2020). Under sparse, exogenous and typically equidistant sampling, many tick-level returns are bundled into one sampling interval, which dilutes the relative contribution of jumps and thus reduces finite-sample power. This practical tension motivates a key question: Can we sample in a way that retains more jump information than equidistant calendar-time sampling?

In this paper, we introduce an innovative nonparametric method to test for jumps in a discretely observed semimartingale based on endogenous sampling. Different from the conventional equidistant calendar-time sampling, our methodology adopts a stochastic and endogenous approach that recursively samples tick-by-tick observations at first exit times from a symmetric double barrier, inspired by Engle and Russell (1998), Andersen et al. (2008), Fukasawa and Rosenbaum (2012), Vetter and Zwingmann (2017), and Hong et al. (2023), among others. This endogenous sampling scheme is tailored to be sensitive to jumps. Jumps of size larger than the barrier width will terminate

the sampling interval immediately and produce large "overshoots", i.e., threshold exceedances. By stopping the sampling interval when the barrier is breached, the sampled return captures the jump in a clean way, without mixing it with post-jump diffusion increments, which amplifies the jump signal. To distinguish between threshold exceedances caused by discrete Brownian steps and those by jumps, we censor the returns between consecutive sampling times with a specific threshold,[1] and construct a standardized test statistic to measure the potential distortion caused by disproportionately large overshoots in the sample moment of returns. While our approach is in the spirit of the standard truncation technique of Mancini (2009), the objects are first-exit ladder increments rather than Brownian increments over equidistant calendar-time intervals, so the relevant limit theorems differ and require new asymptotic results under the first-exit framework. Furthermore, we develop a two-step noise reduction method based on the pre-averaging approach of Jacod et al. (2009) and the wild bootstrap to mitigate the impact of weakly dependent market microstructure noise in the pre-sampling tick-level observations, which helps to bridge the gap between real-world features and the theoretical framework.

Simulation results reveal that our new high-frequency jump test exhibits reliable finite-sample size and power performance across various aggregation levels, and its performance is robust to measurement errors simulated with a realistically calibrated specification. A comparison with commonly used tests constructed from equidistantly sampled observations and some noise-robust versions based on ultra-high-frequency data is conducted thereafter. We find that (i) most calendar-time-sampled tests exhibit less consistent performance across different sampling frequencies and are poorly sized in the presence of noise, which is in line with the Monte Carlo results of Dumitru and Urga (2012) and Maneesoonthorn et al. (2020), (ii) while noise-robust tests achieve reliable sizes in the presence of noise, their power performance is still inferior to our test across a wide range of simulation settings, and (iii) the truncation-based jump filtering and detection techniques commonly applied in the recent literature suffer from spurious detections and become unreliable when noise is substantial at high frequencies, which echoes the findings in Aït-Sahalia et al. (2025). In an empirical application, our test is applied to transaction data of 10 selected stocks listed on the New York Stock Exchange (NYSE). Clear statistical evidence of jumps is found for all selected stocks, with jumps occurring on approximately 10% to 15% of trading days. Furthermore, the test rejections are highly robust to the correction of spurious detections based on the method of Bajgrowicz et al. (2016).

The remainder of this paper is structured as follows: Section 2 lays out the basic setup and key assumptions. Section 3 discusses the test statistic and its asymptotic theory, along with the noise reduction technique. Section 4 assesses the finite-sample performance of our new test with Monte Carlo simulations. After discussing the empirical application for selected NYSE stocks in Section 5, we conclude in Section 6. All proofs and additional simulation and empirical results are relegated to the Online Appendix.

[1] Related works about the boundary crossing problems for random walks, especially those with Gaussian steps, include Rogozin (1964), Lorden (1970), Lotov (1996), and Khaniyev and Kucuk (2004).

2 Setting and Assumptions

On a filtered probability space $(\Omega, \mathcal{F}, \mathbb{F} = (\mathcal{F}_t)_{t\geq 0}, \mathbb{P})$, let the one-dimensional process $X = (X_t)_{t\geq 0}$ denote the efficient logarithmic price of a financial asset. We assume that X follows a possibly discontinuous Itô semimartingale of the following form:

$$\begin{aligned} X &= X' + X'', \\ X'_t &= X_0 + \int_0^t \mu_s ds + \int_0^t \sigma_s dW_s, \\ X''_t &= \int_0^t \int_{\mathbb{R}} \delta(s,x) \mathbb{1}_{\{|\delta(s,x)|\leq 1\}} (\underline{p} - \underline{q})(ds,dx) + \int_0^t \int_{\mathbb{R}} \delta(s,x) \mathbb{1}_{\{|\delta(s,x)|>1\}} \underline{p}(ds,dx), \end{aligned} \tag{1}$$

where t stands for time, W is a standard Brownian motion, $\underline{p}(dt,dx)$ is a Poisson random measure on $\mathbb{R}_+ \times \mathbb{R}$ with a compensator $\underline{q}(dt,dx) = dt \otimes \lambda(dx)$, and λ is a σ-finite measure on $\mathbb{R}_+$. We assume that X satisfies the following regularity conditions:

Assumption 1. The following properties hold for the processes in Eq. (1):

(i) The process μ is optional and locally bounded;

(ii) The process σ is càdlàg (i.e., right-continuous with left limits), adapted, and strictly positive;

(iii) There exists a sequence $(\tau_m)_{m\geq 1}$ of stopping times increasing to ∞, and a sequence $(K_m)_{m\geq 1}$ of finite constants, such that it holds for each $m \geq 1$ that $\mathbb{E}[|\sigma_{t\wedge\tau_m} - \sigma_{s\wedge\tau_m}|^2] \leq K_m|t-s|$ for all $s,t \in [0,T]$ with some finite T;

(iv) The function $\delta(\omega,t,x)$ on $\Omega \times \mathbb{R}_+ \times \mathbb{R}$ is predictable;

(v) There is a localizing sequence $(\tau_n)_{n\geq 1}$ of stopping times increasing to ∞, and a sequence $(f_n)_{n\geq 1}$ of deterministic nonnegative functions on $\mathbb{R}$, which satisfies $|\delta(\omega,t,x)| \wedge 1 \leq f_n(x)$ for all (ω,t,x) with $t \leq \tau_n(\omega)$, and $\int_{\mathbb{R}} |f_n|^r \lambda(dx) < \infty$ for some $r \in [0,1)$.

Remark 1. Assumption 1 entails some very mild technical conditions that the processes in Eq. (1) should meet. Conditions (i), (ii) and (iv) are standard in the literature. Condition (iii) states that the spot volatility process is locally 1/2-Hölder continuous under the L_2-norm. The smoothness condition is satisfied whenever σ is an Itô semimartingale, or a long-memory process driven by a fractional Brownian motion (Li and Liu, 2021). The parameter r in Condition (v) sets a bound on the degree of jump activity, which can be interpreted as a generalized version of the Blumenthal-Getoor index for a Lévy process (Aït-Sahalia and Jacod, 2009a; Jing et al., 2012). With some $r \in [0,1)$, we consider jumps of both finite and infinite activities, but restrict them to be of finite variation, i.e., they are absolutely summable, such that in Eq. (1) we dispense with the integral with $\underline{p} - \underline{q}$; see Jacod et al. (2019) for more details.

The quadratic variation (QV) of X over a finite interval $[0,t]$ is defined as

$$\langle X, X\rangle_t = \int_0^t \sigma_s^2 ds + \sum_{0\leq s\leq t} (\Delta X_s)^2, \quad \text{with } \Delta X_t = X_t - X_{t-}, \tag{2}$$

where the integrated variance (IV), $\int_0^t \sigma_s^2 ds$, summarizes the variation from X'.

Testing for jumps is a procedure to answer the fundamental question of whether the realized sample path $X(\omega)$ is continuous or not over a finite time interval, e.g., $(0,1)$.[2] Technically speaking, we decompose the sample space Ω into two complementary subsets:

$$\begin{aligned} \Omega' &= \{\omega : X_t(\omega) \text{ is continuous on } (0,1)\}, \\ \Omega'' &= \{\omega : X_t(\omega) \text{ is discontinuous on } (0,1)\}, \end{aligned} \tag{3}$$

where Ω' (resp. Ω'') represents the null hypothesis (alternative hypothesis) for a jump test, which assesses the plausibility of these two hypotheses based on discrete observations of $X(\omega)$.

2.1 Observation Scheme

We now describe how observations take place.[3] At stage n, we assume that the successive observations of $X(\omega)$ occur at times $0 = t_{n,0} < t_{n,1} < \dots$ for a sequence $(t_{n,i})$ of discrete times over a fixed interval (such as a trading day), which is normalized to the unit interval $[0,1]$. We set

$$N_t^n = \sum_{i \geq 1} \mathbb{1}_{\{t_{n,i} \leq t\}} \qquad \text{and} \qquad \Delta_{n,i} = t_{n,i} - t_{n,i-1}, \tag{4}$$

where $N \equiv N_1^n$ stands for the number of observations on $(0,1]$, and $\Delta_{n,i}$ is the i-th inter-observation lag at stage n. It is easily seen from the empirical tick-level data that the observation times are far from evenly spaced and usually dependent on $X(\omega)$ itself. Our assumption for the observation scheme over $[0,1]$ is outlined as follows:

Assumption 2. Let Δ_n be a positive sequence of real numbers satisfying $\Delta_n \to 0$ as $n \to \infty$. We define an intensity process of observations $\lambda = (\lambda_t)_{0 \leq t \leq 1}$ with $\lambda_t = K\sigma_t^2$ for some $K > 0$. There exists a localizing sequence $(\tau_m)_{m \geq 1}$ of stopping times and positive constants $K_{m,p}$ and κ such that:

(i) With $(\mathcal{F}_t^n)_{t \geq 0}$ the smallest filtration containing $(\mathcal{F}_t)_{t \geq 0}$ and with respect to which all observation times $t_{n,i}$ are stopping times, for each $i = 1, 2, \dots$, the variable $\Delta_{n,i}$ is, conditionally on $\mathcal{F}_{i-1}^n \equiv \mathcal{F}_{t_{n,i-1}}^n$, independent of $\mathcal{F}_\infty = \bigvee_{t \geq 0} \mathcal{F}_t$.

(ii) With the restriction $\{t_{i-1} < \tau_m\}$, we have for all $p \geq 2$,

$$\begin{aligned} \mathbb{E}[|\Delta_{n,i}\lambda_{t_{n,i-1}} - \Delta_n||\mathcal{F}_{i-1}^n] &\leq K_{m,1}\Delta_n^{2+\kappa}, \\ \mathbb{E}[|\Delta_{n,i}\lambda_{t_{n,i-1}}|^p|\mathcal{F}_{i-1}^n] &\leq K_{m,p}\Delta_n^p. \end{aligned} \tag{5}$$

[2] We restrict the alternative hypothesis to contain at least one jump on $(0,1)$ as it is not feasible for a test to identify jumps occurring right at both endpoints of the interval.

[3] We would like to distinguish the terms "observation scheme" and "sampling scheme" in this paper. We allow both tick-level and sampled observations to form discrete-time processes, and the term "sampling" refers to a subsampling or subset selection procedure for the discrete observations at the highest frequency.

A useful consequence of this Assumption is the following convergence in probability:

$$\Delta_n N_t^n \xrightarrow{\mathbb{P}} \tau(t) = \int_0^t \sigma_s^2 ds. \tag{6}$$

Remark 2. Assumption 2 is inspired by Assumption (O) of Jacod et al. (2017) and Assumption (O-ρ, ρ') of Jacod et al. (2019). The process λ controls for the "spot" observation arrival rates, and the unobserved Δ_n can be interpreted as an "average mesh size" between successive observations in an alternative time scale that evolves with volatility (see Remark 3). Our choice of the intensity $\lambda = K\sigma^2$ implies higher observation frequencies of $X(\omega)$ during periods of high local volatility, which captures the diurnal patterns of transaction activities and intraday volatility. This is motivated by the empirical evidence of the E-mini S&P 500 futures contract in Andersen et al. (2018), which illustrates a notable similarity in the intraday U-shaped patterns of one-minute transaction counts and return variation, where the pronounced spikes, typically align with market openings or announcements, roughly coincide. Note that λ is defined up to scale, which allows $K = 1$ to be set without loss of generality (by scaling Δ_n correspondingly), as further discussed in Jacod et al. (2017).

Remark 3. With the convergence result in Eq. (6), Assumption 2 implies a time-changed regular observation scheme under infill asymptotics: As $n \to \infty$, the observation time $t_{n,i}$ converges to $\breve{t}_{n,i} = \inf\{t \in [0,1] : \tau(t) = i\Delta_n\}$. This limiting observation scheme corresponds to Example 2.2 in Jacod et al. (2017). In contrast to the calendar time t, the "intrinsic time" $\tau(t)$ evolves endogenously with respect to the variation from X'. The time change induces a certain level of endogeneity, and extends the commonly assumed equidistant observation scheme in high-frequency financial econometrics literature (Li et al., 2014; Dimitriadis and Halbleib, 2022). With the irregular calendar-time mesh sizes $\Delta_{n,i}$ regulated by Condition (ii), the deviation of $(t_{n,i})$ from $(\breve{t}_{n,i})$ vanishes as $n \to \infty$. Importantly, this discrepancy does not affect the limit theorems developed in the next section, a conclusion supported by strong approximation results in the spirit of Chernozhukov et al. (2013, 2019). Further details can be found in Remark 6 and Online Appendix A.1.

2.2 Price Duration Sampling

Sparse sampling is widely adopted in both the financial econometrics literature and by practitioners to mitigate the impact of market microstructure noise, with some popular choices like 1-minute and 5-minute sampling in calendar time (Aït-Sahalia et al., 2005; Liu et al., 2015). However, such sparse sampling aggregates a substantial amount of tick-level returns exogenously, which dilutes the relative size of jumps and inevitably reduces the power of jump tests. This phenomenon is evident in the Monte Carlo results of Dumitru and Urga (2012) and Maneesoonthorn et al. (2020): Nearly all traditional tests constructed from calendar-time-sampled returns exhibit rapid power loss as

sampling becomes sparser.[4]

In response to this issue, a path-dependent sampling scheme seems a natural solution. We consider a stochastic and endogenous sampling scheme for all observations of $X(\omega)$ on $[0,1]$: Let $(X_i)_{0\le i\le N}$ collect all observations under Assumption 2. With a selected barrier width $c>0$, the price duration sampling (PDS) is defined as the following sampling algorithm:

1. Set $\Pi_0^{(c)}=0$.
2. For $j=1,2,\dots,$ sample X_i for all $i=\Pi_j^{(c)}$ that are decided recursively by

$$\Pi_j^{(c)}=\inf\Big\{\Pi_{j-1}^{(c)}<i\le N:\Big|X_i-X_{\Pi_{j-1}^{(c)}}\Big|\ge c\Big\}. \tag{7}$$

We therefore obtain a subsequence $X^{(c)}=(X_{\Pi_j^{(c)}})_{0\le j\le N^{(c)}}$, where $N^{(c)}=\max_{j\ge1}\{\Pi_j^{(c)}\le N\}$ counts the total number of sampled observations. Moreover, we define the PDS returns as the increments of $X^{(c)}$, i.e., $r_j^{(c)}=X_{\Pi_j^{(c)}}-X_{\Pi_{j-1}^{(c)}}$ for all $j\in\{1,2,\dots,N^{(c)}\}$.

Remark 4. The above sampling algorithm is a discrete-time version of PDS in Hong et al. (2023). The idea of sampling financial observations based on hitting or exit times was initially proposed by Engle and Russell (1998), and has been further developed since then, see, e.g., Gerhard and Hautsch (2002), Andersen et al. (2008), Tse and Yang (2012), Fukasawa and Rosenbaum (2012), Potiron and Mykland (2017), Vetter and Zwingmann (2017), and Hong et al. (2023). While previous studies have primarily focused on volatility estimation based on this alternative sampling scheme, our contribution stands out as the first to demonstrate that this scheme can be exploited to construct more effective high-frequency jump tests.

From a technical standpoint, our design belongs to the broader class of stochastic and endogenous sampling in high frequency, see, e.g., Fukasawa (2010), Li et al. (2014), and Koike (2017). We work with a symmetric first-exit scheme on the intrinsic-time clock, a tractable special case under which asymptotic properties for realized variance (RV) estimators follow directly from Fukasawa (2010). However, further theoretical developments are needed for a jump test based on this sampling scheme; see Remark 6 for further details.

This endogenous sampling scheme is designed to be highly sensitive to the presence of jumps. Fig. 1 shows examples where $X(\omega)$ is continuous and discontinuous, respectively. When $X(\omega)$ is continuous, each sampled return under PDS ("PDS return", i.e., first ladder height with respect to c) consists of the barrier width c plus a small exceedance, i.e., the extra movement needed before the next discrete observation time is stamped. By contrast, if $X(\omega)$ is discontinuous, a jump with magnitude $>c$ triggers the stopping rule immediately and produces an "overshoot" that is visibly larger than the continuous returns.

[4]Some noise-robust tests constructed from filtered data, such as those proposed by Lee and Mykland (2012) and Aït-Sahalia et al. (2012), can utilize all available observations without sampling. As alternative methods that exploit data more sufficiently than classical approaches, we compare their finite-sample performance with our method through simulations in Section 4.

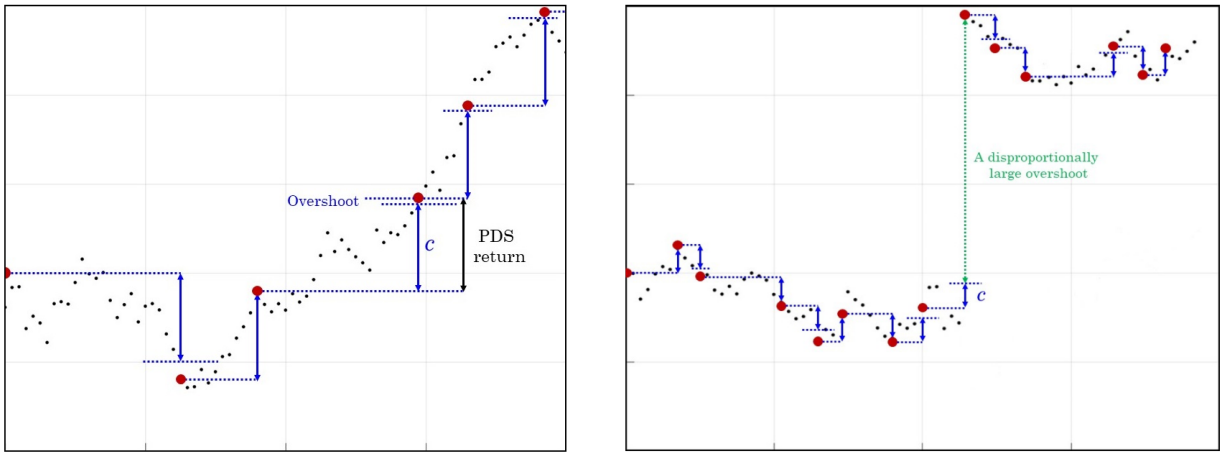

Figure 1: Examples of PDS when $X(\omega)$ is continuous and discontinuous, respectively. Jumps will almost surely lead to the sampling of the next available observation, and induce a large overshoot.

To motivate the use of PDS over exogenous sampling schemes in testing for jumps, we highlight the intuition that, over a given sampling interval, the price return containing a jump is more easily identified when the jump size is large relative to the aggregated continuous price increments in that interval. This relative magnitude can be naturally interpreted as a "signal-to-noise" ratio for jump tests. With a simple motivating Monte Carlo example, we demonstrate that the PDS consistently generates a higher signal-to-noise ratio than equidistant sampling in finite samples under the same sampling frequency. In each replication, we simulate a Gaussian random walk with a fixed number of i.i.d. increments (corresponding to the limiting observation scheme in Remark 3). Under the alternative, we insert one fixed-size jump at a uniformly chosen time index. For each simulated path we then obtain sampled returns with both PDS and equidistant sampling across a broad range of sampling frequencies. A (PDS or equidistantly) sampled return is labelled a jump whenever its absolute value exceeds the 95% quantile of the corresponding null distribution, which by construction fixes the empirical size at 5% for every sampling frequency. In our simulation, both the PDS barrier width and the equidistant interval length are calibrated such that both sampling schemes produce the same expected number of observations. Therefore, any discrepancy in rejection rates under the alternative can be attributed to the effective signal-to-noise ratio achieved by the respective sampling method.

Fig. 2 illustrates the rejection rates under both sampling schemes—under the alternative that the tested interval contains a jump—across a continuum of expected sampling frequencies. For both sampling methods, the rejection rates decline toward the nominal 5% size as sampling becomes increasingly sparse. This is because each sampled return aggregates the jump with an increasing number of Gaussian increments, thereby deteriorating the signal-to-noise ratio. However, the speed of this convergence differs substantially between the two schemes. Intuitively, as the PDS samples the price observations whenever a jump-induced overshoot occurs, the price increments after the jump are excluded from that sampling interval, thus inflating the signal-to-noise ratio. By contrast,

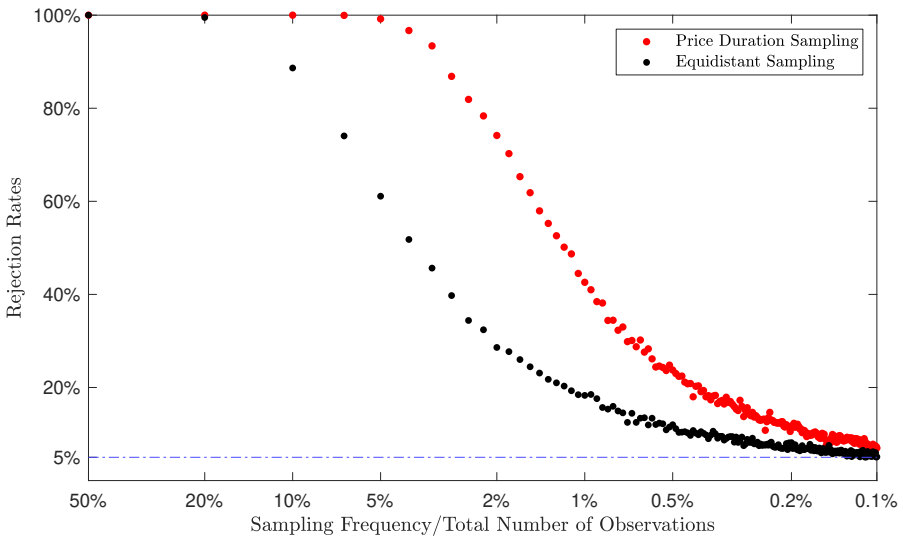

Figure 2: Rejection rates under two different sampling schemes. We simulate 2000 random walk paths with 10^6 standard normal steps (null). A jump of fixed size 10 is randomly inserted in each path. Under two different sampling schemes, the absolute returns containing jumps are compared with the 95% quantiles of absolute sampled returns under the null.

equidistant sampling aggregates returns exogenously at fixed intervals, where the jump size is diluted much more rapidly as the sampling interval lengthens. This advantageous property of PDS contributes to a diminished probability of committing a Type II error, and thereby serves as the main motivation for the new statistical test proposed in the next section.

We now formally introduce our asymptotic setting under PDS: We let the barrier width c shrink proportionally to $\sqrt{\Delta_n}$ under infill asymptotics, i.e.,

$$c \equiv c_n = m\sqrt{\Delta_n}, \quad \text{for some constant } m > 0. \tag{8}$$

When $X(\omega)$ is continuous, each absolute PDS return $|r_i^{(c)}|$ is a sum of the barrier width c and a small threshold exceedance caused by the discreteness of observations, such that the ratio $|r_i^{(c)}|/c$ is bounded in probability. In contrast, jumps of a higher asymptotic order than $\sqrt{\Delta_n}$ will almost surely trigger the stopping rule in Eq. (7), and generate disproportionally large PDS returns for which $|r_i^{(c)}|/c$ diverges in the limit.

To distinguish between the "small" overshoots induced by continuous price increments and the "big" overshoots caused by genuine jumps, we censor the (absolute) PDS returns with a threshold $\varphi_\epsilon(c)$ that shrinks to zero at the same rate $\sqrt{\Delta_n}$ as the barrier width c, i.e., for all $i \in \{1, 2, \ldots, N^{(c)}\}$,

$$|\bar{r}_i^{(c)}| = |r_i^{(c)}| \wedge \varphi_\epsilon(c), \quad \text{where } \varphi_\epsilon(c) = c\,(1+\epsilon) \text{ for some constant } \epsilon > 0. \tag{9}$$

Remark 5. The idea of censored returns is inspired by the standard truncation techniques of Mancini (2009). However, the key difference is that the sampled returns we work with are first-exit ladder increments, rather than Brownian increments over equidistant calendar-time intervals, for which Mancini's threshold is calibrated with local volatility estimates and justified by the Lévy

modulus of continuity. Therefore, the relevant limit theorems are different and require additional theoretical development in the first-exit framework. Furthermore, the fixed choice of ϵ in Eq. (9) is unconventional in the literature. Unlike the standard calendar-time threshold of order slightly higher than $\sqrt{\Delta_n}$, our chosen threshold $\varphi_\epsilon(c) \asymp \sqrt{\Delta_n}$ affects increments from both X' and X'' under infill asymptotics. This circumvents the "perfect correlation" issue of censored and uncensored returns under the null (Podolskij and Ziggel, 2010), and allows the construction of feasible test statistics.[5]

3 Main Results

In this section, we introduce and analyze our new test statistic, which is constructed from the PDS returns between sampled observations collected by $X^{(c)}$. Then we augment the test with an effective noise reduction method to mitigate the impact of market microstructure noise.

3.1 Test Statistic

To prepare for the construction of our test statistic, we first introduce the notation for the moments of PDS returns from a standard Gaussian random walk $(Z_i)_{i=0,1,\ldots}$ with a barrier width m, which is denoted as $Z_1^{(m)}$:

(i) Absolute moment of $Z_1^{(m)}$: $\mu_\gamma(m) = \mathbb{E}[|Z_1^{(m)}|^\gamma]$,
(ii) Absolute moment of censored $Z_1^{(m)}$: $\overline{\mu}_{\gamma,\epsilon}(m) = \mathbb{E}[|\overline{Z}_1^{(m)}|^\gamma] = \mathbb{E}[(|Z_1^{(m)}| \wedge \varphi_\epsilon(m))^\gamma]$,
(iii) Absolute cross moment of censored and uncensored $Z_1^{(m)}$: $\overline{\rho}_{\gamma,\epsilon}(m) = \mathbb{E}[|Z_1^{(m)}|^\gamma |\overline{Z}_1^{(m)}|^\gamma]$,

and two first-order differentiable and invertible functions:

$$h_2(m) = \frac{\mu_2(m)}{m^2} \qquad \text{and} \qquad \overline{h}_{2,\epsilon}(m) = \frac{\overline{\mu}_{2,\epsilon}(m)}{m^2}, \tag{10}$$

with the first-order derivatives $h_2'(m)$ and $\overline{h}_{2,\epsilon}'(m)$, and the inverse functions $h_2^{-1}(x)$ and $\overline{h}_{2,\epsilon}^{-1}(x)$.[6]

We will now proceed to define the testing procedures. For all observations $(X_i)_{0\le i\le N}$ under Assumption 2, we obtain the sampled observations in $X^{(c)}$ with the barrier width c that satisfies Eq. (8). To assess the distortion resulting from "large" overshoots, we compare the sample moments of uncensored and censored PDS returns normalized by the barrier width c, i.e.,

$$S_2 = \frac{1}{N^{(c)}} \sum_{i=1}^{N^{(c)}} \left(\frac{|r_i^{(c)}|}{c} \right)^2 \quad \text{and} \quad \overline{S}_{2,\epsilon} = \frac{1}{N^{(c)}} \sum_{i=1}^{N^{(c)}} \left(\frac{|\overline{r}_i^{(c)}|}{c} \right)^2, \tag{11}$$

[5] In this paper, we can also adopt the truncation technique and discard all absolute PDS returns that are larger than $\varphi_\epsilon(c)$. However, the censoring approach does not change the total number of PDS returns and is therefore more convenient for both our theoretical derivation and empirical implementation.

[6] The invertibility and differentiability of $h_2(m)$ and $\overline{h}_{2,\epsilon}(m)$ are proved in Online Appendix A.2. In practice, we compute the required moments and functionals of $Z_1^{(m)}$ by simulation of standard Gaussian random walks, and obtain numerically the inverses and first-order derivatives of $h_2(m)$ and $\overline{h}_{2,\epsilon}(m)$ with local polynomial interpolation and local linear regression, respectively.

with the functions defined in Eq. (10):

$$M_c = h_2^{-1}\left(S_2\right) \quad \text{and} \quad \overline{M}_{c,\epsilon} = \overline{h}_{2,\epsilon}^{-1}\left(\overline{S}_{2,\epsilon}\right). \tag{12}$$

Theorem 1 (Consistency)**.** Under Assumptions 1 and 2, it holds as $n \to \infty$ that

$$\begin{aligned} (\overline{M}_{c,\epsilon}, M_c)' &\xrightarrow{\mathbb{P}} (m, m)', \qquad \text{if } \omega \in \Omega', \\ (\overline{M}_{c,\epsilon}, M_c)' &\xrightarrow{\mathbb{P}} (m, m^*)', \qquad \text{if } \omega \in \Omega'', \end{aligned} \tag{13}$$

where $m^* = h_2^{-1}(\kappa \cdot h_2(m))$ with κ the ratio between QV and IV over $[0, 1]$.

Both $\overline{M}_{c,\epsilon}$ and M_c are jointly asymptotically normal under the null with a known variance-covariance matrix, which naturally leads to a well-defined ratio test.

Theorem 2 (Asymptotic normality)**.** Under the same conditions as in Theorem 1, the estimators $\overline{M}_{c,\epsilon}$ and M_c are jointly normally distributed when $\omega \in \Omega'$:

$$\sqrt{N}\begin{pmatrix} \overline{M}_{c,\epsilon} - m \\ M_c - m \end{pmatrix} \xrightarrow{\mathcal{L}} \mathcal{N}\left(\begin{pmatrix} 0 \\ 0 \end{pmatrix}, \begin{pmatrix} \phi_{11}(m) & \bullet \\ \phi_{21}(m) & \phi_{22}(m) \end{pmatrix}\right), \tag{14}$$

where

$$\phi_{11}(m) = \frac{\mu_2(m)(\overline{\mu}_{4,\epsilon}(m) - \overline{\mu}_{2,\epsilon}^2(m))}{m^4(\overline{h}'_{2,\epsilon}(m))^2}, \tag{15}$$

$$\phi_{22}(m) = \frac{\mu_2(m)(\mu_4(m) - \mu_2^2(m))}{m^4(h'_2(m))^2}, \tag{16}$$

$$\phi_{21}(m) = \frac{\mu_2(m)(\overline{\rho}_{2,\epsilon}(m) - \mu_2(m)\overline{\mu}_{2,\epsilon}(m))}{m^4(h'_2(m)\overline{h}'_{2,\epsilon}(m))^2}. \tag{17}$$

Remark 6. Based on a strong approximation argument of Chernozhukov et al. (2013, 2019), we couple the complicated observation scheme under Assumption 2 with the much simpler limiting observation scheme $(\breve{t}_{n,i})$ in Remark 3, and the PDS returns $(r_i^{(c)})_{1 \le i \le N^{(c)}}$ are strongly approximated by the sampled returns from a corresponding homogeneous Gaussian random walk in intrinsic time; see Online Appendix A.1.3 for details. The CLT in Theorem 2 is obtained from a joint convergence of the PDS-based RV, its censored version, and the sum of squared sampling thresholds. While the marginal stable CLT of the PDS-based RV can also be derived from Fukasawa (2010), the joint convergence requires additional non-trivial theoretical results, which are new in the literature; see Online Appendix A.4 for details.

Moreover, under the alternative, $\overline{M}_{c,\epsilon}$ remains robust to jumps because $\varphi_\epsilon(c)$ shrinks at the same rate as $\sqrt{\Delta_n}$, so censoring caps jump-induced overshoots. By contrast, M_c is inflated by these overshoots and converges to a different level. The resulting separation implies that the standardized test statistic diverges, as shown in the following Corollary 1.

Theorems 1 and 2 directly imply the following result, which indicates that our test is correctly sized under the null and consistent under the alternative:

Corollary 1. Under the same conditions, the standardized ratio test statistic $T_{c,\epsilon}$ satisfies

$$T_{c,\epsilon} = \frac{\overline{M}_{c,\epsilon}/M_c - 1}{\sqrt{\widehat{V}_\epsilon(\overline{M}_{c,\epsilon})}} \quad \begin{cases} \xrightarrow{\mathcal{L}} \mathcal{N}(0,1) & \text{if } \omega \in \Omega', \\ \xrightarrow{\mathbb{P}} \infty & \text{if } \omega \in \Omega'', \end{cases} \tag{18}$$

where the denominator is the estimated standard deviation of $\overline{M}_{c,\epsilon}/M_c$ with

$$\widehat{V}_\epsilon(m) = \frac{1}{m^2 N}(\phi_{11}(m) + \phi_{22}(m) - 2\phi_{21}(m)). \tag{19}$$

When $X''(\omega) \equiv 0$ on the interval $(0,1)$, the test statistic $T_{c,\epsilon}$ converges in distribution to a standard normal random variable, which is implied by Theorem 2. When $X''(\omega) \neq 0$ for some $t \in (0,1)$, the numerator of $T_{c,\epsilon}$ converges to a finite non-zero level determined by κ, whereas its denominator shrinks to zero as $n \to \infty$. Consequently, the standardized test statistic diverges in the limit, thereby implying the consistency of the test under the alternative hypothesis.

3.2 Noise Mitigation

As discussed in Remark 6, our asymptotic results derived in Section 3.1 are based on the strong approximation result that couples the observation scheme $(t_{n,i})$ under Assumption 2 and the limiting scheme $(\breve{t}_{n,i})$ in Remark 3. However, this rationale becomes untenable when the observations are contaminated by measurement errors, such as market microstructure noise. In this section, we propose an empirically plausible approach to mitigate the impact of the noise. With a two-step noise reduction method, we transform the noise-contaminated observations into a sequence of pseudo-observations, which behaves locally like a Gaussian random walk in the limit. Since each sampled return is only determined by finitely many tick-level returns within a local horizon, our test statistic relying solely on the sample moments of normalized PDS returns remains valid.

To this end, we assume an additive noise term with a weak dependence structure, before which we recall the definition of α-mixing (Fan and Yao, 2003): The α-mixing coefficient of a stationary sequence $(X_i)_{i\in\mathbb{Z}}$ of variables indexed by $i \in \mathbb{Z}$ is defined as

$$\alpha(h) = \sup\{|\mathbb{P}(A \cap B) - \mathbb{P}(A)\mathbb{P}(B)| : A \in \mathcal{F}_i,\ B \in \mathcal{F}^{i+h}\}, \tag{20}$$

where the pre- and post-σ-fields are defined as $\mathcal{F}_j = \sigma(\{X_i : i \leq j\})$ and $\mathcal{F}^j = \sigma(\{X_i : i \geq j\})$. The process (X_i) is said to be α-mixing if $\alpha(h) \to 0$ as $h \to \infty$.

Assumption 3. Let $\varepsilon = (\varepsilon_i)_{0\leq i\leq N}$ be a stationary sequence with $\mathbb{E}[\varepsilon_i] = 0$ and $\mathbb{E}[|\varepsilon_i|^{2+\delta}] < \infty$ for some $\delta > 0$, where ε_i are identically distributed with variance σ_ε^2 and autocovariance function $\Gamma_h = \mathbb{E}[\varepsilon_i \varepsilon_{i+h}]$. The process ε is α-mixing with $\sum_{h=1}^{\infty} \alpha(h)^{\delta/(2+\delta)} < \infty$, and exogenous to X. The

sequence $Y = (Y_i)_{0 \leq i \leq N}$ collects all observations contaminated by noise $Y_i = X_i + \varepsilon_i$, with the log-returns $r_i = Y_i - Y_{i-1}$ for all $1 \leq i \leq N$.

Remark 7. The autocovariance function Γ_h satisfies $\Gamma_0 = \sigma_\varepsilon^2$ and $\Gamma_{-h} = \Gamma_h$. For Γ_h, the standard absolute summability condition, i.e., $\sum_{h \in \mathbb{Z}} |\Gamma_h| < \infty$, is well-known to be sufficient for ergodicity and necessary for α-mixing under stationarity (Ibragimov and Linnik, 1971). Furthermore, the assumed conditions on the $(2+\delta)$-th moment and the α-mixing coefficient $\alpha(h)$ are sufficient for a CLT for the centered, stationary and α-mixing ε (Theorem 1.7, Ibragimov, 1962; Theorem 8.3.7, Durrett, 2019).

Remark 8. The additive noise term ε_i summarizes a diverse array of market frictions. An i.i.d. additive noise with non-zero variance, firstly introduced by Zhou (1996), is commonly assumed in earlier literature of high-frequency volatility estimation, see, e.g., Aït-Sahalia et al. (2005) and Zhang et al. (2005). However, some previous studies including Hansen and Lunde (2006), Ubukata and Oya (2009), and Aït-Sahalia et al. (2011) find empirical evidence of self-dependent noise in financial markets. Recent work by Jacod et al. (2017) summarizes the common statistical properties of market microstructure noise and develops estimators for its autocovariances and autocorrelations, which further confirms this point. Assumption 3 allows for a weak dependence structure of the noise. This standard Itô semimartingale plus locally dependent noise framework has been employed by a number of recent studies, see, e.g., Jacod et al. (2017, 2019), Varneskov (2017), Christensen et al. (2022), and Li and Linton (2022).

However, it is worth noting that Assumption 3 is in fact more stringent than needed, given that Proposition 1 only necessitates the convergence of the pre-averaged returns defined in Eq. (21) to an α-mixing and stationary Gaussian process. This convergence result requires an appropriate limit theorem to hold for a weighted-average of the tick-level returns $r_i = \Delta_i^N Y = \Delta_i^N X + \Delta_i^N \varepsilon$, which is satisfied when the assumed α-mixing and stationary ε is exogenous to X. However, the same result holds when (r_i) itself satisfies such conditions for an appropriate limit theorem, which permits certain dependence structure between X and ε. For brevity, we will stick with the exogenous noise assumption in the analysis henceforward, and examine its potential impact with a more general specification of ε via extensive simulations in Section 4.

With the additive noise under Assumption 3, the noisy observations clearly do not resemble a Gaussian random walk in the limit. There are two main problems:

(i) The noise term dominates the variance of tick-level returns (r_i) and does not shrink as $n \to \infty$;
(ii) The tick-level returns are no longer independent due to the self-dependence of ε.

We now introduce a two-step noise reduction method which facilitates the construction of a sequence of pseudo-observations with desirable properties in the limit:

Step 1: Pre-averaging. We implement the pre-averaging approach of Jacod et al. (2009): We choose a sequence of positive integers k_n satisfying $k_n \sqrt{\Delta_n} = \theta$ for some $\theta > 0$. We calculate

log-returns on $(Y_i)_{0\le i\le N}$ that are pre-averaged in a local neighborhood of k_n observations:

$$r_i^* = \frac{1}{k_n}\sum_{j=k_n/2+1}^{k_n} Y_{i+j} - \frac{1}{k_n}\sum_{j=1}^{k_n/2} Y_{i+j} = \sum_{j=1}^{k_n-1} g\Big(\frac{j}{k_n}\Big) r_{i+j}, \tag{21}$$

where $g(s) = s \wedge (1-s)$, for all $i \in \{1,\dots,N'\}$ with $N' = N - 2k_n/2 + 2$.

Step 2: Random Sign Flip and Permutation. We compute the "wild-bootstrapped" returns based on the pre-averaged returns $(r_i^*)_{1\le i\le N'}$ obtained from Step 1:

$$\tilde{r}_i = r^*_{\pi(i)}\delta_{\pi(i)}, \tag{22}$$

where $(\delta_i)_{1\le i\le N'}$ is a sequence of i.i.d. Rademacher random variables, i.e., $\mathbb{P}(\delta_i = -1) = \mathbb{P}(\delta_i = 1) = 1/2$, and $\pi : \{1,\dots,N'\} \mapsto \{1,\dots,N'\}$ is a uniform random permutation of the index set $\{1,\dots,N'\}$.

Under the null, we show that the sequence of "wild-bootstrapped" returns $(\tilde{r}_i)_{1\le i\le N'}$ behave locally like a sequence of i.i.d. Gaussian random variables in the limit:

Proposition 1. Let ε and Y follow Assumption 3. Under the null hypothesis and as $n \to \infty$, the sequence $(\tilde{r}_i)_{1\le i\le N'}$ converges in distribution to a sequence of locally independent[7] and identically distributed Gaussian random variables with variances of order $\sqrt{\Delta_n}$.

We first discuss why this two-step method can mitigate the impact of noise under the null hypothesis. In Step 1, the standard choice of pre-averaging window balances the orders of X increments and ε, such that the pre-averaged returns $(r_i^*)_{1\le i\le N'}$ converge to a centered, stationary and self-dependent Gaussian process as $n \to \infty$. The dependence structure of (r_i^*) arises from both the assumed self-dependent ε and overlapping pre-averaging windows. Therefore, we proceed to Step 2 to remove the local dependence, which is inspired by the wild bootstrap introduced by Wu (1986). The random sign flip eliminates serial correlations in (r_i^*). The uniform random permutation assigns equal probability to each of the $N'!$ possible permutations, which ensures that any two variables in $(\tilde{r}_i)_{1\le i\le N'}$ are independent when their indices are not sufficiently far apart from each other in $\{1,\dots,N'\}$ under infill asymptotics.

Proposition 1 inspires the construction of our test in the presence of noise as follows: We generate a sequence of pseudo-observations $(\tilde{Y}_i)_{0\le i\le N'}$ as partial sums of $(\tilde{r}_i)$, where $\tilde{Y}_0 = Y_0$ and $\tilde{Y}_i = \sum_{j=1}^{i}\tilde{r}_j$. Next, we choose a sequence of barrier widths $c = m\Delta_n^{1/4}$ and obtain the sampled observations $(\tilde{Y}_i^{(c)})$. Finally, we follow Section 3.1 to construct the standardized test statistic $\tilde{T}_{c,\epsilon}$ from $(\tilde{Y}_i^{(c)})$ in place of $(X_i^{(c)})$. Formal establishment of its asymptotic properties requires further assumptions about the noise, and is left for future research. We next discuss some plausible properties of $\tilde{T}_{c,\epsilon}$, which are verified through comprehensive simulations with a realistically calibrated noise specification in the next section.

[7] A formal definition of local independence is given in Eq. (A.140) in Online Appendix A.5.

The choice of $c = m\Delta_n^{1/4}$ ensures that the normalized increments $\tilde{r}_i/c$ are invariant to Δ_n, which is analogous to the case without noise. Assuming that $(\tilde{r}_i)_{1\leq i\leq N'}$ is a sequence of i.i.d. centered Gaussian random variables, $(\tilde{Y}_i)_{0\leq i\leq N'}$ forms a genuine Gaussian random walk, and thus the same CLT in Theorem 2 would hold for $\tilde{T}_{c,\epsilon}$ under the null. Our simulation results reveal that this CLT still holds for $\tilde{T}_{c,\epsilon}$ constructed from $(\tilde{Y}_i)$. This is because each sampled return is only determined by finitely many increments of $(\tilde{Y}_i)$ within a local horizon, which are indeed asymptotically i.i.d.. Importantly, the convergence rate of $\tilde{T}_{c,\epsilon}$ remains $\sqrt{N}$, which apparently contradicts the optimal $N^{1/4}$ rate of noise-robust IV estimators (Gloter and Jacod, 2001; Xiu, 2010; Reiß, 2011) that also appears in some noise-robust jump tests (Aït-Sahalia et al., 2012). This discrepancy arises because our test statistic does not rely on a noise-robust IV estimator, but rather on a consistent estimator of the scale-invariant barrier width m, which is identified through the variance of $\tilde{r}_i$. As $\tilde{r}_i$ has the same order as the pre-averaged noise, a consistent estimator of m has the same $\sqrt{N}$ rate as that of a noise variance estimator. This finding also reveals that a noise-robust IV estimator is not a pre-requisite for noise-robust jump tests.

4 Monte Carlo Simulations

4.1 Simulation Design

We simulate an empirically realistic discretized diffusion model for asset prices, which incorporates both time varying tick-variances and transaction activities. Firstly, we simulate a Heston model for the efficient price process X and obtain its tick-level observations, to which we add jumps with different sizes:

$$\begin{aligned} dX_t &= \Big(\mu - \frac{\sigma_t^2}{2}\Big)dt + \sigma_t dW_t + dX_t'', \quad t \in [0,1] \\ d\sigma_t^2 &= \alpha(\theta - \sigma_t^2)dt + \eta\sigma_t dB_t, \end{aligned} \tag{23}$$

where $W = (W_t)$ and $B = (B_t)$ are standard Brownian motions with $\mathrm{Corr}(W_t, B_t) = \rho$, and X'' is a compound Poisson process, i.e.,

$$X_t'' = \sum_{i=1}^{N_t} J_i, \tag{24}$$

where $N = (N_t)$ is a Poisson process with rate λ, and jump sizes J_i follow a double exponential distribution (Laplace distribution) with location parameter 0 and scale parameter b. To generate all tick-level observations, we discretize X equidistantly on $t = i/n$ for $n = 23,400$. Then we modify the observation times $0 \leq t_{n,1} < t_{n,2} < \cdots \leq 1$ following an inhomogeneous Poisson process with the rate

$$\alpha(t) = 1 - \frac{1}{2}\cos 2\pi t, \tag{25}$$

where $t \in [0,1]$. The inverted U-shaped rate function $\alpha(t)$ is employed to mimic the empirical feature of more transactions that occur in the early morning and late afternoon than in the middle

of the trading day (Jacod et al., 2017). We draw 10,000 simulated price paths for each experiment.

For the additive noise,[8] we denote

$$\varepsilon_i = 2\sqrt{\frac{\sigma^2_{t_{n,i}}}{n}}\left(\omega_i^A + \omega_i^B\sqrt{\frac{\nu-2}{\nu}}\right), \tag{26}$$

where ω_i^A are autocorrelated Gaussian random variables defined as

$$\omega_i^A = \phi_i + \sum_{j=1}^{\Lambda}\beta_j\phi_{i-j}, \quad \text{with } \phi_i \sim \text{i.i.d.}\,\mathcal{N}(0,1), \text{ and } \beta_j = \frac{d(1+d)\cdots(j-1+d)}{j!}, \tag{27}$$

for $d \in (-0.5, 0.5)$ and a large cutoff value Λ, which form a moving-average series that approximates a fractionally differenced process (Jacod et al., 2019), and ω_i^B are i.i.d. draws from a Student's t distribution with the degree of freedom ν.

The instantaneous standard deviation of the Gaussian-t mixture noise is about four times as much as that of diffusive increments, i.e., $\sqrt{\sigma^2_{t_{n,i}}/n}$, so that the diffusive increments are clearly dominated by the additive noise.[9] This specification of ε_i captures some important features of market microstructure noise in financial markets, e.g., temporal heteroskedasticity, slowly-decaying serial correlation, intraday seasonality, and dependence on the latent prices. The t-distributed noise ω_i^B is introduced to capture the large bouncebacks commonly observed in high-frequency transaction data (Aït-Sahalia et al., 2012). Besides the additive noise, we also consider the rounding errors on the price level, i.e., let the observed prices $e^{Y_i} = e^{X_i+\varepsilon_i}$ be further rounded to cents. The observed logarithmic prices are given as

$$Y_i = \log\left(\left[\frac{e^{X_i+\varepsilon_i}}{0.01}\right]\times 0.01\right), \tag{28}$$

where the function $[x]$ rounds a number x to the nearest integer.[10]

The annualized parameters for the Heston model are fixed at $(\mu, \alpha, \theta, \eta, \rho) = (0.05, 5, 0.16, 0.5, -0.5)$, where the volatility parameters satisfy the Feller's condition $2\alpha\theta \geq \eta^2$ which ensures the positivity of σ. The parameter choices follow both Aït-Sahalia and Jacod (2009b) and Aït-Sahalia et al. (2012), which are calibrated according to the empirical estimates in Aït-Sahalia and Kimmel (2007). For the jump components, we let $\lambda = 1$, and $b = 0.2\sqrt{\theta}$ and $0.4\sqrt{\theta}$ corresponding to moderate and relatively large jump sizes. The moderate (resp. large) jumps contribute about 7% (resp. 25%) of the daily QV on average when noise is absent. For the additive noise term, we let $(d, \Lambda, \nu) = (0.3, 100, 2.5)$ following Aït-Sahalia et al. (2012) and Jacod et al. (2019).

[8] The simulation design of additive noise mainly follows Aït-Sahalia et al. (2012). In addition, we consider its serial correlation using the method of Jacod et al. (2019).

[9] In the simulations, we follow Aït-Sahalia et al. (2012) to truncate the t-distributed ω_i^B at $\pm 50\sqrt{\nu/(\nu-2)}$ to avoid large returns in the absence of jumps, which could lead to very misleading results. Hence, the instantaneous standard deviation of the t-distributed noise $2\omega_i^B\sqrt{\sigma^2_{t_{n,i}}/n}\sqrt{(\nu-2)/\nu}$ is slightly lower than $2\sqrt{\sigma^2_{t_{n,i}}/n}$.

[10] We also consider alternative specifications for the additive heteroscedastic noise, see the results in Online Appendix B.3.

Fig. 3 depicts the intraday variation of some market activity variables of a simulated path in the absence of noise, which include the return, number of trades, and annualized RV in each one-minute interval. Both transaction intensity and return variation exhibit a U-shaped pattern over the trading hours, which is in line with some prior empirical findings (Harris, 1986; Wood et al., 1985; Andersen and Bollerslev, 1997; Andersen et al., 2018, 2019, 2024). Fig. 4 compares the simulated tick-level latent prices and the rounded, noise-contaminated price observations over an intraday episode.

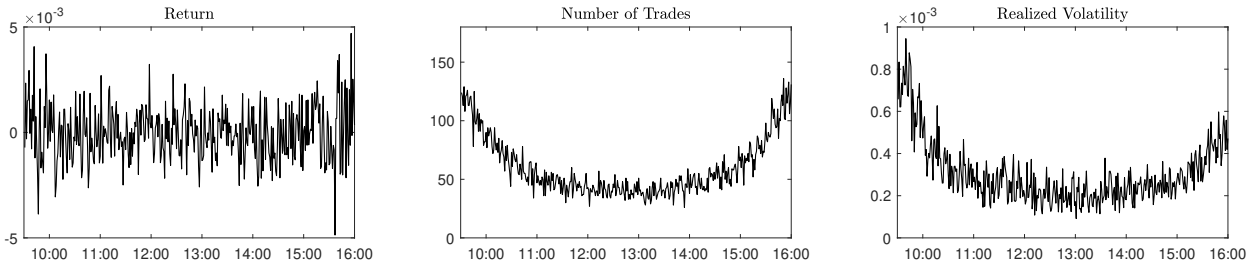

Figure 3: Some market activity variables of simulated prices. The tick-level observations are simulated with the Heston model in Eq. (23), and we assign randomized observation times with an inverted U-shape rate function in Eq. (25) to all observations. The returns, numbers of transactions, and annualized RVs are computed at a granularity of one minute.

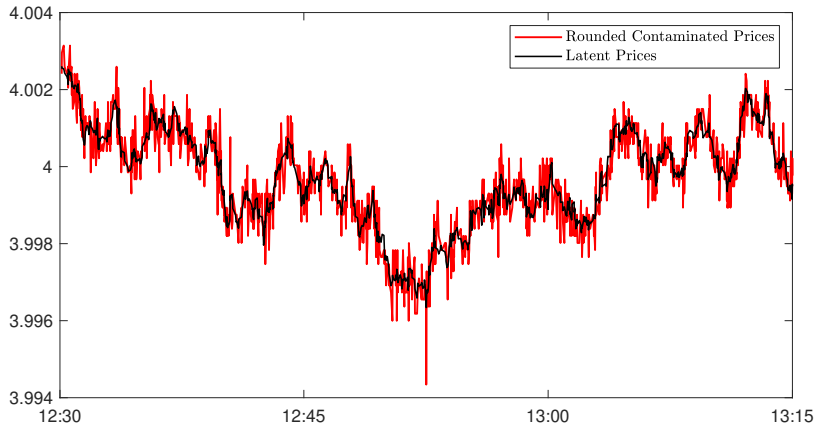

Figure 4: Comparison of the simulated latent prices and the noise-contaminated prices with rounding errors.

4.2 Test Performance in the Absence of Market Microstructure Noise

Table 1 reports the finite-sample size and size-adjusted power (at 5% nominal level) of the standardized test statistic $T_{c,\epsilon}$ when noise is absent. Tick-level observations are sampled with different PDS barrier widths $c = K\sigma(r_i)$, i.e., K times the standard deviation of tick-by-tick returns, where K ranges from 3 to 10. Different censoring thresholds with $\epsilon \in \{0.05, 0.07, 0.1\}$ are also considered. In Table 1, the rejection rates under the null (Panel A) are all closely aligned with the nominal level. For the finite-sample power under the alternative (Panels B and C), we find that the rejection rates are fairly robust across different sampling frequencies. Fig. 5 compares the finite-sample distributions of our test statistic with the limiting standard normal distribution. Under the null, the finite-sample distribution (solid line) closely resembles the standard normal (shaded area), while

the distribution deviates significantly from $\mathcal{N}(0,1)$ when there exist jumps of either moderate or large sizes.

Table 1: Finite-sample size and power (%)

Nominal size: 5%	Panel A No Jump				Panel B Moderate Price Jumps				Panel C Large Price Jumps			
		ϵ				ϵ				ϵ		
$c/\sigma(r_i)$	$N^{(c)}$	0.05	0.07	0.10	$N^{(c)}$	0.05	0.07	0.10	$N^{(c)}$	0.05	0.07	0.10
3	1786	5.26	5.31	5.48	1697	58.21	61.68	65.22	1564	76.29	78.47	80.37
4	1100	5.51	5.58	5.89	1043	61.24	64.54	67.46	959	77.95	80.18	81.99
5	744	5.39	5.56	5.77	705	63.01	66.29	69.55	647	79.10	81.00	82.83
6	536	4.99	5.20	5.61	508	63.77	67.13	70.30	466	80.16	82.01	83.92
7	405	5.28	5.56	5.71	383	65.19	68.47	71.07	351	80.59	82.23	84.01
8	316	5.20	5.61	5.93	299	65.86	68.90	72.07	274	80.76	82.51	84.36
9	254	5.28	5.46	6.01	240	66.33	68.88	71.47	220	81.36	82.78	84.42
10	208	5.07	5.29	5.49	197	66.66	69.33	72.16	181	81.20	83.18	84.85

This table reports the finite-sample size and size-adjusted power (%) of 10,000 simulations of the test statistic $T_{c,\epsilon}$ at 5% nominal level in the absence of market microstructure noise. Tick-level observations are sampled with different PDS barrier widths $c = K\sigma(r_i)$, i.e., K times the standard deviation of tick-by-tick returns, where K ranges from 3 to 10. Different censoring thresholds with $\epsilon \in \{0.05, 0.07, 0.1\}$ are considered. $N^{(c)}$ stands for the average sampling frequencies.

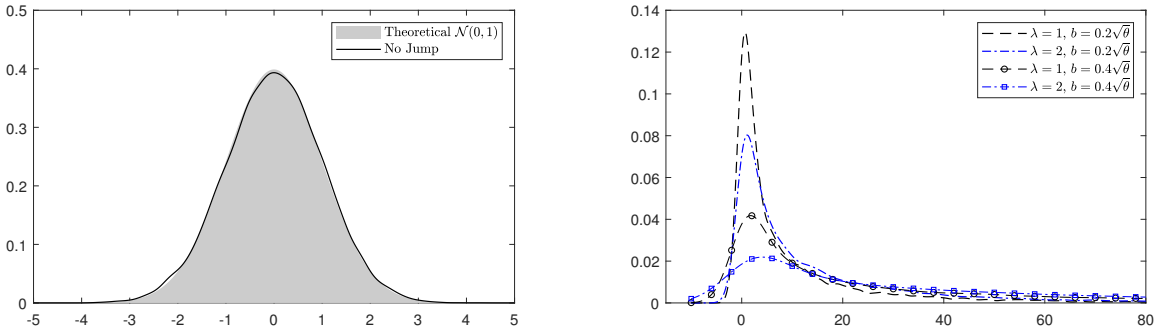

Figure 5: Finite-sample distributions of the standardized test statistic $T_{c,\epsilon}$ in the absence of noise. We plot the finite-sample distribution under the null (solid line) and compare it with the simulated standard normal (shaded area). Jumps are simulated with a compounded Poisson process with the intensity λ, and their sizes follow a double exponential distribution with location parameter 0 and scale parameter b. We consider different parameter choices: (i) $\lambda = 1$, $b = 0.2\sqrt{\theta}$ (dash), (ii) $\lambda = 2$, $b = 0.2\sqrt{\theta}$ (dash-dot), (iii) $\lambda = 1$, $b = 0.4\sqrt{\theta}$ (dash-circle), and (iv) $\lambda = 2$, $b = 0.4\sqrt{\theta}$ (dash-square). In all cases, the PDS barrier width $c = 5\sigma(r_i)$, and the censoring parameter $\epsilon = 0.05$.

4.3 Test Performance in the Presence of Market Microstructure Noise

Panel A in Table 2 summarizes the finite-sample size (at 5% nominal level) of the standardized test statistic $T_{c,\epsilon}$ constructed from the rounded noise-contaminated observations. We employ the two-step noise reduction method in Section 3.2 to construct the sequence of pseudo-observations with three different pre-averaging windows, i.e., $k_n = \lceil \theta\sqrt{N} \rceil$ with $\theta \in \{0.3, 0.4, 0.5\}$. The choices of θ follow the rule of thumb in Hautsch and Podolskij (2013). Similar to the results in the absence of noise, the rejection rates under the null are close to the nominal level across almost all choices of bandwidth c and censoring parameter ϵ. Panels B and C in Table 2 report the size-adjusted power

under the alternative with moderate and large jumps, respectively. Compared with the simulation results in Table 1, the finite-sample power experiences a marginal reduction but remains above 40% for most of the parameter choices. Fig. 6 compares the finite-sample distributions of $T_{c,\epsilon}$ with $\mathcal{N}(0,1)$. It is observed that $T_{c,\epsilon}$ is almost a standard normal under the null, but it has a notably larger magnitude than $\mathcal{N}(0,1)$ under the alternative. Comparing this with Fig. 5, we observe that the right tails of the test statistic become smaller with the same jump specifications. This explains the slightly reduced power of our test in the presence of market microstructure noise.

Table 2: Finite-sample size and power (%) in the presence of market microstructure noise

Nominal size: 5%		$\theta = 0.3$				$\theta = 0.4$				$\theta = 0.5$			
			ϵ				ϵ				ϵ		
	$c/\sigma(\tilde{r}_i)$	$N^{(c)}$	0.05	0.07	0.10	$N^{(c)}$	0.05	0.07	0.10	$N^{(c)}$	0.05	0.07	0.10
Panel A No Jump	3	1784	4.90	5.15	5.20	1784	4.80	5.35	5.71	1783	5.06	5.07	5.70
	4	1099	4.84	4.95	5.42	1098	5.29	5.10	5.51	1098	5.14	5.08	5.79
	5	743	4.94	5.01	5.20	743	5.19	5.02	5.57	742	4.81	5.02	5.70
	6	536	4.74	4.89	5.57	536	4.78	5.11	5.58	535	4.96	5.11	5.47
	7	404	4.99	5.11	5.29	404	4.86	5.05	5.76	404	4.86	5.17	5.46
	8	316	5.15	5.37	5.54	316	4.82	5.08	5.43	315	4.81	5.30	5.82
	9	253	5.04	5.41	5.13	254	4.84	5.10	5.63	253	4.96	5.28	5.73
	10	208	5.18	5.10	5.60	208	4.84	5.34	5.54	208	5.04	5.08	5.66
Panel B Moderate Jumps	3	1716	46.00	49.28	51.77	1717	44.98	46.84	49.27	1718	43.08	45.18	47.52
	4	1058	45.89	48.56	50.92	1059	43.31	46.76	48.56	1061	41.35	44.77	46.22
	5	717	44.95	47.45	50.42	719	42.99	45.50	47.53	720	40.81	43.12	44.93
	6	519	44.60	46.65	48.86	519	42.82	43.97	47.01	520	40.25	42.06	45.01
	7	392	43.79	45.31	48.98	393	41.00	43.15	46.29	394	40.08	41.95	45.04
	8	307	42.45	45.21	48.64	308	40.97	42.47	46.81	308	39.98	41.03	43.83
	9	247	41.38	43.95	48.57	248	40.54	42.58	45.62	248	38.45	41.21	43.67
	10	203	41.08	44.57	47.51	204	40.04	41.30	45.45	204	38.12	40.03	43.86
Panel C Large Jumps	3	1594	68.85	70.38	72.44	1596	68.06	69.14	70.54	1599	66.37	68.54	69.68
	4	983	68.79	70.51	72.17	986	66.37	68.97	70.42	990	65.60	67.26	68.97
	5	668	67.26	69.92	71.80	671	66.37	68.22	69.52	673	65.11	66.50	68.19
	6	484	67.69	69.41	70.48	486	65.92	67.13	69.67	489	64.38	66.05	68.07
	7	367	66.78	68.71	70.81	369	65.14	66.46	68.54	371	63.68	65.35	67.61
	8	288	65.84	68.11	70.24	290	64.22	66.40	68.42	292	62.93	64.89	66.90
	9	233	65.83	67.44	70.32	234	64.08	66.29	68.38	236	62.29	64.68	66.67
	10	192	65.00	66.96	69.70	193	63.44	65.54	68.23	194	61.91	64.12	66.69

This table reports the finite-sample size and size-adjusted power (%) of 10,000 simulations of the test statistic $T_{c,\epsilon}$ at 5% nominal level. All simulated prices are contaminated by the additive Gaussian-t mixture noise and rounding errors. We utilize the two-step noise reduction method in Section 3.2 to construct the sequence of pseudo-observations with three different pre-averaging windows, i.e., $k_n = \lceil \theta\sqrt{N} \rceil$ with $\theta \in \{0.3, 0.4, 0.5\}$. The observations are sampled with different PDS barrier widths $c = K\sigma(\tilde{r}_i)$, where K ranges from 3 to 10. Different censoring thresholds with $\epsilon \in \{0.05, 0.07, 0.1\}$ are considered. $N^{(c)}$ stands for the average sampling frequencies.

We then compare the empirical rejection rates of our test with those of 8 classical high-frequency jump tests constructed from equidistantly calendar-time-sampled observations (Table 3). These tests include BNS (Barndorff-Nielsen and Shephard, 2006), JO (Jiang and Oomen, 2008), LM (Lee and Mykland, 2008), ASJ (Aït-Sahalia and Jacod, 2009b), CPR (Corsi et al., 2010), PZ (Podolskij and Ziggel, 2010), MinRV and MedRV (Andersen et al., 2012). The parameter choices for all these

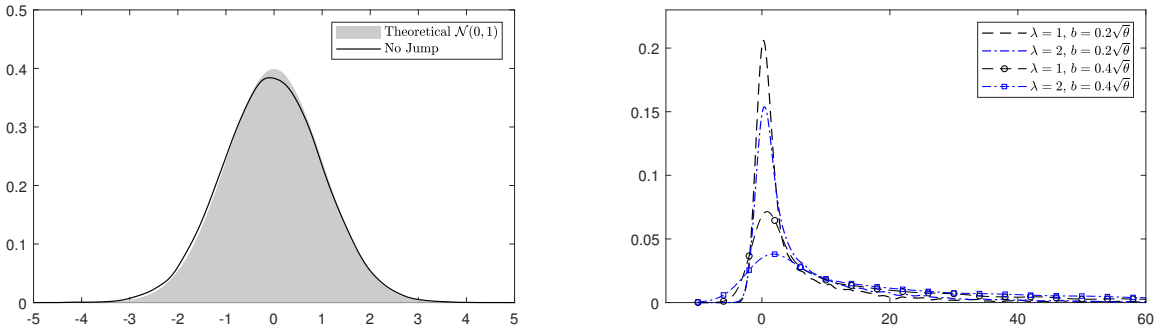

Figure 6: Finite-sample distributions of the standardized test statistic $T_{c,\epsilon}$ in the presence of noise. We plot the finite-sample distribution under the null (solid line) and compare it with the simulated standard normal (shaded area). Jumps are simulated with a compounded Poisson process with the intensity λ, and their sizes follow a double exponential distribution with location parameter 0 and scale parameter b. We consider different parameter choices: (i) $\lambda = 1$, $b = 0.2\sqrt{\theta}$ (dash), (ii) $\lambda = 2$, $b = 0.2\sqrt{\theta}$ (dash-dot), (iii) $\lambda = 1$, $b = 0.4\sqrt{\theta}$ (dash-circle), and (iv) $\lambda = 2$, $b = 0.4\sqrt{\theta}$ (dash-square). In all cases, we select the pre-averaging window $k_n = \lceil \theta\sqrt{N} \rceil = 46$ with $\theta = 0.3$, the PDS barrier width $c = 5\sigma(\tilde{r}_i)$, and the censoring parameter $\epsilon = 0.05$.

tests are determined in accordance with the recommendations from their original literature.[11] Our analysis, in line with the Monte Carlo results of Dumitru and Urga (2012) and Maneesoonthorn et al. (2020), demonstrates that nearly all the tests constructed from equidistantly calendar-time-sampled observations suffer from size distortion and their results become highly unstable under the assumed additive Gaussian-t mixture noise and rounding errors. This noise significantly distorts their finite-sample null distributions, particularly at higher sampling frequencies. It might be interesting to see that the size of the JO test is close to the nominal level. However, a closer examination reveals that this is caused by two cancelling distortions due to the mixture of Gaussian and t-distributed noise specification, see Online Appendix B.3 for details. While sparse sampling can alleviate size distortion, it also substantially weakens the power of these tests.

For more appropriate benchmarks when noise is present, we also consider some noise-robust versions of classical tests (Table 4) constructed from tick-level or finely sampled observations: the noise-adjusted PZ (Podolskij and Ziggel, 2010), LM12 (Lee and Mykland, 2012), and ASJL (Aït-Sahalia et al., 2012). Similar to our test, all these noise-robust tests rely on the pre-averaging approach of Jacod et al. (2009) to "pre-filter" the noise-contaminated observations.[12] The "optimal" tuning parameters for those tests are selected by minimizing the absolute distance between the nominal size and the empirical size with the simulated tick-level noise-contaminated observations.[13] We find that, while these noise-robust tests reliably control size, their power performance slightly falls short of that achieved by our proposed test.

Furthermore, we consider the widely employed jump filtering and detection technique from the recent literature (see, e.g., Aït-Sahalia et al., 2025; Aleti et al., 2025) as an alternative benchmark.

[11] The parameter choices of the competing tests are reported in Online Appendix B.1.

[12] With a simplified i.i.d. noise specification, Jiang and Oomen (2008) propose an analytically modified form of JO. However, it cannot achieve comparable performance under the simulated Gaussian-t mixture noise.

[13] Note that the optimal tuning parameters are not empirically feasible in practice. Therefore, the results presented should be interpreted as upper bounds of the performance for these benchmark tests.

Table 3: Finite-sample size and power (%) of other tests

Nominal size: 5%										
	Int. (sec)	N_{spl}	BNS	JO	LM	ASJ	CPR	PZ	MinRV	MedRV
Panel A No Jump	5	4680	0.33	6.19	98.40	99.98	33.39	89.61	0.00	0.00
	15	1560	0.42	5.23	71.12	99.42	18.20	52.91	0.00	0.12
	30	780	3.30	5.25	46.82	76.71	13.02	30.25	0.99	2.53
	60	390	5.16	5.75	30.82	29.50	8.47	19.57	3.35	5.30
	120	195	6.46	8.08	17.73	10.60	7.86	16.76	4.78	6.91
	180	130	6.90	8.95	15.10	7.52	8.05	15.96	5.29	8.16
	300	78	7.65	10.87	12.12	4.84	8.97	15.58	5.34	8.98
Panel B Moderate Jumps	5	4680	30.08	31.95	15.80	97.25	10.93	12.40	16.91	26.45
	15	1560	36.42	36.33	24.78	94.76	21.13	20.59	32.89	36.17
	30	780	33.20	33.89	32.00	77.29	28.64	28.39	28.95	33.25
	60	390	28.25	28.25	36.63	45.44	29.58	37.36	24.96	28.61
	120	195	21.64	20.90	32.73	24.43	24.18	30.47	20.07	23.51
	180	130	17.40	17.16	28.97	16.57	19.34	25.51	16.34	19.42
	300	78	13.83	11.33	20.56	11.44	15.93	19.09	13.32	14.74
Panel C Large Jumps	5	4680	56.35	59.11	43.00	95.12	32.58	36.63	42.72	53.55
	15	1560	60.94	61.18	52.39	95.31	47.32	47.58	58.68	60.84
	30	780	59.06	59.05	58.46	83.73	54.54	55.57	54.79	58.43
	60	390	54.36	54.57	62.78	59.83	56.25	62.88	50.60	54.90
	120	195	46.78	46.16	58.81	36.76	50.12	56.74	44.11	49.20
	180	130	41.21	40.86	54.93	26.94	44.83	51.91	39.32	44.13
	300	78	34.07	33.19	45.73	16.14	38.76	43.76	33.66	37.49

This table reports the finite-sample size and size-adjusted power (%) of 10,000 simulations of 8 classical tests at 5% nominal level: BNS (Barndorff-Nielsen and Shephard, 2006), JO (Jiang and Oomen, 2008), LM (Lee and Mykland, 2008), ASJ (Aït-Sahalia and Jacod, 2009b), CPR (Corsi et al., 2010), PZ (Podolskij and Ziggel, 2010), MinRV and MedRV (Andersen et al., 2012). All these tests are constructed on observations equidistantly sampled with various intervals in calendar time: 5, 15, 30, 60, 120, 180 and 300 seconds, and "N_{spl}" stands for the sampling frequencies.

Table 4: Finite-sample size and power (%) of other noise-robust tests

Nominal size: 5%					
	Int. (sec)	N_{spl}	PZ*	LM12	ASJL
Panel A: No Jump	tick	23400	5.29	5.03	5.12
	5	4680	4.96	8.83	8.79
Panel B: Moderate Jumps	tick	23400	38.57	22.70	38.22
	5	4680	30.38	18.79	17.66
Panel C: Large Jumps	tick	23400	64.78	40.76	63.50
	5	7680	56.49	31.38	41.96

This table reports the finite-sample size and size-adjusted power (%) of 10,000 simulations of 3 noise-robust tests at 5% nominal level: Noise-adjusted PZ (Podolskij and Ziggel, 2010), LM12 (Lee and Mykland, 2012), and ASJL (Aït-Sahalia et al., 2012). All these tests are constructed on tick-level and 5-second-sampled observations. The tuning parameters for those tests are selected by minimizing the absolute distance between the nominal size and the empirical size with the simulated tick-level noise-contaminated observations.

This method is based on the sequential detection approach of Andersen et al. (2007b) and the thresholding technique of Mancini (2009). Specifically, returns are classified as jumps if their absolute value exceeds the threshold $k\sigma_{t_{n,i}}\Delta_{n,i}^{\varpi}$, where the spot volatility is typically estimated recursively on a backward-looking window with a jump- and noise-robust procedure. With the rolling spot volatility estimates, one periodically checks (e.g., every few transactions or every few

minutes) whether a return has exceeded k standard deviations. Since our focus is to test for the existence of jumps over a fixed interval (a trading day), we adjust the threshold parameter k using both the Šidák and Bonferroni corrections—two widely used methods for controlling the family-wise error rate (FWER)—to maintain a nominal size of 5% for the overall procedure and address the multiple testing issue.[14]

Table 5: Finite-sample size and power (%) of truncation-based filtering technique

Nominal size: 5%					
		Panel A		Panel B	Panel C
		No Jump (with FWER control)			
Ticks	N_{spl}	Šidák	Bonferroni	Moderate Jumps	Large Jumps
1	23400	100.00	100.00	9.64	29.57
5	4680	100.00	100.00	15.33	39.49
15	1560	99.97	99.96	23.41	49.80
30	780	83.41	82.53	31.92	57.67
60	390	37.31	35.72	38.12	62.78
120	195	15.54	15.18	37.22	61.23
180	130	10.19	10.04	33.09	57.26
300	78	6.99	7.10	26.45	50.42

This table reports the finite-sample size and size-adjusted power (%) of 10,000 simulations of the truncation-based jump filtering technique. Observations are sampled at various multiples of ticks, where "N_{spl}" stands for the corresponding sampling frequencies. The truncation thresholds are constructed from the localized pre-averaged bipower variation of Podolskij and Vetter (2009) computed within each backward-looking window of 1,800 ticks. The threshold parameter k is adjusted with both the Šidák and Bonferroni corrections, and $\varpi = 0.5$.

Table 5 presents the finite-sample size and size-adjusted power of the truncation-based filtering technique, where we estimate the spot volatilities with the localized pre-averaged bipower variation of Podolskij and Vetter (2009) and evaluate returns every few ticks.[15] Although the filtering technique exhibits reliable size and power performance in the absence of noise with various choices of volatility estimators (see Table B.1 in Online Appendix B.2), our empirically calibrated simulations under noise contamination reveal that it tends to spuriously detect normal returns as jumps, particularly when sampled at a very high frequency. Furthermore, similar to the empirical applications of Aït-Sahalia et al. (2025), we consider a wide range of k from 3.5 to 9, and test for both tick-time- and calendar-time-sampled returns across various sampling frequencies. We find that both inadequate downsampling and low k-values lead to considerable overrejection under the null, whereas further sparse sampling and more stringent truncation thresholds result in a loss of power under the alternatives (see Figs. B.1 and B.2 in Online Appendix B.2), which indicates the difficulty of balancing such trade-offs when employing the truncation-based filtering technique.

[14] We note that both the Šidák and Bonferroni corrections are highly conservative, as the standardized returns may exhibit serial correlation. A simulation-based procedure adopted by Christensen et al. (2022) can generate data-driven critical values from AR(1) processes that account for serial correlations. However, as the critical values need to be adjusted downwards to achieve the correct size, it results in more inflated rejection rates than those reported in Table 5, and is therefore omitted here.

[15] We also examine returns sampled in equidistant calendar-time intervals, with the adjustments for intraday volatility pattern incorporated, and observe similar finite-sample performance, see Table B.2 in Online Appendix B.2.

As illustrated in Table 2, our PDS-based test demonstrates robustness across various parameter choices: (i) barrier width c, (ii) censoring parameter ϵ, and (iii) pre-averaging window $k_n = \lceil \theta\sqrt{N} \rceil$, even when we consider such a complicated and realistic noise specification. Furthermore, our test remains competitive and, often superior, to those noise-robust tests with optimal parameter choices. While we refrain from providing optimal parameter choices, we offer recommended ranges for practitioners:

(i) Choose c as a multiple of the standard deviation of $\tilde{r}_i$, i.e., $c = K\sigma(\tilde{r}_i)$, with $3 \leq K \leq 10$.
(ii) Choose ϵ in $[0.03, 0.15]$.
(iii) Choose the pre-averaging window $k_n = \lceil \theta\sqrt{N} \rceil$ with $\theta \in [0.2, 0.8]$.

Through extensive simulation studies with different specifications of market frictions, we believe that the recommended parameter choices work reasonably well in finite samples when the number of intraday tick-level observations is no less than 10,000. Additional simulation results can be found in Online Appendix B.3.

5 Empirical Analysis

In this section, we employ our new jump test on the high-frequency transaction data of 10 stocks listed on the New York Stock Exchange (NYSE): American Express (AXP), Boeing (BA), Disney (DIS), IBM, Johnson & Johnson (JNJ), JP Morgan (JPM), Merck (MRK), McDonald's (MCD), Procter & Gamble (PG), and Walmart (WMT). Our Trade and Quote (TAQ) dataset includes all transactions from 9:30 am to 4:00 pm on each trading day in 2020. As is standard in empirical research involving high-frequency financial data, we apply filters, as outlined in Barndorff-Nielsen et al. (2009), to eliminate obvious data errors, remove all transactions in the original record that are later corrected, canceled or otherwise invalidated, and retain only transactions from NYSE. Table 6 reports descriptive statistics of trades on these selected NYSE stocks, which include the number of trades, observed transaction prices in dollar terms, and intraday log-returns in basis points. Our PDS-based test utilizes the same tuning parameters as those in Section 4: the PDS barrier width $c = K\sigma(\tilde{r}_i)$ with K ranging from 4 to 6, the censoring parameter $\epsilon = 0.05$, and three pre-averaging windows $k_n = \lceil \theta\sqrt{N} \rceil$ with $\theta \in \{0.3, 0.4, 0.5\}$.

Table 7 reports the proportions of trading days with rejections in 2020, as determined by our PDS-based test. For the selected stocks, the proportions of trading days with identified jumps are no more than 20%, with only AXP and MCD identified to exhibit over 15% of trading days containing jumps. There is little variation in the rejection rates across different stocks, and the results are relatively stable with different parameter choices. For each stock, there is a slight decrease in the percentage of identified jumps when we employ a larger barrier width c for PDS, i.e., sample less frequently. To visualize the testing results for the selected stocks in 2020, we aggregate all stock-day outcomes, which yields a total of 2530 stock-day pairs. Fig. 7 illustrates the empirical distributions of the standardized test statistic (solid line) and compares it with the standard normal distribution $\mathcal{N}(0, 1)$. Relative to the limiting distribution under the null hypothesis of no jump (shaded area),

Table 6: Descriptive statistics of daily trades on selected NYSE stocks

Stock		AXP	BA	DIS	IBM	JNJ
Number of trades	Min	3171	10556	9785	5047	6383
	Max	59273	245802	125550	49178	71733
	Mean	19351	55314	37962	17818	22966
	Std Dev	9205	38352	20390	8265	11561
Transaction prices	Min	67.03	89.00	79.07	90.56	109.16
	Max	138.16	349.45	183.40	158.78	157.66
	Mean	100.88	181.46	121.78	123.16	143.33
	Std Dev	14.72	51.15	20.12	11.57	8.53
Intraday log-returns (1×10^{-4})	Min	−123.24	−163.29	−100.49	−143.49	−110.04
	Max	97.48	129.22	75.30	143.49	200.25
	Mean	0.00	0.00	0.00	0.00	0.00
	Std Dev	1.78	1.85	1.17	1.44	1.23
Stock		JPM	MRK	MCD	PG	WMT
Number of trades	Min	12593	5787	3968	7516	9845
	Max	156987	71570	55024	76337	90546
	Mean	44738	22833	16096	23224	26148
	Std Dev	25335	11058	7838	10422	13032
Transaction prices	Min	76.92	65.26	124.23	94.31	102.00
	Max	141.10	92.14	231.91	146.92	153.60
	Mean	103.17	79.86	195.17	125.19	128.55
	Std Dev	14.28	4.55	21.74	11.63	12.04
Intraday log-returns (1×10^{-4})	Min	−103.80	−177.00	−154.39	−132.25	−305.08
	Max	103.80	117.50	142.80	207.58	190.19
	Mean	0.00	0.00	0.00	0.00	0.00
	Std Dev	1.06	1.26	1.74	1.33	1.13

This table contains summary statistics for the number of trades, observed transaction prices in dollars, and intraday log-returns in basis points for 10 selected NYSE stocks in 2020. Data are collected from the TAQ database which includes all transactions from 9:30 am to 4:00 pm in each trading day. We apply filters, as outlined in Barndorff-Nielsen et al. (2009), to eliminate clear data errors, remove all transactions in the original record that are later corrected, cancelled or otherwise invalidated, and keep transactions on NYSE only.

the empirical distribution of our test statistic deviates slightly towards the right side, but maintains a bell shape centered around 0.5.

Table 7: Empirical rejection rates (%) for selected NYSE stocks

k_n	$c/\sigma(\tilde{r}_i)$	AXP	BA	DIS	IBM	JNJ	JPM	MRK	MCD	PG	WMT
$\theta = 0.3$	4	17.00	10.67	9.88	13.04	13.83	10.67	10.67	16.60	13.44	11.07
	5	15.81	10.67	9.49	12.25	11.86	10.67	10.28	16.21	11.86	10.67
	6	14.23	9.88	9.09	12.25	11.46	10.28	9.88	15.02	11.86	11.07
$\theta = 0.4$	4	16.21	9.88	10.28	13.44	12.65	10.67	9.88	15.81	12.65	12.25
	5	15.02	9.88	9.49	12.25	12.25	10.67	9.49	15.42	11.86	11.07
	6	14.23	9.49	9.49	11.46	11.07	9.88	9.49	14.23	11.46	10.28
$\theta = 0.5$	4	15.81	10.28	10.28	12.25	13.04	10.28	10.28	15.81	12.25	11.46
	5	14.23	9.09	9.88	12.25	11.46	9.49	9.09	15.02	11.86	10.67
	6	13.44	8.70	9.09	11.46	11.07	9.88	9.09	14.62	11.07	10.67

This table reports the proportions of days with jumps identified by the PDS-based test for 10 NYSE stocks in 2020. We use three pre-averaging windows $k_n = \lceil \theta\sqrt{N} \rceil$ with $\theta \in \{0.3, 0.4, 0.5\}$, different PDS barrier widths $c = K\sigma(\tilde{r}_i)$, i.e., the integer multiple of the standard deviation of pre-averaged returns, with K ranging from 4 to 6, and the censoring parameter $\epsilon = 0.05$. The total number of trading days is 253.

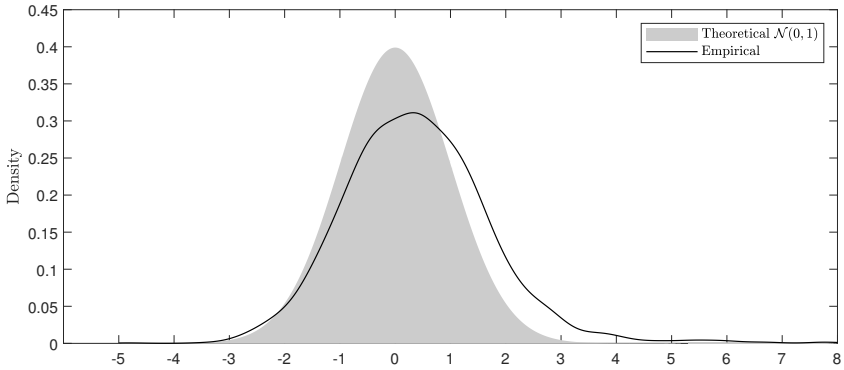

Figure 7: Testing results for selected NYSE stocks in 2020. We plot the empirical distribution of the standardized test statistic for all 2530 stock-day pairs and, for comparison, the simulated standard normal distribution (shaded area). We use the PDS barrier width $c = 4\sigma(\tilde{r}_i)$, the censoring parameter $\epsilon = 0.05$, and the pre-averaging window $k_n = \lceil \theta\sqrt{N} \rceil$ with $\theta = 0.3$, which corresponds to the first row in Table 7.

To eliminate spurious detections due to the multiple testing issue, Bajgrowicz et al. (2016) propose a formal treatment of the over-identification bias with double asymptotics when the jump tests are applied over a sample of many days. We apply their thresholding methods to our results: (i) the universal threshold $\sqrt{2\ln 253}$, and (ii) the threshold based on the false discovery rate (FDR).[16] The adjusted results of our test for all selected stocks are reported in Table 8. It is noteworthy that our testing results are fairly robust to the control of spurious detections, which underscores the empirical reliability of our PDS-based test.

The empirical results for alternative calendar-time-sampling-based and noise-robust tests—both with and without the control of spurious detections—are reported in Online Appendix B.4. We find that the outcomes of calendar-time-based tests vary substantially with the sampling frequency, whereas the noise-robust tests constructed from all available tick-level observations generally identify fewer days with jumps. Especially, the truncation-based detection method flags jumps on over 60% of trading days when returns are sampled every 30 seconds, which echoes the findings of Aït-Sahalia et al. (2025), but this proportion drops to about 20% when the data are down-sampled to 5-minute intervals. Our proposed test yields results comparable to certain noise-robust benchmarks—such as the ASJL test constructed from tick-level data—but exhibits superior robustness to the control of spurious detections.

6 Conclusions

This paper introduces a novel nonparametric high-frequency jump test for a discretely observed Itô semimartingale. Our approach utilizes a path-dependent sampling scheme for the tick-level

[16] For the vector of one-side test statistics $(S_1, S_2, \ldots, S_N)'$ which converge to i.i.d. standard normal random variables under the null, the universal threshold is $\sqrt{2\ln N}$ (Bajgrowicz et al., 2016). The data-adaptive FDR threshold is determined from the observed p-value distribution by the Benjamini–Hochberg procedure.

Table 8: Adjusted empirical rejection rates (%) for selected NYSE stocks

	k_n	$c/\sigma(\tilde{r}_i)$	AXP	BA	DIS	IBM	JNJ	JPM	MRK	MCD	PG	WMT
Panel A Universal threshold	$\theta = 0.3$	4	15.02	9.49	9.09	12.25	12.25	7.91	9.49	14.62	11.07	9.49
		5	13.83	9.88	8.70	11.07	10.28	8.30	9.09	14.62	9.88	8.70
		6	12.65	8.70	8.30	11.07	10.28	7.91	8.70	13.44	9.88	9.09
	$\theta = 0.4$	4	14.23	8.70	9.49	12.25	11.07	8.30	8.70	14.23	10.28	9.88
		5	13.44	8.70	8.70	11.46	11.07	8.30	8.30	13.83	9.88	9.09
		6	13.04	8.70	8.70	10.67	9.88	7.91	8.30	12.65	9.49	8.70
	$\theta = 0.5$	4	13.83	9.09	9.09	11.46	11.86	8.30	9.09	13.83	10.28	9.49
		5	12.65	8.30	9.09	11.07	10.28	7.51	7.91	13.44	9.88	8.70
		6	11.86	7.91	8.30	10.67	9.88	7.51	8.30	13.04	9.49	9.09
Panel B FDR threshold	$\theta = 0.3$	4	13.44	9.09	8.70	11.86	11.07	7.11	9.09	13.44	9.88	8.70
		5	12.65	9.49	8.70	11.07	9.88	7.51	8.70	13.44	9.09	8.30
		6	11.86	8.30	8.30	10.67	9.88	7.51	8.30	12.65	9.09	8.30
	$\theta = 0.4$	4	13.04	8.70	9.09	11.86	10.28	7.51	8.30	13.04	9.88	9.09
		5	12.25	8.30	8.30	11.07	10.67	7.51	8.30	12.65	9.09	8.70
		6	12.25	8.70	8.30	9.88	9.49	7.51	7.91	11.86	9.09	8.30
	$\theta = 0.5$	4	12.65	9.09	8.30	11.07	11.07	7.51	9.09	12.25	9.09	9.09
		5	11.46	7.91	8.70	10.67	9.49	7.11	7.91	12.25	9.09	7.91
		6	11.07	7.91	8.30	10.28	9.49	6.72	7.91	12.25	9.09	8.30

This table reports the proportions of days with jumps identified by the PDS-based test for 10 NYSE stocks in 2020, with the control of spurious detections using (i) the universal threshold and (ii) the FDR threshold of Bajgrowicz et al. (2016). We use three pre-averaging windows $k_n = \lceil \theta\sqrt{N} \rceil$ with $\theta \in \{0.3, 0.4, 0.5\}$, different PDS barrier widths $c = K\sigma(\tilde{r}_i)$, i.e., the integer multiple of the standard deviation of pre-averaged returns, with K ranging from 4 to 6, and the censoring parameter $\epsilon = 0.05$. The total number of trading days is 253.

price observations. The key intuition behind the construction of our test is that, different from a continuous price increase or decrease over a certain time interval, a discontinuous shift with a larger magnitude will always trigger an exit-time event and induce a disproportionately large threshold exceedance under infill asymptotics. Additionally, a two-step noise reduction technique is designed to alleviate the impact of weakly dependent market microstructure noise. Through extensive simulations, we validate the reliable finite-sample performance of our test under empirically realistic specifications for price observations, which is convincingly superior to a comprehensive collection of "classical" methods. The Monte Carlo results demonstrate that the performance of our test is robust to various aggregation levels and tuning parameter choices. An empirical analysis of NYSE-traded stocks provides strong statistical evidence for jumps across all selected stocks, and the results are robust to the correction of spurious detections. This methodology stands as the first exploration of the duration-based approach to test for jumps, which offers a robust and easy-to-implement tool for researchers and practitioners.

Acknowledgements

We thank the Co-Editor Torben Andersen, the Associate Editor, and two anonymous referees for their constructive comments and suggestions. We also thank Leopoldo Catania (discussant), Carsten Chong, Kim Christensen, Dobrislav Dobrev, Roxana Halbleib, Seok Young Hong, Aleksey Kolokolov, Sébastien Laurent, Manh Pham, Roberto Renò, George Tauchen, Stephen Taylor, Viktor Todorov,

Giovanni Urga, as well as participants at the CFE-CMStatistics 2020, 6th KoLaMaFr Workshop on Financial Econometrics, XXIII Workshop on Quantitative Finance, Conference on Intrinsic Time in Finance, Economics of Financial Technology Conference 2022, EcoSta 2022, QFFE 2022, IAAE 2022, Econometric Society Asian Meeting 2022, SoFiE 2022, AsianFA 2022, Workshop on Volatility, Jumps and Bursts, Econometric Society Australasian Meeting 2022, 25th Dynamic Econometrics Conference, and seminars at various institutions, for helpful comments and suggestions. Shifan Yu acknowledges financial support from the Economic and Social Research Council (ESRC) North West Social Science Doctoral Training Partnership (ES/P000665/1). The MATLAB code example can be founded at https://github.com/Shifan-Yu/Jumps_Endogenous_Sampling.

References

Aït-Sahalia, Y. and Jacod, J. (2009a). Estimating the degree of activity of jumps in high frequency data. *Annals of Statistics*, 37(5A):2202–2244.

Aït-Sahalia, Y. and Jacod, J. (2009b). Testing for jumps in a discretely observed process. *Annals of Statistics*, 37(1):184–222.

Aït-Sahalia, Y., Jacod, J., and Li, J. (2012). Testing for jumps in noisy high frequency data. *Journal of Econometrics*, 168(2):207–222.

Aït-Sahalia, Y. and Kimmel, R. (2007). Maximum likelihood estimation of stochastic volatility models. *Journal of Financial Economics*, 83(2):413–452.

Aït-Sahalia, Y., Li, C. X., and Li, C. (2025). So many jumps, so little news. Working Paper.

Aït-Sahalia, Y., Mykland, P. A., and Zhang, L. (2005). How often to sample a continuous-time process in the presence of market microstructure noise. *Review of Financial Studies*, 18(2):351–416.

Aït-Sahalia, Y., Mykland, P. A., and Zhang, L. (2011). Ultra high frequency volatility estimation with dependent microstructure noise. *Journal of Econometrics*, 160(1):160–175.

Aleti, S., Bollerslev, T., and Siggaard, M. (2025). Intraday market return predictability culled from the factor zoo. *Management Science*, forthcoming.

Andersen, T. G. and Bollerslev, T. (1997). Intraday periodicity and volatility persistence in financial markets. *Journal of Empirical Finance*, 4(2-3):115–158.

Andersen, T. G., Bollerslev, T., and Diebold, F. X. (2007a). Roughing it up: Including jump components in the measurement, modeling, and forecasting of return volatility. *Review of Economics and Statistics*, 89(4):701–720.

Andersen, T. G., Bollerslev, T., and Dobrev, D. (2007b). No-arbitrage semi-martingale restrictions for continuous-time volatility models subject to leverage effects, jumps and i.i.d. noise: Theory and testable distributional implications. *Journal of Econometrics*, 138(1):125–180.

Andersen, T. G., Bondarenko, O., Kyle, A. S., and Obizhaeva, A. A. (2018). Intraday trading invariance in the E-mini S&P 500 futures market. Working Paper.

Andersen, T. G., Dobrev, D., and Schaumburg, E. (2008). Duration-based volatility estimation. Working Paper.

Andersen, T. G., Dobrev, D., and Schaumburg, E. (2012). Jump-robust volatility estimation using nearest neighbor truncation. *Journal of Econometrics*, 169(1):75–93.

Andersen, T. G., Su, T., Todorov, V., and Zhang, Z. (2024). Intraday periodic volatility curves. *Journal of the American Statistical Association*, 119(546):1181–1191.

Andersen, T. G., Thyrsgaard, M., and Todorov, V. (2019). Time-varying periodicity in intraday volatility. *Journal of the American Statistical Association*, 114(528):1695–1707.

Asmussen, S. (2003). *Applied Probability and Queues*. Springer.

Bajgrowicz, P., Scaillet, O., and Treccani, A. (2016). Jumps in high-frequency data: Spurious detections, dynamics, and news. *Management Science*, 62(8):2198–2217.

Barndorff-Nielsen, O. E., Hansen, P. R., Lunde, A., and Shephard, N. (2009). Realized kernels in practice: Trades and quotes. *Econometrics Journal*, 12(3):1–32.

Barndorff-Nielsen, O. E. and Shephard, N. (2004). Power and bipower variation with stochastic volatility and jumps. *Journal of Financial Econometrics*, 2(1):1–37.

Barndorff-Nielsen, O. E. and Shephard, N. (2006). Econometrics of testing for jumps in financial economics using bipower variation. *Journal of Financial Econometrics*, 4(1):1–30.

Barndorff-Nielsen, O. E. and Shiryaev, A. N. (2015). *Change of Time and Change of Measure*. World Scientific Publishing.

Bibinger, M. and Winkelmann, L. (2015). Econometrics of co-jumps in high-frequency data with noise. *Journal of Econometrics*, 184(2):361–378.

Bollerslev, T., Li, S. Z., and Zhao, B. (2020). Good volatility, bad volatility, and the cross section of stock returns. *Journal of Financial and Quantitative Analysis*, 55(3):751–781.

Bollerslev, T., Todorov, V., and Xu, L. (2015). Tail risk premia and return predictability. *Journal of Financial Economics*, 118(1):113–134.

Borodin, A. N. and Salminen, P. (2002). *Handbook of Brownian Motion: Facts and Formulae*. Springer, Second edition.

Caporin, M., Kolokolov, A., and Renò, R. (2017). Systemic co-jumps. *Journal of Financial Economics*, 126(3):563–591.

Chernozhukov, V., Chetverikov, D., and Kato, K. (2013). Gaussian approximations and multiplier bootstrap for maxima of sums of high-dimensional random vectors. *Annals of Statistics*, 41(6):2786–2819.

Chernozhukov, V., Chetverikov, D., and Kato, K. (2019). Inference on causal and structural parameters using many moment inequalities. *Review of Economic Studies*, 86(5):1867–1900.

Christensen, K., Oomen, R., and Renò, R. (2022). The drift burst hypothesis. *Journal of Econometrics*, 227(2):461–497.

Corsi, F., Pirino, D., and Renò, R. (2010). Threshold bipower variation and the impact of jumps on volatility forecasting. *Journal of Econometrics*, 159(2):276–288.

Cremers, M., Halling, M., and Weinbaum, D. (2015). Aggregate jump and volatility risk in the cross-section of stock returns. *Journal of Finance*, 70(2):577–614.

Dimitriadis, T. and Halbleib, R. (2022). Realized quantiles. *Journal of Business & Economic Statistics*, 40(3):1346–1361.

Dumitru, A.-M. and Urga, G. (2012). Identifying jumps in financial assets: A comparison between nonparametric jump tests. *Journal of Business & Economic Statistics*, 30(2):242–255.

Durrett, R. (2019). *Probability: Theory and Examples*. Cambridge University Press, Fifth edition.

Engle, R. F. and Russell, J. R. (1998). Autoregressive conditional duration: A new model for irregularly spaced transaction data. *Econometrica*, 66(5):1127–1162.

Fan, J. and Yao, Q. (2003). *Nonlinear Time Series: Nonparametric and Parametric Methods*. Springer.

Feller, W. (1991). *An Introduction to Probability Theory and Its Applications, Volume 2*. John Wiley & Sons; Second edition.

Fukasawa, M. (2010). Realized volatility with stochastic sampling. *Stochastic Processes and their Applications*, 120(6):829–852.

Fukasawa, M. and Rosenbaum, M. (2012). Central limit theorems for realized volatility under hitting times of an irregular grid. *Stochastic Processes and their Applications*, 122(12):3901–3920.

Gerhard, F. and Hautsch, N. (2002). Volatility estimation on the basis of price intensities. *Journal of Empirical Finance*, 9(1):57–89.

Gloter, A. and Jacod, J. (2001). Diffusions with measurement errors. I. Local asymptotic normality. *ESAIM: Probability and Statistics*, 5:225–242.

Gut, A. (2009). *Stopped Random Walks: Limit Theorems and Applications*. Springer, Second edition.

Hansen, P. R. and Lunde, A. (2006). Realized variance and market microstructure noise. *Journal of Business & Economic Statistics*, 24(2):127–161.

Harris, L. (1986). A transaction data study of weekly and intradaily patterns in stock returns. *Journal of Financial Economics*, 16(1):99–117.

Hautsch, N. and Podolskij, M. (2013). Preaveraging-based estimation of quadratic variation in the presence of noise and jumps: Theory, implementation, and empirical evidence. *Journal of Business & Economic Statistics*, 31(2):165–183.

Hong, S. Y., Nolte, I., Taylor, S. J., and Zhao, X. (2023). Volatility estimation and forecasts based on price durations. *Journal of Financial Econometrics*, 21(1):106–144.

Huang, X. and Tauchen, G. (2005). The relative contribution of jumps to total price variance. *Journal of Financial Econometrics*, 3(4):456–499.

Ibragimov, I. A. (1962). Some limit theorems for stationary processes. *Theory of Probability & Its Applications*, 7(4):349–382.

Ibragimov, I. A. and Linnik, Y. V. (1971). *Independent and Stationary Sequences of Random Variables*. Wolters-Noordhoff.

Jacod, J. (1997). On continuous conditional Gaussian martingales and stable convergence in law. *Séminaire de probabilités de Strasbourg*, 31:232–246.

Jacod, J., Li, Y., Mykland, P. A., Podolskij, M., and Vetter, M. (2009). Microstructure noise in the continuous case: The pre-averaging approach. *Stochastic Processes and their Applications*, 119(7):2249–2276.

Jacod, J., Li, Y., and Zheng, X. (2017). Statistical properties of microstructure noise. *Econometrica*, 85(4):1133–1174.

Jacod, J., Li, Y., and Zheng, X. (2019). Estimating the integrated volatility with tick observations. *Journal of Econometrics*, 208(1):80–100.

Jacod, J. and Protter, P. (2012). *Discretization of Processes*. Springer.

Jacod, J. and Shiryaev, A. (2003). *Limit Theorems for Stochastic Processes*. Springer, Second edition.

Jiang, G. J. and Oomen, R. C. (2008). Testing for jumps when asset prices are observed with noise – a "swap variance" approach. *Journal of Econometrics*, 144(2):352–370.

Jiang, G. J. and Yao, T. (2013). Stock price jumps and cross-sectional return predictability. *Journal of Financial and Quantitative Analysis*, 48(5):1519–1544.

Jing, B.-Y., Kong, X.-B., Liu, Z., and Mykland, P. (2012). On the jump activity index for semimartingales. *Journal of Econometrics*, 166(2):213–223.

Khaniyev, T. and Kucuk, Z. (2004). Asymptotic expansions for the moments of the Gaussian random walk with two barriers. *Statistics & Probability Letters*, 69(1):91–103.

Koike, Y. (2017). Time endogeneity and an optimal weight function in pre-averaging covariance estimation. *Statistical Inference for Stochastic Processes*, 20(1):15–56.

Kolokolov, A. and Renò, R. (2024). Jumps or staleness? *Journal of Business & Economic Statistics*, 24(2):516–532.

Laurent, S. and Shi, S. (2020). Volatility estimation and jump detection for drift-diffusion processes. *Journal of Econometrics*, 217(2):259–290.

Lee, S. S. and Mykland, P. A. (2008). Jumps in financial markets: a new nonparametric test and jump dynamics. *Review of Financial Studies*, 21(6):2535–2563.

Lee, S. S. and Mykland, P. A. (2012). Jumps in equilibrium prices and market microstructure noise. *Journal of Econometrics*, 168(2):396–406.

Li, J. and Liu, Y. (2021). Efficient estimation of integrated volatility functionals under general volatility dynamics. *Econometric Theory*, 37(4):664–707.

Li, Y., Mykland, P. A., Renault, E., Zhang, L., and Zheng, X. (2014). Realized volatility when sampling times are possibly endogenous. *Econometric Theory*, 30(3):580–605.

Li, Z. M. and Linton, O. (2022). A ReMeDI for microstructure noise. *Econometrica*, 90(1):367–389.

Liu, L. Y., Patton, A. J., and Sheppard, K. (2015). Does anything beat 5-minute RV? a comparison of realized measures across multiple asset classes. *Journal of Econometrics*, 187(1):293–311.

Lorden, G. (1970). On excess over the boundary. *Annals of Mathematical Statistics*, 41(2):520–527.

Lotov, V. I. (1996). On some boundary crossing problems for Gaussian random walks. *Annals of Probability*, 24(4):2154–2171.

Mancini, C. (2009). Non-parametric threshold estimation for models with stochastic diffusion coefficient and jumps. *Scandinavian Journal of Statistics*, 36(2):270–296.

Maneesoonthorn, W., Martin, G. M., and Forbes, C. S. (2020). High-frequency jump tests: Which test should we use? *Journal of Econometrics*, 219(2):478–487.

Mykland, P. A. and Zhang, L. (2009). Inference for continuous semimartingales observed at high frequency. *Econometrica*, 77(5):1403–1445.

Nolte, I. and Xu, Q. (2015). The economic value of volatility timing with realized jumps. *Journal of Empirical Finance*, 34:45–59.

Pelger, M. (2020). Understanding systematic risk: A high-frequency approach. *Journal of Finance*, 75(4):2179–2220.

Podolskij, M. and Vetter, M. (2009). Bipower-type estimation in a noisy diffusion setting. *Stochastic Processes and their Applications*, 119(9):2803–2831.

Podolskij, M. and Vetter, M. (2010). Understanding limit theorems for semimartingales: A short survey. *Statistica Neerlandica*, 64(3):329–351.

Podolskij, M. and Ziggel, D. (2010). New tests for jumps in semimartingale models. *Statistical Inference for Stochastic Processes*, 13(1):15–41.

Potiron, Y. and Mykland, P. A. (2017). Estimation of integrated quadratic covariation with endogenous sampling times. *Journal of Econometrics*, 197(1):20–41.

Reiß, M. (2011). Asymptotic equivalence for inference on the volatility from noisy observations. *Annals of Statistics*, 39(2):772–802.

Rényi, A. (1963). On stable sequences of events. *Sankhyā, Series A*, 25(3):293–302.

Rogozin, B. A. (1964). On the distribution of the first jump. *Theory of Probability & Its Applications*, 9(3):450–465.

Shepp, L. A. (1967). A first passage problem for the Wiener process. *Annals of Mathematical Statistics*, 38(6):1912–1914.

Tse, Y.-K. and Yang, T. T. (2012). Estimation of high-frequency volatility: An autoregressive conditional duration approach. *Journal of Business & Economic Statistics*, 30(4):533–545.

Ubukata, M. and Oya, K. (2009). Estimation and testing for dependence in market microstructure noise. *Journal of Financial Econometrics*, 7(2):106–151.

Varneskov, R. T. (2017). Estimating the quadratic variation spectrum of noisy asset prices using generalized flat-top realized kernels. *Econometric Theory*, 33(6):1457–1501.

Vetter, M. and Zwingmann, T. (2017). A note on central limit theorems for quadratic variation in case of endogenous observation times. *Electronic Journal of Statistics*, 11(1):963–980.

Wood, R. A., McInish, T. H., and Ord, J. K. (1985). An investigation of transactions data for NYSE stocks. *Journal of Finance*, 40(3):723–739.

Wu, C.-F. J. (1986). Jackknife, bootstrap and other resampling methods in regression analysis. *Annals of Statistics*, 14(4):1261–1295.

Xiu, D. (2010). Quasi-maximum likelihood estimation of volatility with high frequency data. *Journal of Econometrics*, 159(1):235–250.

Yan, S. (2011). Jump risk, stock returns, and slope of implied volatility smile. *Journal of Financial Economics*, 99(1):216–233.

Zhang, L., Mykland, P. A., and Aït-Sahalia, Y. (2005). A tale of two time scales: Determining integrated volatility with noisy high-frequency data. *Journal of the American Statistical Association*, 100(472):1394–1411.

Zhou, B. (1996). High-frequency data and volatility in foreign-exchange rates. *Journal of Business & Economic Statistics*, 14(1):45–52.

Appendix A Proofs

A.1 Strong Approximation and Some Useful Lemmas

In this section, we establish a strong approximation result in the spirit of Chernozhukov et al. (2013, 2019), which couples the complicated observation scheme under Assumption 2 with the much simpler limiting observation scheme $(\check{t}_{n,i})$ in Remark 3. Unless specifically stated, we assume $X(\omega)$ to be continuous, i.e., $\omega \in \Omega'$.

In all the sequel, the positive constants K, K', K'' varies from line to line, but never depends on n, N, and $N^{(c)}$, and the various indices i, j. We use $\langle M, N\rangle$ to denote the quadratic covariation of M and N. When M and N are d- and r-dimensional, respectively, then $\langle M, N\rangle = (\langle M^i, N^j\rangle)_{1\le i\le d, 1\le j\le r}$ is a $(d \times r)$-dimensional process, and also $\langle M\rangle \equiv \langle M, M\rangle$.

Similar to the Assumption (S-HON) of Jacod et al. (2019), we impose the following stronger assumption without loss of generality by a classical localization procedure:

Assumption A.1. We have Assumptions 1 and 2 with $\tau_1 = \infty$. Moreover, the function δ and the processes μ, σ, λ, X are bounded, and we have $N \le K\Delta_n^{-1}$ and $\mathbb{E}[\Delta_{n,i}^p] \le K'\Delta_n^p$.

A.1.1 Intrinsic time. With an absolutely continuous time change from the calendar time t to intrinsic time $\tau(t)$:

$$t \to \tau(t) = \int_0^t \sigma_s^2 ds, \tag{A.1}$$

the intrinsic-time counterpart of X adapted to $(\mathcal{F}_t)_{t\ge 0}$ is

$$\widetilde{X}_{\tau(t)} = \widetilde{X}_0 + \int_0^{\tau(t)} \widetilde{\mu}_s ds + \widetilde{W}_{\tau(t)}, \tag{A.2}$$

where $\widetilde{\mu}$ is time-changed processes corresponding to μ in Eq. (1), and $\widetilde{W} = (\widetilde{W}_\tau)_{\tau\ge 0}$ is a Brownian motion evolving in intrinsic time. The relation $\widetilde{X}_{\tau(t)} = X_t$ holds for all t, and the τ-time process $\widetilde{X} = (\widetilde{X}_{\tau(t)})_{t\ge 0}$ is adapted to $(\widetilde{\mathcal{F}}_{\tau(t)})_{t\ge 0}$ with the τ-time σ-algebra satisfying $\widetilde{\mathcal{F}}_{\tau(t)} = \mathcal{F}_t$ (Lemma 1.2, Barndorff-Nielsen and Shiryaev, 2015). Particularly, when X is a calendar-time local martingale, $\widetilde{X}$ is an intrinsic-time Brownian motion (with an initial condition), which is implied by the Dambis-Dubins-Schwarz theorem. Following Mykland and Zhang (2009), the drift can be harmlessly assumed away, as the results on convergence in probability and stable convergence—established in Appendix A.3 and Appendix A.4, respectively—remain valid by a contiguity argument.

A.1.2 Observation schemes. We start with two sequences of observations of $X(\omega)$:

(I) Under Assumption 2: X_{t_i}, for all $i = 0, 1, 2, \ldots, N$,
(II) Equidistant observations in intrinsic time: $\widetilde{X}_{i\Delta_n}$, for all $i = 0, 1, 2, \ldots, N$.

For the ease of notation, we denote $t_i \equiv t_{n,i}$ under Assumption 2, and $\breve{t}_i \equiv \tau^{-1}(i\Delta_n)$. The increments between successive observations are denoted by

$$r_i = X_{t_i} - X_{t_{i-1}} \qquad \text{and} \qquad \breve{r}_i = X_{\breve{t}_i} - X_{\breve{t}_{i-1}}, \tag{A.3}$$

for all $i \in \{1, 2, \ldots, N\}$. Lemma A.1 of Jacod et al. (2017) indicates the sequence (I) is an $(\mathcal{F}_t^n)$-martingale with Gaussian increments. Different from the independent but not identically distributed increments r_i, the increments $\breve{r}_i$ are i.i.d. normal with zero mean and variance Δ_n, which make the sequence (II) a homogenous Gaussian random walk.

Remark A.1. We assume both sequences have the same number $N \equiv N_1^n$ of observations. Assumption A.1 and Eq. (6) indicate that $T = \tau^{-1}(N\Delta_n)$ is bounded and $T \xrightarrow{\mathbb{P}} 1$ as $n \to \infty$. Moreover, by the triangle inequality and law of iterated expectations, Assumption 2 further implies $\mathbb{E}[|N\Delta_n - \tau(1)|] \leq K\Delta_n$, hence $|T - 1| = O_p(\Delta_n)$. That being said, the probability of jump occurrence in the "differenced part" of observation interval is negligible; see more discussions in Section 2.3 of Aït-Sahalia and Jacod (2009b). To fix ideas, let $\delta \to 0$, then $\mathbb{P}(X_t'' \neq 0 \text{ for some } t \in [0, T] \triangle [0, 1]) \leq \mathbb{P}(|T-1| > \delta) + \mathbb{P}(X_t'' \neq 0 \text{ for some } t \in [1-\delta, 1+\delta]) = o(1)$, since we only assume potential jumps in $(0, 1)$.

For each sequence of observations, we conduct the PDS with the barrier width $c = m\sqrt{\Delta_n}$. We denote the PDS returns from each sequence of sampled observations by $(r_i^{(c)})_{i\in\{1,2,\ldots,N^{(c)}\}}$ and $(\breve{r}_i^{(c)})_{i\in\{1,2,\ldots,\breve{N}^{(c)}\}}$, respectively. Note that the PDS returns $\breve{r}_i^{(c)}$ are i.i.d., as implied by the strong Markov property of the Gaussian random walk (II) and the symmetric feature of the stopping rule in Eq. (7).

A.1.3 Strong Approximation. We define two supremum processes $(Y_j)_{1\leq j\leq N}$ and $(\breve{Y}_j)_{1\leq j\leq N}$:

$$Y_j = \sup_{1\leq i\leq j} |X_{t_i}| \qquad \text{and} \qquad \breve{Y}_j = \sup_{1\leq i\leq j} |X_{\breve{t}_i}|. \tag{A.4}$$

Lemma A.1. For any fixed $1 \leq j \leq N$, it holds for the supremum processes that

$$|Y_j - \breve{Y}_j| = O_p(j^2 \Delta_n^{1+\kappa/2} \sqrt{L_n}), \tag{A.5}$$

where for the ease of notation, $L_n \equiv \log N \asymp \log(\Delta_n^{-1})$.

Proof. Let $\mathcal{D}_n \equiv \sigma(\Delta_{n,1}, \Delta_{n,2}, \ldots)$ denote the σ-algebra generated by observation times. Note that by the triangle inequality of ℓ_∞-norm

$$\begin{aligned} |Y_j - \breve{Y}_j| &= \left| \max_{1\leq i\leq j} |X_{t_i}| - \max_{1\leq i\leq j} |X_{\breve{t}_i}| \right| \\ &\leq \max_{1\leq i\leq j} |X_{t_i} - X_{\breve{t}_i}|. \end{aligned} \tag{A.6}$$

Note that by definition, we have with probability approaching 1,

$$\begin{aligned} X_{t_i} - X_{\check{t}_i} &= \sum_{\ell=1}^{i} \left(\int_{t_{\ell-1}}^{t_\ell} \sigma_s dW_s - \int_{\check{t}_{\ell-1}}^{\check{t}_\ell} \sigma_s dW_s \right) \\ &= \sum_{\ell=1}^{i} \left(\sigma_{t_{\ell-1}} (W_{t_\ell} - W_{t_{\ell-1}}) - \sigma_{\check{t}_{\ell-1}} (W_{\check{t}_\ell} - W_{\check{t}_{\ell-1}}) \right) \\ &+ \sum_{\ell=1}^{i} \left(\int_{t_{\ell-1}}^{t_\ell} (\sigma_s - \sigma_{t_{\ell-1}}) dW_s - \int_{\check{t}_{\ell-1}}^{\check{t}_\ell} (\sigma_s - \sigma_{\check{t}_{\ell-1}}) dW_s \right) \\ &\equiv A_{n,i}^{(1)} + A_{n,i}^{(2)}. \end{aligned} \tag{A.7}$$

For the first term, by the maximal inequality of Gaussian variables, we have

$$\mathbb{E}\Big[\max_{1 \le i \le j} |A_{n,i}^{(1)}| \Big| \mathcal{D}_n \Big] \le K \sqrt{L_n \max_{1 \le i \le j} \Big| \sum_{\ell=1}^{i} (\Delta_{n,\ell} \lambda_{t_{\ell-1}} - \Delta_n) \Big|}. \tag{A.8}$$

For the right hand side, note that by the triangle inequality and Assumption 2 (ii),

$$\max_{1 \le i \le j} \Big| \sum_{\ell=1}^{i} \mathbb{E}\big[|\Delta_{n,\ell} \lambda_{t_{\ell-1}} - \Delta_n| \big| \mathcal{F}_{\ell-1}^n \big] \Big| \le K j \Delta_n^{2+\kappa}. \tag{A.9}$$

Combining Eq. (A.8) and Eq. (A.9), it follows the law of iterated expectation that

$$\max_{1 \le i \le j} |A_{n,i}^{(1)}| = O_p(j \Delta_n^{1+\kappa/2} \sqrt{L_n}). \tag{A.10}$$

For the second term in Eq. (A.7), by the maximal inequality, we have

$$\mathbb{E}\Big[\max_{1 \le i \le j} |A_{n,i}^{(2)}| \Big] \le K j \max_{1 \le i \le j} \mathbb{E}[|A_{n,i}^{(2)}|] \le K j^2 \Delta_n^{3/2+\kappa/2}, \tag{A.11}$$

where the last step is by the Burkholder-Davis-Gundy inequality and smoothness of σ regulated by Assumption 1 (ii). The proof of required statement is completed by the triangle inequality and Eqs. (A.6), (A.7), (A.10) and (A.11).

□

We consider the first sampled observation times for both sequences:

$$\Pi_1^{(c)} = \inf\{i : |X_{t_i} - X_0| \ge c\} \qquad \text{and} \qquad \breve{\Pi}_1^{(c)} = \inf\{i : |\widetilde{X}_{i\Delta_n} - \widetilde{X}_0| \ge c\}, \tag{A.12}$$

which means that the $\Pi_1^{(c)}$-th and the $\breve{\Pi}_1^{(c)}$-th observations in (I) and (II), respectively, are the first to breach the symmetric double barrier. Lemma A.2 indicates that the first exit times of both sequences coincide with probability approaching 1 under infill asymptotics.

Lemma A.2. For $c = m\sqrt{\Delta_n}$, let $\overline{N}^{(c)} \equiv N^{(c)} \wedge \breve{N}^{(c)}$.

(i) For all integer $p \geq 1$, $\mathbb{E}[(\breve{\Pi}_1^{(c)})^p] < \infty$.

(ii) The first exit times for both sequences (I) and (II) satisfy

$$\mathbb{P}\Big(\max_{1 \leq i \leq \overline{N}^{(c)}} |\Pi_i^{(c)} - \breve{\Pi}_i^{(c)}| \geq 1 \Big) \leq K \Delta_n^{\kappa/2} \sqrt{L_n}. \tag{A.13}$$

Proof. (i) Note that $\breve{\Pi}_1^{(c)}$ has the same distribution as the number of steps for a standard Gaussian random walk $(Z_i)_{i=1,2,\ldots}$ to exit the double barrier $(-m, m)$. Let $h = \inf\{\tau : \widetilde{W}_\tau \notin (-m, m)\}$ denote the first exit time of the time-changed Brownian motion $\widetilde{W}$ from $(-m, m)$, then it is clear that $\breve{\Pi}_1^{(c)} - 1 \leq h$ by the continuity of Brownian motion, thus $\mathbb{E}[(\breve{\Pi}_1^{(c)} - 1)^p] \leq \mathbb{E}[h^p]$ for all $p > 0$. The Laplace transform of h is well-known in the literature, see, e.g., Eq. (3.0.1) in Borodin and Salminen (2002): $\mathbb{E}[e^{-\lambda h}] = \cosh^{-1} \sqrt{2\lambda} m$, and its Maclaurin series implies that $\mathbb{E}[h^p] < \infty$ for all integer $p \geq 1$. This completes the proof.

(ii) We start from the first term. By definition, we have

$$\mathbb{P}(\Pi_1^{(c)} \geq k) = \mathbb{P}(Y_k \leq c) \quad \text{and} \quad \mathbb{P}(\breve{\Pi}_1^{(c)} \geq k) = \mathbb{P}(\breve{Y}_k \leq c). \tag{A.14}$$

Let $\epsilon > 0$ be a positive number that can be arbitrarily small but not depend on N, it follows Lemma A.1 and the Markov inequality that

$$\begin{aligned}
\mathbb{P}(\Pi_1^{(c)} - \breve{\Pi}_1^{(c)} \geq 1) &= \sum_{k=1}^{N} \mathbb{P}(\breve{\Pi}_1^{(c)} = k) \mathbb{P}(\Pi_1^{(c)} > k | \breve{\Pi}_1^{(c)} = k) \\
&\leq \sum_{k=1}^{N} \mathbb{P}(\breve{\Pi}_1^{(c)} = k) \mathbb{P}(\breve{Y}_k - Y_k > \epsilon) \\
&\leq K \Delta_n^{1+\kappa/2} \sqrt{L_n} \Big[\sum_{k=1}^{N} k^2 \mathbb{P}(\breve{\Pi}_1^{(c)} = k) \Big] \\
&\leq K \Delta_n^{1+\kappa/2} \sqrt{L_n},
\end{aligned} \tag{A.15}$$

where the last line uses $\sum_{k=1}^{N} k^2 \mathbb{P}(\breve{\Pi}_1^{(c)} = k) \leq \mathbb{E}[(\breve{\Pi}_1^{(c)})^2] \leq K$ by Lemma A.2 (i). Similarly, we can also show

$$\mathbb{P}(\breve{\Pi}_1^{(c)} - \Pi_1^{(c)} \geq 1) \leq K \Delta_n^{1+\kappa/2} \sqrt{L_n}. \tag{A.16}$$

Combining above results, we have

$$\mathbb{P}(|\Pi_1^{(c)} - \breve{\Pi}_1^{(c)}| \geq 1) \leq K \Delta_n^{1+\kappa/2} \sqrt{L_n}. \tag{A.17}$$

Now, note that for any $2 \le q \le \overline{N}^{(c)}$, we have

$$\begin{aligned}\mathbb{P}\Big(\max_{1\le i\le q}|\Pi_i^{(c)}-\breve{\Pi}_i^{(c)}|\ge 1\Big) \le \mathbb{P}\Big(\max_{1\le i\le q-1}|\Pi_i^{(c)}-\breve{\Pi}_i^{(c)}|\ge 1\Big) \\ + \mathbb{P}\big(|\Pi_q^{(c)}-\breve{\Pi}_q^{(c)}|\ge 1\big|\Pi_i^{(c)}=\breve{\Pi}_i^{(c)} \text{ for all } 1\le i\le q-1\big).\end{aligned} \tag{A.18}$$

By the renewal property, we have $\Pi_q^{(c)}-\breve{\Pi}_q^{(c)} \overset{\mathcal{L}}{=} \Pi_1^{(c)}-\breve{\Pi}_1^{(c)}$ conditional on $\Pi_i^{(c)}=\breve{\Pi}_i^{(c)}$ for all $1\le i\le q-1$. Therefore, using the same argument as in driving Eq. (A.17), we can show that the second term is bounded by $K\Delta_n^{1+\kappa/2}\sqrt{L_n}$. Applying the above argument recursively, we have

$$\begin{aligned}\mathbb{P}\Big(\max_{1\le i\le \overline{N}^{(c)}}|\Pi_i^{(c)}-\breve{\Pi}_i^{(c)}|\ge 1\Big) &\le K\overline{N}^{(c)}\Delta_n^{1+\kappa/2}\sqrt{L_n} \\ &\le K\Delta_n^{\kappa/2}\sqrt{L_n},\end{aligned} \tag{A.19}$$

for which we use $\overline{N}^{(c)} \asymp \Delta_n^{-1}$; see Lemma A.6 (ii). The proof is then completed. □

Lemma A.3. (Strong Approximation for Sampled Returns) It holds that

$$\mathbb{P}\Big(\max_{1\le i\le \overline{N}^{(c)}}|r_i^{(c)}-\breve{r}_i^{(c)}|>K\Delta_n^{1+\kappa/8}\Big)\le K'\Delta_n^{\kappa/8}\sqrt{L_n}. \tag{A.20}$$

Proof. It follows from the maximal inequality of Gaussian variables that

$$\mathbb{E}\Big[\max_{1\le i\le N}|r_i-\breve{r}_i|\Big|\mathcal{D}_n\Big]\le K\sqrt{L_n}\max_{1\le i\le N}\sqrt{\big|\mathbb{E}[\Delta_{n,i}\lambda_{t_{i-1}}|\mathcal{F}_{i-1}^n]-\Delta_n\big|}\le K\Delta_n^{1+\kappa/2}\sqrt{L_n}. \tag{A.21}$$

Let $E_n \equiv \{\Pi_i^{(c)}=\breve{\Pi}_i^{(c)} \text{ for all } 1\le i\le N^{(c)}=\breve{N}^{(c)}\}$, we have $\mathbb{P}(E_n^{\complement})\le K\Delta_n^{\kappa/2}\sqrt{L_n}$ by Lemma A.2 (ii). Note that by the maximal inequality, we have for any $p>1$,

$$\mathbb{E}\Big[\max_{1\le i\le \breve{N}^{(c)}}|\breve{\Pi}_i^{(c)}-\breve{\Pi}_{i-1}^{(c)}|^p\Big]\le \breve{N}^{(c)}\max_{1\le i\le \breve{N}^{(c)}}\mathbb{E}[|\breve{\Pi}_i^{(c)}-\breve{\Pi}_{i-1}^{(c)}|^p]\le K_p\Delta_n^{-1}, \tag{A.22}$$

where the last step is by Lemma A.2 (i). Taking $p>4/\kappa$ gives

$$\mathbb{E}\Big[\max_{1\le i\le \breve{N}^{(c)}}|\breve{\Pi}_i^{(c)}-\breve{\Pi}_{i-1}^{(c)}|^2\Big]\le K\Delta_n^{-\kappa/2}. \tag{A.23}$$

Moreover, by Cauchy-Schwarz inequality, we obtain

$$\begin{aligned}\mathbb{E}\Big[\max_{1\le i\le \breve{N}^{(c)}}|r_i^{(c)}-\breve{r}_i^{(c)}|\Big|E_n\Big] &\le \sqrt{\mathbb{E}\Big[\max_{1\le i\le \breve{N}^{(c)}}|\breve{\Pi}_i^{(c)}-\breve{\Pi}_{i-1}^{(c)}|^2\Big]\mathbb{E}\Big[\max_{1\le \ell\le n}|r_\ell-\breve{r}_\ell|^2\Big]} \\ &\le K\Delta_n^{1+\kappa/4}\sqrt{L_n}.\end{aligned} \tag{A.24}$$

Therefore, we have

$$\begin{aligned}
&\mathbb{P}\Big(\max_{1\le i\le \overline{N}^{(c)}} |r_i^{(c)} - \breve{r}_i^{(c)}| > K\Delta_n^{1+\kappa/8}\Big) \\
&\le \mathbb{P}\Big(\max_{1\le i\le \breve{N}^{(c)}} |r_i^{(c)} - \breve{r}_i^{(c)}| > K\Delta_n^{1+\kappa/8}\Big| E_n\Big) + \mathbb{P}(E_n^{\complement}) \qquad \text{(A.25)} \\
&\le K'(\Delta_n^{\kappa/8}\sqrt{L_n} + \Delta_n^{\kappa/2}\sqrt{L_n}).
\end{aligned}$$

This completes the proof.

□

Lemma A.3 shows the statistics constructed from sampled returns under observation schemes (I) and (II) are equivalent up to a $\Delta_n^{-1-\kappa/8}$ normalization, which is sufficient for the $c^{-1} \asymp \Delta_n^{-1/2}$ or $\sqrt{\breve{N}^{(c)}} \asymp \Delta_n^{-1/2}$ order in conventional CLT. The requirement is only $\kappa > 0$.

The above type of strong approximation results are similarly used in, e.g., the proof of Theorem 5.1 in Chernozhukov et al. (2013) and the proof of Theorem 4.3 in Chernozhukov et al. (2019). It allows us to focus on the limiting behavior of functionals of $(|\breve{r}_i^{(c)}|/c)^2$, the result can be sufficiently extended to those of $(|r_i^{(c)}|/c)^2$. To fix ideas, consider a possibly multi-dimensional Lipschitz function $f(\cdot)$. Suppose that

$$\frac{1}{\breve{N}^{(c)}}\sum_{i=1}^{\breve{N}^{(c)}} f\Big(\frac{(\breve{r}_i^{(c)})^2}{c^2}\Big) \xrightarrow{\mathbb{P}} \mu_f, \quad \text{and} \quad \frac{1}{\sqrt{\breve{N}^{(c)}}}\sum_{i=1}^{\breve{N}^{(c)}}\Big(f\Big(\frac{(\breve{r}_i^{(c)})^2}{c^2}\Big) - \mu_f\Big) \xrightarrow{\mathcal{L}} \mathcal{N}(0, \Sigma_f). \qquad \text{(A.26)}$$

Let $E_n' \equiv \{\Pi_i^{(c)} = \breve{\Pi}_i^{(c)} \text{ for all } 1 \le i \le \breve{N}^{(c)}\} \cap \{\max_{1\le i\le \breve{N}^{(c)}} |(r_i^{(c)})^2 - (\breve{r}_i^{(c)})^2|/c^2 > K\Delta_n^{1/2+\kappa/16}\}$. Note that $a^2 - b^2 = (a-b)^2 + 2b(a-b)$, it follows from triangle inequality that

$$\max_{1\le i\le \breve{N}^{(c)}} |(r_i^{(c)})^2 - (\breve{r}_i^{(c)})^2| \le \Big(\max_{1\le i\le \breve{N}^{(c)}} |r_i^{(c)} - \breve{r}_i^{(c)}|\Big)^2 + 2\Big(\max_{1\le i\le \breve{N}^{(c)}} |\breve{r}_i^{(c)}|\Big)\Big(\max_{1\le i\le \breve{N}^{(c)}} |r_i^{(c)} - \breve{r}_i^{(c)}|\Big). \qquad \text{(A.27)}$$

Note that $\max_{1\le i\le \breve{N}^{(c)}} |\breve{r}_i^{(c)}| = O_p(\Delta_n^{1/2}\sqrt{L_n}) = o_p(\Delta_n^{1/2-\kappa/16})$ by the maximal inequality of sub-Gaussian variables. Then it follows from Lemma A.2 (ii), A.3, and Eq. (A.27) that $\mathbb{P}(E_n') \ge 1 - K\Delta_n^{\kappa/8}\sqrt{L_n}$. Therefore, for each $\varepsilon > 0$,

$$
\begin{aligned}
&\mathbb{P}\Big(\Big\|\frac{1}{N^{(c)}}\sum_{i=1}^{N^{(c)}} f\Big(\frac{(r_i^{(c)})^2}{c^2}\Big)-\mu_f\Big\|>\varepsilon\Big)\\
&\le \mathbb{P}\Big(\Big\|\frac{1}{\breve{N}^{(c)}}\sum_{i=1}^{\breve{N}^{(c)}} f\Big(\frac{(\breve{r}_i^{(c)})^2}{c^2}\Big)-\mu_f\Big\|>\frac{\varepsilon}{2}\Big)+\mathbb{P}\Big(\Big\|\frac{1}{N^{(c)}}\sum_{i=1}^{N^{(c)}} f\Big(\frac{(r_i^{(c)})^2}{c^2}\Big)-\frac{1}{\breve{N}^{(c)}}\sum_{i=1}^{\breve{N}^{(c)}} f\Big(\frac{(\breve{r}_i^{(c)})^2}{c^2}\Big)\Big\|>\frac{\varepsilon}{2}\Big)\\
&\le \mathbb{P}\Big(\Big\|\frac{1}{\breve{N}^{(c)}}\sum_{i=1}^{\breve{N}^{(c)}} f\Big(\frac{(\breve{r}_i^{(c)})^2}{c^2}\Big)-\mu_f\Big\|>\frac{\varepsilon}{2}\Big)+\mathbb{P}\Big(K\max_{1\le i\le \breve{N}^{(c)}}\frac{|(r_i^{(c)})^2-(\breve{r}_i^{(c)})^2|}{c^2}>\frac{\varepsilon}{2}\Big|E_n'\Big)+\mathbb{P}(E_n'^{\complement})\\
&= \mathbb{P}\Big(\Big\|\frac{1}{\breve{N}^{(c)}}\sum_{i=1}^{\breve{N}^{(c)}} f\Big(\frac{(\breve{r}_i^{(c)})^2}{c^2}\Big)-\mu_f\Big\|>\frac{\varepsilon}{2}\Big)+K\Delta_n^{\kappa/8}\sqrt{L_n}.
\end{aligned}
\tag{A.28}
$$

Let $Z\sim\mathcal{N}(0,\Sigma_f)$. For each $A\subset\mathbb{R}^{\dim(f)}$ and $\varepsilon>0$, let $A^\varepsilon\equiv\{x\in\mathbb{R}^{\dim(f)}:\inf_{y\in A}\|x-y\|\le\varepsilon\}$ denote the ε-enlargement of A, then we have

$$
\begin{aligned}
&\mathbb{P}\Big(\frac{1}{\sqrt{N^{(c)}}}\sum_{i=1}^{N^{(c)}}\Big(f\Big(\frac{(r_i^{(c)})^2}{c^2}\Big)-\mu_f\Big)\in A\Big)\\
&\le \mathbb{P}\Big(\frac{1}{\sqrt{\breve{N}^{(c)}}}\sum_{i=1}^{\breve{N}^{(c)}}\Big(f\Big(\frac{(\breve{r}_i^{(c)})^2}{c^2}\Big)-\mu_f\Big)\in A^\varepsilon\Big)+\mathbb{P}\Big(\Big\|\frac{1}{\sqrt{N^{(c)}}}\sum_{i=1}^{N^{(c)}} f\Big(\frac{(r_i^{(c)})^2}{c^2}\Big)-\frac{1}{\sqrt{\breve{N}^{(c)}}}\sum_{i=1}^{\breve{N}^{(c)}} f\Big(\frac{(\breve{r}_i^{(c)})^2}{c^2}\Big)\Big\|>\varepsilon\Big)\\
&\le \mathbb{P}\Big(\frac{1}{\sqrt{\breve{N}^{(c)}}}\sum_{i=1}^{\breve{N}^{(c)}}\Big(f\Big(\frac{(\breve{r}_i^{(c)})^2}{c^2}\Big)-\mu_f\Big)\in A^\varepsilon\Big)+\mathbb{P}\Big(K\sqrt{\breve{N}^{(c)}}\max_{1\le i\le \breve{N}^{(c)}}\frac{|(r_i^{(c)})^2-(\breve{r}_i^{(c)})^2|}{c^2}>\varepsilon\Big|E_n'\Big)+\mathbb{P}(E_n'^{\complement})\\
&= \mathbb{P}(Z\in A)+\mathbb{P}(Z\in A^\varepsilon\setminus A)+K\Delta_n^{\kappa/8}\sqrt{L_n}.
\end{aligned}
\tag{A.29}
$$

Taking $\varepsilon\to 0$, the right-hand side becomes $\mathbb{P}(Z\in A)+o(1)$. Similarly, one can show

$$
\mathbb{P}\Big(\frac{1}{\sqrt{N^{(c)}}}\sum_{i=1}^{N^{(c)}}\Big(f\Big(\frac{(r_i^{(c)})^2}{c^2}\Big)-\mu_f\Big)\in A\Big)\ge\mathbb{P}(Z\in A)-o(1),
\tag{A.30}
$$

which is the desired result.

A.1.4 Impact of Small Jumps. Under Assumption 1, we consider the jump component of X in the following form, which is valid as the jumps are of finite variation:

$$
X_t''=\int_0^t\int_{\mathbb{R}}\delta(s,x)\underline{p}(ds,dx),
\tag{A.31}
$$

where $\delta(\omega, t, x)$ on $\Omega \times \mathbb{R}_+ \times \mathbb{R}$ is predictable, $\underline{p}(dt, dx)$ is a Poisson random measure on $\mathbb{R}_+ \times \mathbb{R}$ with a compensator $\underline{q}(dt, dx) = dt \otimes \lambda(dx)$, and λ is a σ-finite measure on $\mathbb{R}_+$. Moreover, we have

$$\lim_{u \to 0^+} u^r \int_{\{|f_m| \geq u\}} \lambda(dx) \leq \int_{\{|f_m| \geq u\}} |f_m|^r \lambda(dx) < \infty, \tag{A.32}$$

which implies, as $u \to 0$,

$$\lambda(\{x : |f_m(x)| \geq u\}) \equiv \int_{\{|f_m| \geq u\}} \lambda(dx) = O(u^{-r}). \tag{A.33}$$

We split the jumps into "big" and "small" ones by selecting a sequence (u_n) of positive real numbers satisfying:

$$\frac{u_n}{\sqrt{\Delta_n}} \to \infty \qquad \text{and} \qquad u_n \Delta_n^{\beta - 1/2} \to 0, \tag{A.34}$$

for any $0 < \beta \leq 1/2$. Then we rewrite the Itô semimartingale $X = X' + X''$ in Eq. (1) as:

$$X_t = X'_t + \underbrace{\int_0^t \int_{\{|\delta(s,x)| \geq u_n\}} \delta(s, x) \underline{p}(ds, dx)}_{\text{"Big" Jumps: } J^n_{1,t}} + \underbrace{\int_0^t \int_{\{|\delta(s,x)| < u_n\}} \delta(s, x) \underline{p}(ds, dx)}_{\text{"Small" Jumps: } J^n_{2,t}}, \tag{A.35}$$

where the component X'' is partitioned into two n-dependent processes J^n_1 and J^n_2. This "optimal" cutoff level $u_n \asymp \Delta_n^{\varpi}$ with ϖ arbitrarily close to but below $1/2$ separates all jumps that either prevail over or are diluted within Brownian increments.

Next, we show that the existence of small jumps in J^n_2 has no impact on Lemma A.1.

Lemma A.4. For the purely discontinuous process J^n_2 defined in Eq. (A.35), with the sequence (u_n) of thresholds satisfying Eq. (A.34), it holds that for all $p \geq 1$,

$$\sup_{t_{i-1} \leq s \leq t_i} |J^n_{2,s} - J^n_{2,t_{i-1}}|^p = O_p(\Delta_n u_n^{p-r}). \tag{A.36}$$

Proof. Following Assumption A.1, we have Assumption 1 (v) with $\tau_1 = \infty$ without loss of generality by a standard localization procedure, such that $|\delta(\omega, t, x)| \wedge 1 \leq f(x)$ holds uniformly on $\Omega \times \mathbb{R}_+ \times \mathbb{R}$. We start with the notation for a local p-th order variation of small jumps, which resembles the first quantity in Eq. (2.1.35) of Jacod and Protter (2012):

For some $p \geq 1$, we define

$$\widehat{\delta}_{p,i} = \frac{1}{t_i - t_{i-1}} \int_{t_{i-1}}^{t_i} ds \int_{\{|\delta(s,x)| < u_n\}} |\delta(s, x)|^p \lambda(dx). \tag{A.37}$$

For all $1 \le i \le n$, it holds that

$$\begin{aligned}
\mathbb{E}[\widehat{\delta}_{p,i}|\mathcal{F}_{t_{i-1}}] &\le \frac{1}{t_i - t_{i-1}}\mathbb{E}\left[\int_{t_{i-1}}^{t_i} ds \int_{\{|\delta(s,x)|<u_n\}} |\delta(s,x)|^p \lambda(dx)\middle|\mathcal{F}_{t_{i-1}}\right] \\
&\le \frac{1}{t_i - t_{i-1}}\mathbb{E}\left[\int_{t_{i-1}}^{t_i} ds \int_{\{|\delta(s,x)|<u_n\}} u_n^{p-r}|\delta(s,x)|^r \lambda(dx)\middle|\mathcal{F}_{t_{i-1}}\right] \\
&\le u_n^{p-r}\int_{\mathbb{R}} |f(x)|^r \lambda(dx),
\end{aligned} \tag{A.38}$$

since $\delta(\omega,t,x)$ is bounded by the deterministic function $f(x)$, and $t_i - t_{i-1}$ is independent of $\mathcal{F}_{t_{i-1}}$. Denote the integral as a constant $C_r = \int_{\mathbb{R}} |f(x)|^r \lambda(dx)$, we have

$$\mathbb{E}[\widehat{\delta}_{p,i}|\mathcal{F}_{t_{i-1}}] \le C_r u_n^{p-r}. \tag{A.39}$$

Similarly, for another conditional expectation $\mathbb{E}[\widehat{\delta}^p_{1,i}|\mathcal{F}_{t_{i-1}}]$, we have

$$\begin{aligned}
\mathbb{E}[\widehat{\delta}^p_{1,i}|\mathcal{F}_{t_{i-1}}] &= \frac{1}{(t_i - t_{i-1})^p}\mathbb{E}\left[\left(\int_{t_{i-1}}^{t_i} ds \int_{\{|\delta(s,x)|<u_n\}} |\delta(s,x)|\lambda(dx)\right)^p\middle|\mathcal{F}_{t_{i-1}}\right] \\
&\le \frac{1}{(t_i - t_{i-1})^p}\mathbb{E}\left[\left(\int_{t_{i-1}}^{t_i} ds \int_{\{|\delta(s,x)|<u_n\}} u_n^{1-r}|\delta(s,x)|^r\lambda(dx)\right)^p\middle|\mathcal{F}_{t_{i-1}}\right] \\
&\le u_n^{p(1-r)}\left(\int_{\mathbb{R}} |f(x)|^r\lambda(dx)\right)^p \\
&\le C_r^p u_n^{p(1-r)}.
\end{aligned} \tag{A.40}$$

Then by Lemma 2.1.7 of Jacod and Protter (2012), with the bounds for both $\mathbb{E}[\widehat{\delta}_{p,i}|\mathcal{F}_{t_{i-1}}]$ and $\mathbb{E}[\widehat{\delta}^p_{1,i}|\mathcal{F}_{t_{i-1}}]$ in Eqs. (A.39) and (A.40), respectively, we have for all $p \ge 1$,

$$\begin{aligned}
\mathbb{E}\left[\sup_{t_{i-1}\le s\le t_i} |J^n_{2,s} - J^n_{2,t_{i-1}}|^p\middle|\mathcal{F}_{t_{i-1}}\right] &\le K\left(\Delta_n\mathbb{E}[\widehat{\delta}_{p,i}|\mathcal{F}_{t_{i-1}}] + \Delta_n^p\mathbb{E}[\widehat{\delta}^p_{1,i}|\mathcal{F}_{t_{i-1}}]\right) \\
&\le K\left(C_r\Delta_n u_n^{p-r} + C_r^p\Delta_n^p u_n^{p(1-r)}\right) \\
&\le K'\Delta_n u_n^{p-r},
\end{aligned} \tag{A.41}$$

where the latter term $KC_r^p\Delta_n^p u_n^{p(1-r)}$ reduces to $K'\Delta_n u_n^{p-r}$ since $1 < 1+\varpi(p-r) < p < p+p\varpi(1-r)$ for some ϖ slightly smaller than $1/2$. The desired result in Lemma A.4 follows from the law of iterated expectation and Markov's inequality. □

To examine the impact of small jumps on Lemma A.1, we rewrite the supremum processes into

$$Y_j = \sup_{1\le i\le j} |X'_{t_i} + J^n_{2,t_i}| \qquad \text{and} \qquad \breve{Y}_j = \sup_{1\le i\le j} |X'_{\breve{t}_i}|. \tag{A.42}$$

In this case, by the triangle inequality, we have

$$|Y_j - \breve{Y}_j| = \Big|\max_{1\le i\le j}|X'_{t_i} + J^n_{2,t_i}| - \max_{1\le i\le j}|X'_{\breve{t}_i}|\Big| \le \max_{1\le i\le j}|X'_{t_i} - X'_{\breve{t}_i}| + \max_{1\le i\le j}|J^n_{2,t_i}|, \tag{A.43}$$

where, by Lemma A.4,

$$\max_{1\le i\le j}|J^n_{2,t_i}| \le \sum_{i=1}^{j}\sup_{(i-1)\Delta_n\le s\le i\Delta_n}|J^n_{2,s} - J^n_{2,(i-1)\Delta_n}| = O_p(j\Delta_n u_n^{1-r}). \tag{A.44}$$

For some $0 < \kappa < 1 - r$ such that $\kappa/2(1-r) \le \varpi < 1/2$, we have $\max_{1\le i\le j}|J^n_{2,t_i}| = O_p(j\Delta_n^{1+\kappa/2})$. Therefore, for any fixed $1 \le j \le N$, the small jumps in J^n_2 do not affect Lemma A.1 and any subsequent results in Appendix A.1.3.

A.2 Properties of Functions $h_2(m)$ and $\overline{h}_{2,\epsilon}(m)$

In this section, we prove some properties of the functions $h_2(\cdot)$ and $\overline{h}_{2,\epsilon}(\cdot)$ defined in Eq. (10), which are important for the construction of our test statistic.

Proposition 2. The functions $h_2(\cdot)$ and $\overline{h}_{2,\epsilon}(\cdot)$ are invertible and differentiable with nonvanishing derivatives.

Proof. For the standard Gaussian random walk Z, let $\Pi_1^{(m)} \equiv \min\{n \ge 1 : |Z_n| > m\}$ be the first passage time across $\pm m$, then by definition $Z_1^{(m)} = Z_{\Pi_1^{(m)}}$. We start with $h_{2,\epsilon}(\cdot)$, it follows Fubini's theorem that

$$\begin{aligned}\overline{h}_{2,\epsilon}(m) &= \mathbb{E}\left[\frac{|Z_1^{(m)}|^2}{m^2} \wedge (1+\epsilon)^2\right] = \int_0^{(1+\epsilon)^2}\mathbb{P}(|Z_1^{(m)}| > m\sqrt{u})du \\ &= 1 + 2\int_0^{\epsilon}(1+v)\mathbb{P}\big(|Z_1^{(m)}| > m(1+v)\big)dv,\end{aligned} \tag{A.45}$$

where the second line is by a change of variable $u = (1+v)^2$, and the fact that $\mathbb{P}\big(|Z_1^{(m)}| > m(1+v)\big) = 1$ for $v \in [-1, 0)$. Note that for fixed $v > 0$, $\mathbb{P}\big(|Z_1^{(m)}| > m(1+v)\big)$ is strictly decreasing in m, since for a larger m the annulus $\big(m, m(1+v)\big)$ becomes wider hence it is less likely that a Gaussian increment makes Z first exit $\pm m$ also clear $\pm m(1+v)$. Therefore, $\overline{h}_{2,\epsilon}(\cdot)$ is also strictly decreasing, the invertibility readily follows.

The differentiability relies on an integral representation of tail probability using renewal identity. Let $(H_n)_{n\ge1}$ denote the strong ascending ladder heights, with F_H its distribution. By the standard Wiener–Hopf renewal representation for ladder heights (see Chapter XVIII.3 in Feller, 1991), F_H is absolutely continuous with density $f_H(x) = \int_{[0,\infty)}\varphi(x+y)U^-(dy)$ where U^- is the descending ladder height renewal measure. Further denote U_m^+ the renewal measure killed upon hitting $-m$, i.e., $U_m^+(E) \equiv \sum_{n\ge0}\mathbb{P}\big(\sum_{i=1}^n H_i \in E, \tau_m < \tau_{-m}\big)$ for Borel E. Then by symmetry and the renewal

identity (see, e.g., Section 2.6 in Gut, 2009),

$$\mathbb{P}\big(|Z_1^{(m)}| > m(1+v)\big) = 2\int_{[0,m]} \big[1 - F_H\big(m(1+v) - x\big)\big] U_m^+(dx) \equiv \phi_v(m). \tag{A.46}$$

Note that U_m^+ has an atom $U_m^+(\{0\}) = \mathbb{P}(\tau_m < \tau_{-m}) = \frac{1}{2}$, by Theorem VII.1.1 in Asmussen (2003), it admits Stone's decomposition on compact sets, i.e., $U_m^+(dx) = \frac{1}{2}\delta_0(dx) + u_m^+(x)dx$ for a bounded continuous density $u_m^+(\cdot)$. It follows Leibniz rule that

$$\phi_v'(m) = 2\bigg[u_m^+(m)\big(1 - F_H(mv)\big) - (1+v)\int_{[0,m]} f_H\big(m(1+v) - x\big) U_m^+(dx)\bigg], \tag{A.47}$$

where we use the fact that $\partial_m U_m^+$ vanishes except for the boundary $x = m$. Combining Eqs. (A.45) and (A.47) gives the differentiability and $\overline{h}_{2,\epsilon}'(m) = 2\int_0^\epsilon (1+v)\phi_v'(m)dv$ which is strictly negative for $m > 0$ and $\epsilon > 0$.

We now turn to $h_2(\cdot)$. Taking $\epsilon \to \infty$ in Eq. (A.45) yields

$$h_2(m) = 1 + 2\int_0^\infty (1+v)\phi_v(m)dv. \tag{A.48}$$

Since for Gaussian increments, the tails of ladder height $1 - F_H(\cdot)$ are exponentially small, by Eq. (A.46) we have $\phi_v(m) \le 2U_m^+([0,m])\big(1 - F_H(mv)\big) \le K_m \exp\{-Kv^2m^2\}$. Therefore, $\int_0^\infty 2(1+v)\phi_v(m)dv$ is finite. The rest of the proof follows the similar argument as $\overline{h}_{2,\epsilon}(\cdot)$ and dominated convergence.

□

A.3 Proof of Theorem 1

Following the strong approximation results in Appendix A.1.3, it suffices to consider the limit theorems of the test statistics constructed from $(\breve{r}_i^{(c)})_{1 \le i \le \breve{N}^{(c)}}$. For ease of notation, we drop the breve mark ($\breve{}$) in the subsequent proofs.

Under the null. We shall prove the following three convergence results under $\omega \in \Omega'$:

$$\sum_{i=1}^{N^{(c)}} (r_i^{(c)})^2 \xrightarrow{\mathbb{P}} \tau(1), \qquad \sum_{i=1}^{N^{(c)}} (\overline{r}_i^{(c)})^2 \xrightarrow{\mathbb{P}} \tau(1)\frac{\overline{h}_{2,\epsilon}(m)}{h_2(m)}, \qquad c^2 N^{(c)} \xrightarrow{\mathbb{P}} \frac{\tau(1)}{h_2(m)}. \tag{A.49}$$

To verify these results over the unit interval in Eq. (A.49), we establish a more general result on uniform convergence in probability (u.c.p.). Specifically, for any processes Z^n and Z, where n indexes the stages of statistical experiments, we say that Z^n converges uniformly in probability to Z on compact sets, written as $Z^n \xrightarrow{\text{u.c.p.}} Z$, if and only if $\sup_{0 \le t \le T} |Z_t^n - Z_t| \xrightarrow{\mathbb{P}} 0$ for all finite $T > 0$.

We start with some notation for clarity: Let $N_{n,t}^{(c)}$ denote the number of sampled observations with the barrier width c_n over $[0,t]$ at stage n. Let $\tau_{n,i}^{(c)} = \tau(t_{n,\Pi_{n,i}^{(c)}})$ denote the intrinsic time (defined

in Appendix A.1.1) at the i-th sampled observation, and $\Delta\tau_{n,i}^{(c)} = \tau_{n,i}^{(c)} - \tau_{n,i-1}^{(c)}$ the i-th duration in intrinsic time. We define the discretized filtration $\mathbb{F}^n = (\mathcal{F}^n_{N_{n,t}^{(c)}+1})_{t\geq 0}$, where $\mathcal{F}_i^n = \mathcal{F}_{t_{n,\Pi_{n,i}^{(c)}}} = \widetilde{\mathcal{F}}_{\tau_{n,i}^{(c)}}$.

Lemma A.5 extends Wald's identity to sums of independent, non-negative, and potentially non-identically distributed random variables. Lemma A.6 establishes some properties of the sequence $(\Delta\tau_{n,i}^{(c)})$, the sampled returns $(r_{n,i}^{(c)})$, and the counting process $(N_{n,t}^{(c)})$. Lemma A.7 provides some results for the discretized filtration $\mathbb{F}^n$ that will be used in subsequent proofs.

Lemma A.5. Let $S_n = \sum_{i=1}^n X_i$, where $(X_i)_{i\geq 1}$ is a sequence of independent, non-negative random variables satisfying $\mathbb{E}[X_i] \leq C$ for all i. Suppose that N is an integer-valued stopping time with respect to the filtration $\mathcal{G}_i = \sigma(X_1, \ldots, X_i)$. Then the expectation of the stopped sum satisfies the bound $\mathbb{E}[S_N] \leq C\mathbb{E}[N]$.

Proof. It holds that

$$\mathbb{E}[S_N] = \mathbb{E}\left[\sum_{i=1}^{\infty} X_i \mathbb{1}_{\{i\leq N\}}\right] = \sum_{i=1}^{\infty} \mathbb{E}[X_i \mathbb{1}_{\{i\leq N\}}] = \sum_{i=1}^{\infty} \mathbb{E}[X_i]\mathbb{E}[\mathbb{1}_{\{i\leq N\}}] \leq C\sum_{i=1}^{\infty} \mathbb{P}(N \geq i) = C\mathbb{E}[N], \tag{A.50}$$

where the interchange of infinite sum and expectation is valid by Tonelli's theorem since all the summands are non-negative. This completes the proof of Lemma A.5. □

Lemma A.6. For any finite $t > 0$, it holds that

(i) $\mathbb{E}[r_{n,i}^{(c)}] = 0$, and $\mathbb{E}[(r_{n,i}^{(c)})^2] = c_n^2 h_2(m)$;
(ii) $\mathbb{E}[N_{n,t}^{(c)} + 1] \leq Kc_n^{-2}$;
(iii) $\max_{1\leq i\leq N_{n,t}^{(c)}+1} \Delta\tau_{n,i}^{(c)} = o_p(c_n)$;
(iv) $\mathbb{E}[\Delta\tau_{n,i}^{(c)} r_{n,i}^{(c)} | \mathcal{F}_{i-1}^n] = 0$ for all i and n.

Proof. (i) Since $\mathbb{E}[\tau_{n,1}^{(c)}] < \infty$, the claims follow from Theorem 1 of Shepp (1967).

(ii) We express $\mathbb{E}[N_{n,t}^{(c)}]$ as an infinite sum of probabilities related to $\Delta\tau_{n,i}^{(c)}$:

$$\mathbb{E}[N_{n,t}^{(c)}] = \sum_{k=1}^{\infty} \mathbb{P}(N_{n,t}^{(c)} \geq k) = \sum_{k=1}^{\infty} \mathbb{P}\left(\sum_{i=1}^{k} \Delta\tau_{n,i}^{(c)} \leq \tau(t)\right). \tag{A.51}$$

By the Markov property of $\widetilde{X}$, the sequence $(\Delta\tau_{n,i}^{(c)})$ consists of positively-valued, conditionally independent random variables for each n, which satisfy $\Delta\tau_{n,i}^{(c)} \overset{\mathcal{L}}{=} c_n^2 \Delta t_i^n$, where (Δt_i^n) is a sequence of i.i.d. random variables, representing the durations for a standard Gaussian random walk to exit the double barrier $(-1, 1)$. Specifically, $\Delta t_i^n = \Delta_n(\Pi_{n,i}^{(1)} - \Pi_{n,i-1}^{(1)})$, where $\Pi_{n,i}^{(1)}$ denote the number of steps to breach the barrier for the i-th time. Therefore, for some constant $K > 0$, we obtain the bound:

$$\sum_{k=1}^{\infty} \mathbb{P}\left(\sum_{i=1}^{k} \Delta\tau_{n,i}^{(c)} \leq \tau(t)\right) \leq \sum_{k=1}^{\infty} \mathbb{P}\left(\sum_{i=1}^{k} \Delta t_i^n \leq Kc_n^{-2}\right) = \mathbb{E}[\mathbb{N}^{(1)}_{n,Kc_n^{-2}}], \tag{A.52}$$

where

$$\mathtt{N}_{n,t}^{(1)} = \sum_{k=1}^{\infty} \mathbb{1}_{\{\sum_{i=1}^{k} \Delta t_i^n \le t\}} \tag{A.53}$$

is a counting process associated with the standard Gaussian random walk. Next we show that $\mathbb{E}[\mathtt{N}^{(1)}_{n,Kc_n^{-2}}] \le Kc_n^{-2}$. Following an approach similar to the proof of the elementary renewal theorem (see, e.g., Theorem 4.1, Gut, 2009), we censor the durations Δt_i^n for some $a > 0$:

$$\Delta \bar{t}_i^n = \begin{cases} \Delta t_i^n, & t_i^n \le a, \\ a, & t_i^n > a, \end{cases} \tag{A.54}$$

and consider another renewal process with the sequence of durations $(\Delta \bar{t}_i^n)$, and the corresponding counting process

$$\overline{\mathtt{N}}_{n,t}^{(1)} = \sum_{k=1}^{\infty} \mathbb{1}_{\{\sum_{i=1}^{k} \Delta \bar{t}_i^n \le t\}}, \tag{A.55}$$

which satisfies

$$\mathbb{E}[\mathtt{N}_{n,t}^{(1)}] \le \mathbb{E}[\overline{\mathtt{N}}_{n,t}^{(1)}], \tag{A.56}$$

for all $t > 0$. Note that $\overline{\mathtt{N}}_{n,t}^{(1)}$ is not a stopping time (with respect to the renewal process), while $\overline{\mathtt{N}}_{n,t}^{(1)} + 1$ is a stopping time for all $t > 0$; see details in Section 2.3 of Gut (2009). Moreover, for any $a > 0$ and $t > 0$, we have $\sum_{i=1}^{\overline{\mathtt{N}}_{n,t}^{(1)}+1} \Delta \bar{t}_i^n \le t + a$. For large enough n such that $Kc_n^{-2} > 1$, take $t = Kc_n^{-2}$ and by Wald's identity, we have

$$\mathbb{E}\left[\sum_{i=1}^{\overline{\mathtt{N}}^{(1)}_{n,Kc_n^{-2}}+1} \Delta \bar{t}_i^n\right] = \mathbb{E}[\Delta \bar{t}_i^n]\mathbb{E}\big[\overline{\mathtt{N}}^{(1)}_{n,Kc_n^{-2}} + 1\big] + \underbrace{a'}_{O(1)} \le Kc_n^{-2} + a' \quad \Rightarrow \quad \mathbb{E}\big[\overline{\mathtt{N}}^{(1)}_{n,Kc_n^{-2}} + 1\big] \le Kc_n^{-2}. \tag{A.57}$$

Therefore, it follows from Eqs. (A.51), (A.52), (A.56) and (A.57) that $\mathbb{E}[N_{n,t}^{(c)} + 1] \le Kc_n^{-2}$.

(iii) By the maximal inequality, Lemma A.5, and Lemma A.6 (ii), it holds that for some $p > 1$,

$$\mathbb{E}\left[\left(\max_{1 \le i \le N_{n,t}^{(c)}+1} \Delta \tau_{n,i}^{(c)}\right)^p\right] \le \mathbb{E}\left[\sum_{i=1}^{N_{n,t}^{(c)}+1} (\Delta \tau_{n,i}^{(c)})^p\right] \le Kc_n^{2p}\mathbb{E}[N_{n,t}^{(c)} + 1] \le Kc_n^{2p-2}. \tag{A.58}$$

Then, by Markov's and Jensen's inequalities, for any $\delta > 0$,

$$\mathbb{P}\left(\max_{1 \le i \le N_{n,t}^{(c)}+1} \Delta \tau_{n,i}^{(c)} \ge \delta\right) \le K\mathbb{E}\left[\left(\max_{1 \le i \le N_{n,t}^{(c)}+1} \Delta \tau_{n,i}^{(c)}\right)^p\right]^{1/p} \le Kc_n^{2-2/p} = o(c_n). \tag{A.59}$$

(iv) By the Markov property of $\widetilde{X}$, it suffices to show that $\mathbb{E}[\tau_{n,1}^{(c)} \widetilde{X}_{\tau_{n,1}^{(c)}}] = 0$. To justify this result intuitively, we appeal to the reflection principle of Brownian motion. It states that for any sample path of $\widetilde{X}$ stopped at $\widetilde{X}_{\tau_{n,1}^{(c)}}$, there exists a corresponding mirrored path where the process evolves

identically up to $\tau_{n,1}^{(c)}$, but with the final position flipped, i.e., $-\widetilde{X}_{\tau_{n,1}^{(c)}}$. As a result, the distribution of $\widetilde{X}_{\tau_{n,1}^{(c)}}$ conditional on $\tau_{n,1}^{(c)}$ is symmetric about zero, which yields $\mathbb{E}[\widetilde{X}_{\tau_{n,1}^{(c)}}|\tau_{n,1}^{(c)}] = 0$, and hence $\mathbb{E}[\tau_{n,1}^{(c)}\widetilde{X}_{\tau_{n,1}^{(c)}}] = 0$ by the law of iterated expectations.

This completes the proof of Lemma A.6.

□

Lemma A.7. The following results hold for each n:

(i) For a $\mathbb{F}$-martingale M, if M is bounded or square-integrable with $\langle M\rangle_t < Ct$ almost surely for some $C < \infty$, then its discretized version $M(n)$ with $M(n)_t = M_{T_n(t)}$ is an $\mathbb{F}^n$-martingale, where $T_n(t) = t_{n,\Pi_{n,i'}^{(c)}}$ with $i' = N_{n,t}^{(c)} + 1$ represents the first sampling time after t.

(ii) The process $\sum_{i=1}^{N_{n,t}^{(c)}+1}(\Delta\tau_{n,i}^{(c)} - h_2(m)c_n^2)$ is an $\mathbb{F}^n$-martingale.

Proof. (i) Note that $N_{n,t}^{(c)} + 1 = \inf\{i \geq 1 : \tau_{n,i}^{(c)} > t\}$ is an $\mathbb{F}^n$-stopping time. For some finite $\overline{T} > 0$, it holds that $M_{T_n(t)\wedge\overline{T}}$ is a discrete-time $\mathbb{F}^n$-martingale by optional stopping. For $0 \leq s \leq t$, since $N_s^{(c)} + 1 \leq N_t^{(c)} + 1$ are both stopping times, the optional sampling theorem implies that

$$\mathbb{E}\left[M_{T_n(t)\wedge\overline{T}}\middle|\mathcal{F}^n_{N_{n,s}^{(c)}+1}\right] = M_{T_n(s)\wedge\overline{T}}. \tag{A.60}$$

To obtain the desired result $\mathbb{E}[M_{T_n(t)}|\mathcal{F}^n_{N_{n,s}^{(c)}+1}] = M_{T_n(s)}$, it remains to prove $\mathbb{E}[|M_{T_n(t)} - M_{T_n(t)\wedge\overline{T}}|] \to 0$ as $\overline{T} \to \infty$.

If M is bounded, then

$$|M_{T_n(t)} - M_{T_n(t)\wedge\overline{T}}| \leq 2\left(\sup_{0\leq s\leq T_n(t)}|M_s|\right)\mathbb{1}_{\{T_n(t)>\overline{T}\}}, \tag{A.61}$$

and the desired result is directly implied by $\mathbb{1}_{\{T_n(t)>\overline{T}\}} \to 0$ as $\overline{T} \to \infty$.

If M is square-integrable with $\langle M\rangle_t < Ct$, it holds that

$$\mathbb{E}[|M_{T_n(t)} - M_{T_n(t)\wedge\overline{T}}|^2] = \mathbb{E}[|\langle M\rangle_{T_n(t)} - \langle M\rangle_{T_n(t)\wedge\overline{T}}|] < C\mathbb{E}[T_n(t)\mathbb{1}_{\{T_n(t)>\overline{T}\}}]. \tag{A.62}$$

Note that $T_n(t) \leq t + \max_{1\leq i\leq N_{n,t}^{(c)}+1}\Delta t_{n,i}^{(c)}$, where $\Delta t_{n,i}^{(c)}$ is the i-th calendar time duration under PDS. By the smoothness of σ under Assumption 1, Lemma A.5, and Lemma A.6 (iii),

$$\mathbb{E}\left[\max_{1\leq i\leq N_{n,t}^{(c)}+1}\Delta t_{n,i}^{(c)}\right] \leq K\mathbb{E}\left[\max_{1\leq i\leq N_{n,t}^{(c)}+1}\Delta\tau_{n,i}^{(c)}\right] \leq K\mathbb{E}\left[\sum_{i=1}^{N_{n,t}^{(c)}+1}\Delta\tau_{n,i}^{(c)}\right] \leq K'c_n\mathbb{E}[N_{n,t}^{(c)} + 1] < \infty, \tag{A.63}$$

such that $\mathbb{E}[T_n(t)] < \infty$, and $\lim_{\overline{T}\to\infty}\mathbb{E}[T_n(t)\mathbb{1}_{\{T_n(t)>\overline{T}\}}] = 0$ by the dominated convergence theorem. Then the desired result follows from Eq. (A.62).

(ii) By the Markov property in intrinsic time and the first-exit scaling, it holds that $c_n^{-2}\Delta\tau_{n,i}^{(c)} \overset{\mathcal{L}}{=} m^{-2}(Z_1^{(m)})^2$ with $\mathbb{E}[m^{-2}(Z_1^{(m)})^2] = h_2(m)$, and thus $\mathbb{E}[\Delta\tau_{n,i}^{(c)}|\mathcal{F}_{i-1}^n] = h_2(m)c_n^2$. Therefore, $M_{n,k} =$

$\sum_{i=1}^{k}(\Delta\tau_{n,i}^{(c)} - h_2(m)c_n^2)$ is a discrete-time martingale with respect to $\mathcal{F}^n$. For any fixed $n > 0$, the stopping time $\mathbb{E}[N_{n,t}^{(c)} + 1] < \infty$ by Lemma A.6 (ii), and $\mathbb{E}\big[|M_{n,i} - M_{n,i-1}|\big|\mathcal{F}_{i-1}^n\big] \le \mathbb{E}[\Delta\tau_{n,i}^{(c)}|\mathcal{F}_{i-1}^n] + h_2(m)c_n^2 = 2h_2(m)c_n^2 \le K$, such that the optional sampling theorem implies that

$$\mathbb{E}\Big[M_{n,N_{n,t}^{(c)}+1}\Big|\mathcal{F}^n_{N_{n,s}^{(c)}+1}\Big] = M_{n,N_{n,s}^{(c)}+1}, \tag{A.64}$$

for $0 \le s \le t$. Therefore, $(M_{n,N_{n,t}^{(c)}+1})$ is a discrete-time martingale with respect to $\mathbb{F}^n = (\mathcal{F}^n_{N_{n,t}^{(c)}+1})_{t\ge 0}$.

This completes the proof of Lemma A.7. □

Next, we define the following three scaled processes at stage n:

$$V_{1,t}^n = \sum_{i=1}^{N_{n,t}^{(c)}} \zeta_1 (r_{n,i}^{(c)})^2, \qquad V_{2,t}^n = \sum_{i=1}^{N_{n,t}^{(c)}} \zeta_2 (\overline{r}_{n,i}^{(c)})^2, \qquad V_{3,t}^n = \zeta_3 c_n^2 N_{n,t}^{(c)}, \tag{A.65}$$

where the scaling factors are given by $(\zeta_1, \zeta_2, \zeta_3) = (1, h_2(m)/\overline{h}_{2,\epsilon}(m), h_2(m))$. Our goal is to show that for each $k = 1, 2, 3$, the process V_k^n satisfies $V_k^n \xrightarrow{\text{u.c.p.}} \tau = (\tau(t))_{t\ge 0}$. To establish this, it suffices to show that for any $T > 0$,

$$\sup_{t\in[0,T]} |V_{k,t}^n - \tau(t)| = O_p(c_n). \tag{A.66}$$

We begin by proving (A.66) for V_3^n: Define an auxiliary pre-limiting process $U_t^n = \sum_{i=1}^{N_{n,t}^{(c)}} \Delta\tau_{n,i}^{(c)}$. By the triangle inequality,

$$\sup_{t\in[0,T]} |V_{3,t}^n - \tau(t)| \le \sup_{t\in[0,T]} |V_{3,t}^n - U_t^n| + \sup_{t\in[0,T]} |U_t^n - \tau(t)|. \tag{A.67}$$

For the first supremum, we have

$$\sup_{t\in[0,T]} |V_{3,t}^n - U_t^n| = \sup_{t\in[0,T]} \left|\sum_{i=1}^{N_{n,t}^{(c)}} (\zeta_3 c_n^2 - \Delta\tau_{n,i}^{(c)})\right| \le K \sup_{t\in[0,T]} \left|\sum_{i=1}^{N_{n,t}^{(c)}+1} (\zeta_3 c_n^2 - \Delta\tau_{n,i}^{(c)})\right|, \tag{A.68}$$

where the inequality holds because adding one more term to the sum cannot decrease the supremum of the process. By Lemma A.6 (iii), it holds that $\mathbb{E}[(\zeta_3 c_n^2 - \Delta\tau_{n,i}^{(c)})^2] \le K c_n^4$. Note that $\sum_{i=1}^{N_{n,t}^{(c)}+1}(\zeta_3 c_n^2 - \Delta\tau_{n,i}^{(c)})$ is an $\mathbb{F}^n$-martingale, i.e., Lemma A.7 (ii). Applying the Burkholder-Davis-Gundy inequality, Lemma A.5, and Lemma A.6 (ii), we have

$$\mathbb{E}\left[\sup_{t\in[0,T]} \left|\sum_{i=1}^{N_{n,t}^{(c)}+1} (\zeta_3 c_n^2 - \Delta\tau_{n,i}^{(c)})\right|^2\right] \le K\mathbb{E}\left[\sum_{i=1}^{N_{n,t}^{(c)}+1} (\zeta_3 c_n^2 - \Delta\tau_{n,i}^{(c)})^2\right] \le K' c_n^4 \mathbb{E}[N_{n,t}^{(c)}] \le K'' c_n^2. \tag{A.69}$$

Then, by Markov's and Jensen's inequalities, for any $\delta > 0$,

$$\mathbb{P}\left(\sup_{t\in[0,T]} \left| \sum_{i=1}^{N_{n,t}^{(c)}+1} (\zeta_3 c_n^2 - \Delta\tau_{n,i}^{(c)}) \right| > \delta \right) \leq \frac{1}{\delta}\mathbb{E}\left[\sup_{t\in[0,T]} \left| \sum_{i=1}^{N_{n,t}^{(c)}+1} (\zeta_3 c_n^2 - \Delta\tau_{n,i}^{(c)}) \right|^2 \right]^{1/2} \leq K c_n, \tag{A.70}$$

which shows that $\sup_{t\in[0,T]} |V_{3,t}^n - U_t^n| = O_p(c_n)$.

For the second term, we have

$$\sup_{t\in[0,T]} |U_t^n - \tau(t)| = \sup_{t\in[0,T]} \left| \tau_{N_{n,t}^{(c)}}^n - \tau(t) \right| \leq K \max_{1\leq i\leq N_{n,t}^{(c)}+1} \Delta\tau_{n,i}^{(c)} = o_p(c_n), \tag{A.71}$$

where the final equation follows from Lemma A.6 (iii). Combining Eqs. (A.68) and (A.71), we conclude that the u.c.p. result in Eq. (A.66) holds for V_3^n.

To prove the u.c.p. result for V_1^n, we write the corresponding supremum process into:

$$\sup_{t\in[0,T]} |V_{1,t}^n - \tau(t)| \leq \sup_{t\in[0,T]} |V_{1,t}^n - V_{3,t}^n| + \sup_{t\in[0,T]} |V_{3,t}^n - \tau(t)|, \tag{A.72}$$

thus it suffices to prove that

$$\sup_{t\in[0,T]} |V_{1,t}^n - V_{3,t}^n| = \sup_{t\in[0,T]} \left| \sum_{i=1}^{N_{n,t}^{(c)}} ((r_{n,i}^{(c)})^2 - \zeta_3 c_n^2) \right| \leq K \sup_{t\in[0,T]} \left| \sum_{i=1}^{N_{n,t}^{(c)}+1} ((r_{n,i}^{(c)})^2 - \zeta_3 c_n^2) \right| = O_p(c_n). \tag{A.73}$$

With a similar martingale argument as for V_3^n (Lemma A.7 (ii)), and $\mathbb{E}\big[\big((r_{n,i}^{(c)})^2 - \zeta_3 c_n^2\big)^2\big] \leq K c_n^4$ implied by the Burkholder-Davis-Gundy inequality, we have

$$\mathbb{E}\left[\sup_{t\in[0,T]} \left| \sum_{i=1}^{N_{n,t}^{(c)}+1} ((r_{n,i}^{(c)})^2 - \zeta_3 c_n^2) \right|^2 \right] \leq K\mathbb{E}\left[\sum_{i=1}^{N_{n,t}^{(c)}+1} ((r_{n,i}^{(c)})^2 - \zeta_3 c_n^2)^2 \right] \leq K' c_n^4 \mathbb{E}[N_{n,t}^{(c)}] \leq K'' c_n^2. \tag{A.74}$$

and then, similarly to Eq. (A.70), we conclude that Eq. (A.73), and thus the u.c.p. result in Eq. (A.66), holds for V_1^n. Moreover, the u.c.p. result for V_2^n can be verified with the same steps, and thus omitted here.

Since the u.c.p. results in Eq. (A.66) hold for all three processes V_1^n, V_2^n, and V_3^n, it follows that the three limits in Eq. (A.49) also hold uniformly over the unit interval, such that

$$\frac{\sum_{i=1}^{N^{(c)}} (r_i^{(c)})^2}{c^2 N^{(c)}} \xrightarrow{\mathbb{P}} h_2(m) \quad \text{and} \quad \frac{\sum_{i=1}^{N^{(c)}} (\overline{r}_i^{(c)})^2}{c^2 N^{(c)}} \xrightarrow{\mathbb{P}} \overline{h}_{2,\epsilon}(m). \tag{A.75}$$

The consistency of both $\overline{M}_{c,\epsilon}$ and M_c in Theorem 1 is a direct result from Eq. (A.75) and the continuous mapping theorem.

Under the alternative. We denote by (Λ_t^n) the counting process of all jumps in J_1^n in Eq. (A.35), then Λ_t^n is bounded for each n, and for all n, we have

$$\sum_{0\le s\le t} |\Delta J_{1,s}^n|^r < \infty, \qquad \text{where } \Delta J_{1,s}^n = J_{1,s}^n - J_{1,s^-}^n, \tag{A.76}$$

which implies for large enough n (such that $u_n \to 0$),

$$u_n^r \Lambda_t^n \le \sum_{0\le s\le t} |\Delta J_{1,s}^n|^r < \infty, \tag{A.77}$$

with u_n defined in Appendix A.1.4. From Eq. (A.77), we deduce that $\Lambda_t^n = O_p(\Delta_n^{-r\varpi})$ for all fixed t, where ϖ is arbitrarily close to but below $1/2$.

When $X(\omega)$ is discontinuous within $(0,1)$, we denote by $\{s_1, s_2 \ldots, s_\Lambda\}$ the sequence of all jump times in chronological order, where $\Lambda \equiv \Lambda_1^n(\omega)$ counts the number of all jumps on $(0,1]$. We define

$$k^-(s) = \inf_{0\le i\le n} \{t_i \ge s : |t_i - s|\} \quad \text{and} \quad k^+(s) = \inf_{0\le i\le n} \{t_i < s : |t_i - s|\} \tag{A.78}$$

as the index of the first observations no earlier than and strictly before s, respectively. We split the sequence of observations $(X_{t_i})_{0\le i\le N}$ into $\Lambda+1$ segments with $i = k^+(s_j)$ for all $1 \le j \le \Lambda$ as cutoff points. As $N \to \infty$, we have $k^+(s_j) - k^+(s_{j-1}) \to \infty$ (also, $k^+(s_1) \to \infty$), since any intervals of length of order Δ_n mostly contain a single jump of size larger than u_n, see Section 2.3 of Aït-Sahalia and Jacod (2009b).

For each segment $(X_{t_i})_{k^+(s_{j-1})\le i\le k^+(s_j)}$, we obtain the PDS returns $(r_i^{(c)})_{N_{j-1}^{(c)}+1\le i\le N_j^{(c)}}$ with the barrier width $c = m\sqrt{\Delta_n}$. For each $i \in A_n = \{N_1^{(c)}, N_2^{(c)}, \ldots, N_\Lambda^{(c)}\}$, the PDS return $|r_i^{(c)}| \ge u_n \gg c$ contains jumps and will be censored by $\varphi_\epsilon(c)$. For all $i \in A_n^{\complement}$, the PDS return $r_i^{(c)}$ contains only aggregated Brownian increments. For the censored PDS returns, we have

$$\frac{\sum_{i=1}^{N^{(c)}} (\overline{r}_i^{(c)})^2}{c^2 N^{(c)}} = \frac{\sum_{i\in A_n^{\complement}} (\overline{r}_i^{(c)})^2}{c^2 N^{(c)}} + \frac{\sum_{i\in A_n} (\overline{r}_i^{(c)})^2}{c^2 N^{(c)}}. \tag{A.79}$$

For the first term above, since the cardinality of A_n is $\Lambda = O_p(\Delta_n^{-r\varpi}) \ll \Delta_n^{-1} \asymp N^{(c)}$, we have

$$\frac{\sum_{i\in A_n^{\complement}} (\overline{r}_i^{(c)})^2}{c^2 N^{(c)}} = \frac{N^{(c)} - \Lambda}{N^{(c)}} \frac{\sum_{i\in A_n^{\complement}} (\overline{r}_i^{(c)})^2}{c^2 (N^{(c)} - \Lambda)}, \quad \text{where } \frac{N^{(c)} - \Lambda}{N^{(c)}} \xrightarrow{\mathbb{P}} 1, \tag{A.80}$$

such that it coincides with the limit theorems under the null. For the second term, it holds that

$$\frac{\sum_{i\in A_n} (\overline{r}_i^{(c)})^2}{c^2 N^{(c)}} \le K \frac{\Lambda}{N^{(c)}} \le K' \Delta_n^{1-r\varpi}, \tag{A.81}$$

which has no impact on the LLN result. It still vanishes after multiplying by $\sqrt{N^{(c)}} \asymp \Delta_n^{-1/2}$ for any $r \in [0,1)$, and thus does not affect the CLT.

Consider the PDS returns. Under infill asymptotics, we claim that

$$\sum_{i=1}^{N^{(c)}}(r_i^{(c)})^2=\sum_{i\in A_n^{\complement}}(r_i^{(c)})^2+\sum_{i\in A_n}(r_i^{(c)})^2\xrightarrow{\mathbb{P}}\tau(1)+\sum_{0<s\leq 1}|\Delta J_{1,s}^n|^2, \tag{A.82}$$

where the jump variation is given by

$$\sum_{0<s\leq 1}|\Delta J_{1,s}^n|^2=\int_0^1 ds\int_{\{|\delta(s,x)|\geq u_n\}}|\delta(s,x)|^2\lambda(dx). \tag{A.83}$$

The convergence $\sum_{i\in A_n^{\complement}}(r_i^{(c)})^2\xrightarrow{\mathbb{P}}\tau(1)$ is a direct result from Eq. (A.49), with the cardinality of $A_n^{\complement}$, $N^{(c)}-\Lambda$, satisfying Eq. (A.80). For the PDS returns with $i\in A_n$, we have

$$\sum_{i\in A_n}|r_i^{(c)}|^2-\sum_{0<s\leq 1}|\Delta J_{1,s}|^2\leq\sum_{i\in A_n}||r_i^{(c)}|^2-|\Delta_i J_1^n|^2|, \tag{A.84}$$

where $\Delta_i J_1^n=J_{1,t_{\Pi_i^{(c)}}}^n-J_{1,t_{\Pi_i^{(c)}-1}}^n$. For all $i\in A_n$, it holds that

$$|r_i^{(c)}|\leq\left|\sum_{i=\Pi_{i-1}^{(c)}}^{\Pi_i^{(c)}}(X'_{t_i}-X'_{t_{i-1}})\right|+|\Delta_i J_1^n|+\left|\sum_{i=\Pi_{i-1}^{(c)}}^{\Pi_i^{(c)}}(J_{2,t_i}^n-J_{2,t_i-1}^n)\right|, \tag{A.85}$$

such that

$$||r_i^{(c)}|^2-|\Delta_i J_1^n|^2|\leq(|r_i^{(c)}|+|\Delta_i J_1^n|)\left(\left|\sum_{i=\Pi_{i-1}^{(c)}}^{\Pi_i^{(c)}}(X'_{t_i}-X'_{t_{i-1}})\right|+\left|\sum_{i=\Pi_{i-1}^{(c)}}^{\Pi_i^{(c)}}(J_{2,t_i}^n-J_{2,t_i-1}^n)\right|\right)=O_p(\sqrt{\Delta_n}), \tag{A.86}$$

where, by Lemma A.5 and Lemma A.2 (i),

$$\mathbb{E}\left[\left|\sum_{i=\Pi_{i-1}^{(c)}}^{\Pi_i^{(c)}}(X'_{t_i}-X'_{t_{i-1}})\right|\right]\leq\mathbb{E}\left[\sum_{i=\Pi_{i-1}^{(c)}}^{\Pi_i^{(c)}}|X'_{t_i}-X'_{t_{i-1}}|\right]\leq\mathbb{E}[\Pi_1^{(c)}]\max_{1\leq i\leq N}\mathbb{E}[|X'_{t_i}-X'_{t_{i-1}}|]\leq K\sqrt{\Delta_n}, \tag{A.87}$$

and, by Lemma A.4,

$$\begin{aligned}\mathbb{E}\left[\left|\sum_{i=\Pi_{i-1}^{(c)}}^{\Pi_i^{(c)}}(J_{2,t_i}^n-J_{2,t_i-1}^n)\right|\right]&\leq\mathbb{E}\left[\sum_{i=\Pi_{i-1}^{(c)}}^{\Pi_i^{(c)}}|J_{2,t_i}^n-J_{2,t_i-1}^n|\right]\leq\mathbb{E}[\Pi_1^{(c)}]\max_{1\leq i\leq N}\mathbb{E}[|J_{2,t_i}^n-J_{2,t_i-1}^n|]\\&\leq\mathbb{E}[\Pi_1^{(c)}]\max_{1\leq i\leq N}\mathbb{E}\left[\sup_{t_{i-1}\leq s\leq t_i}|J_{2,s}^n-J_{2,t_{i-1}}^n|\right]\leq K\Delta_n^{1+(1-r)\varpi}.\end{aligned} \tag{A.88}$$

Therefore, we have

$$\sum_{i\in A_n} |r_i^{(c)}|^2 - \sum_{0<s\leq 1} |\Delta J_{1,s}|^2 \leq \sum_{i\in A_n} ||r_i^{(c)}|^2 - |\Delta_i J_1^n|^2| = O_p(\Delta_n^{1/2-r\varpi}) = o_p(1), \tag{A.89}$$

which implies the convergence of $\sum_{i\in A_n}(r_i^{(c)})^2$ and thus Eq. (A.82), such that it holds that

$$\frac{\sum_{i=1}^{N^{(c)}}(r_i^{(c)})^2}{c^2 N^{(c)}} \xrightarrow{\mathbb{P}} \frac{h_2(m)\langle X,X\rangle_1}{\tau(1)}. \tag{A.90}$$

This completes the proof.

A.4 Proof of Theorem 2

We start with some definitions and notation for clarity in the proof: We follow the design of statistical experiments in the proof of Theorem 1 (Appendix A.3), where $N_{n,t}^{(c)}$ counts the number of sampled observations with the barrier width c_n over $[0,t]$ at stage n, and we define a sequence $(U_{n,i}^{(c)})$ of random variables as scaled intrinsic-time durations, i.e., $U_{n,i}^{(c)} = c_n^{-2}\Delta\tau_{n,i}^{(c)}$.

By Wald's identity, we have $\mathbb{E}[U_{n,i}^{(c)}] = m^{-2}\mathbb{E}[|Z_1^{(m)}|^2] = h_2(m)$ and $\mathbb{E}[(U_{n,i}^{(c)})^2] = h_4(m)$. For simplicity, we denote the scaled cross moments of $U_{n,i}^{(c)}$ with the squared censored and uncensored PDS returns as $\overline{\lambda}(m) = c_n^{-2}\mathbb{E}[U_{n,i}^{(c)}(\overline{r}_{n,i}^{(c)})^2]$ and $\lambda(m) = c_n^{-2}\mathbb{E}[U_{n,i}^{(c)}(r_{n,i}^{(c)})^2]$, respectively. Additionally, we denote the scaled cross moment between the squared censored and uncensored PDS returns as $\overline{\lambda}_r(m) = c_n^{-2}\mathbb{E}[(r_{n,i}^{(c)})^2(\overline{r}_{n,i}^{(c)})^2] = m^{-4}\overline{\rho}_{2,\epsilon}(m)$.

Stable convergence. We state a key theorem from Jacod (1997) to establish $\mathcal{F}$-stable convergence for a sequence of local martingales.[17] We say that Z^n converges $\mathcal{F}$-stably in law to Z, written as $Z^n \xrightarrow{\mathcal{L}-s} Z$, if for all $\mathcal{F}$-measurable processes Y, we have the joint convergence $(Z^n, Y) \xrightarrow{\mathcal{L}} (Z, Y)$; see more details in Rényi (1963) and Jacod and Protter (2012).

We start with the general setting of Jacod (1997): Let X be a continuous-time local martingale on $(\Omega, \mathcal{F}, \mathbb{F} = (\mathcal{F}_t)_{t\geq 0}, \mathbb{P})$, and denote by $\mathcal{M}_b$ the set of all bounded martingales on the same basis. A sequence of filtrations $\mathbb{F}^n = (\mathcal{F}_t^n)_{t\geq 0}$ on $(\Omega, \mathcal{F})$ is said to satisfy Property (F) if the following conditions hold for each $n \in \mathbb{N}$:

Property (F). We have a square-integrable $\mathbb{F}^n$-martingale $X(n)$ and, for each $Z \in \mathcal{M}_b$, a bounded $\mathbb{F}^n$-martingale $Z(n)$, such that for all $t \geq 0$,

(i) $\sup_{n,t,\omega} |Z(n)_t(\omega)| < \infty$;
(ii) $\langle X(n)\rangle_t \xrightarrow{\mathbb{P}} \langle X\rangle_t$;
(iii) For any finite family $(Z^1, \ldots, Z^m) \subset \mathcal{M}_b$, we have the following convergence for the Skorokhod

[17] See also Chapter IX.7 of Jacod and Shiryaev (2003).

topology on $\mathbb{D}(\mathbb{R}^{d+m})$:

$$(X(n), Z^1(n), \ldots, Z^m(n)) \xrightarrow{\mathbb{P}} (X, Z^1, \ldots, Z^m). \tag{A.91}$$

The following theorem is a simplified version of Theorem IX.7.13 of Jacod and Shiryaev (2003):

Theorem A.1. Assume Property (F). Let H^n denote a sequence of square-integrable $\mathbb{F}^n$-local martingales, and let ΔH^n collects all jumps of H^n. Suppose that there is a C_∞-valued adapted process η starting from zero, such that for all $Z \in \mathcal{M}_b$ orthogonal to X, we have for all $t \geq 0$ and $\varepsilon > 0$:

(i) $\sum_{s \leq t} |\Delta H^n_s|^2 \mathbb{1}_{\{|\Delta H^n_s| > \varepsilon\}} \xrightarrow{\mathbb{P}} 0$;
(ii) $\langle H^n, X(n) \rangle_t \xrightarrow{\mathbb{P}} 0$;
(iii) $\langle H^n, Z(n) \rangle_t \xrightarrow{\mathbb{P}} 0$;
(iv) $\langle H^n \rangle_t \xrightarrow{\mathbb{P}} \eta_t$.

Then it holds that $H^n \xrightarrow{\mathcal{L}-\mathrm{s}} H$, where H is an $\mathcal{F}$-conditional Gaussian martingale on the filtered extension $(\Omega^*, \mathcal{F}^*, (\mathcal{F}^*_t)_{t \geq 0}, \mathbb{P}^*)$ with $\langle H \rangle_t = \eta_t$.

We consider a 3-dimensional $\mathbb{F}^n$-martingale H^n, we aim to show that for $\omega \in \Omega'$:

$$H^n_t = c_n^{-1} \left\{ \sum_{i=1}^{N^{(c)}_{n,t}+1} \begin{pmatrix} (r^{(c)}_{n,i})^2 \\ (\overline{r}^{(c)}_{n,i})^2 \\ c_n^2 \end{pmatrix} - \sum_{i=1}^{N^{(c)}_{n,t}+1} c_n^2 U^{(c)}_{n,i} \begin{pmatrix} \zeta_1^{-1} \\ \zeta_2^{-1} \\ \zeta_3^{-1} \end{pmatrix} \right\} \xrightarrow{\mathcal{L}-\mathrm{s}} H_t, \quad \text{with } \langle H \rangle_t = \frac{\tau(t)}{h_2(m)} \Sigma, \tag{A.92}$$

where $\Sigma = (\sigma_{ij})_{1 \leq i,j \leq 3}$ is symmetric with

$$\sigma_{11} = 2(h_4(m) - \lambda(m)), \tag{A.93}$$

$$\sigma_{22} = \overline{h}_{4,\epsilon}(m) - \frac{2\overline{h}_{2,\epsilon}(m)\overline{\lambda}(m)}{h_2(m)} + \frac{\overline{h}_{4,\epsilon}(m)\overline{h}^2_{2,\epsilon}(m)}{h_2^2(m)}, \tag{A.94}$$

$$\sigma_{33} = \frac{h_4(m) - h_2^2(m)}{h_2^2(m)}, \tag{A.95}$$

$$\sigma_{12} = \overline{\rho}_{2,\epsilon}(m) - \frac{\overline{h}_{2,\epsilon}(m)\lambda(m)}{h_2(m)} - \overline{\lambda}(m) + \frac{h_4(m)\overline{h}_{2,\epsilon}(m)}{h_2(m)}, \tag{A.96}$$

$$\sigma_{13} = \frac{h_4(m) - \lambda(m)}{h_2(m)}, \tag{A.97}$$

$$\sigma_{23} = \frac{h_4(m)\overline{h}_{2,\epsilon}(m)}{h_2^2(m)} - \frac{\overline{\lambda}(m)}{h_2(m)}, \tag{A.98}$$

Note that the martingality of H^n with respect to $\mathbb{F}^n$ can be similarly verified as in Lemma A.7 (ii).

We prove the claimed stable CLT in Eq. (A.92) by verifying the conditions of Theorem A.1. First, we check Property (F) for the discretized filtration $\mathbb{F}^n = (\mathcal{F}^n_{N^{(c)}_{n,t}+1})_{t \geq 0}$. Given the continuous martingale $X \equiv X'$ adapted to $\mathbb{F}$, we define its $\mathbb{F}^n$-discretized version $X(n)$ as in Lemma A.7 (i),

which is square-integrable by construction. Pick some $Z \in \mathcal{M}_b$ and consider its discretized version $Z(n)$, then the boundedness of Z ensures that condition (i) of Property (F) holds. Condition (ii) follows from the u.c.p. result of V_1^n in the proof of Theorem 1 (Appendix A.3). Condition (iii) follows from Proposition VI.6.37 of Jacod and Shiryaev (2003) and Eq. (2.2.13) of Jacod and Protter (2012) by virtue of Lemma A.6 (iii). Therefore, Property (F) is satisfied for the specific PDS-based $\mathbb{F}^n$.

Now we verify the conditions in Theorem A.1 for $H^n = (H_1^n, H_2^n, H_3^n)^\top$. We write

$$H_t^n = \sum_{i=1}^{N_{n,t}^{(c)}+1} \Delta H_i^n, \qquad \text{where } \Delta H_i^n = \begin{pmatrix} \Delta H_{1,i}^n \\ \Delta H_{2,i}^n \\ \Delta H_{3,i}^n \end{pmatrix} = c_n^{-1} \begin{pmatrix} (r_{n,i}^{(c)})^2 - \Delta \tau_{n,i}^{(c)} \\ (\overline{r}_{n,i}^{(c)})^2 - \zeta_2^{-1} \Delta \tau_{n,i}^{(c)} \\ c_n^2 - \zeta_3^{-1} \Delta \tau_{n,i}^{(c)} \end{pmatrix}. \tag{A.99}$$

For Condition (i), we need to show that

$$\sum_{i=1}^{N_{n,t}^{(c)}+1} (\Delta H_{k,i}^n)^2 \mathbb{1}_{\{|\Delta H_{k,i}^n| > \varepsilon\}} \xrightarrow{\mathbb{P}} 0, \tag{A.100}$$

for all $t \geq 0$ and $\varepsilon > 0$. This condition corresponds to a classical (conditional) Lindeberg condition, which ensures that the limiting process H has no jumps; see Remark 3 of Podolskij and Vetter (2010). Note that the conditional expectation of the summand can be bounded by:

$$\begin{aligned} \mathbb{E}[(\Delta H_{k,i}^n)^2 \mathbb{1}_{\{|\Delta H_{k,i}^n| > \varepsilon\}} | \mathcal{F}_{i-1}^n] &\leq (\mathbb{E}[(\Delta H_{k,i}^n)^r | \mathcal{F}_{i-1}^n])^{2/r} (\mathbb{P}(|\Delta H_{k,i}^n| > \varepsilon | \mathcal{F}_{i-1}^n))^{1-2/r} \\ &\leq (\mathbb{E}[(\Delta H_{k,i}^n)^r | \mathcal{F}_{i-1}^n])^{2/r} (\varepsilon^{-r} \mathbb{E}[(\Delta H_{k,i}^n)^r | \mathcal{F}_{i-1}^n])^{1-2/r} \\ &\leq \varepsilon^{2-r} \mathbb{E}[(\Delta H_{k,i}^n)^r | \mathcal{F}_{i-1}^n] \\ &\leq K \mathbb{E}[(\Delta H_{k,i}^n)^r | \mathcal{F}_{i-1}^n], \end{aligned} \tag{A.101}$$

for some $r > 2$, by Hölder's and Markov's inequalities. Then we have

$$\mathbb{E}[|\Delta H_i^n|^r | \mathcal{F}_{i-1}^n] \leq K c_n^r \begin{pmatrix} \mathbb{E}[|c_n^{-2}(r_{n,i}^{(c)})^2 - U_{n,i}^{(c)}|^r | \mathcal{F}_{i-1}^n] \\ \mathbb{E}[|c_n^{-2}(\overline{r}_{n,i}^{(c)})^2 - \zeta_2^{-1} U_{n,i}^{(c)}|^r | \mathcal{F}_{i-1}^n] \\ \mathbb{E}[|1 - \zeta_3^{-1} U_{n,i}^{(c)}|^r | \mathcal{F}_{i-1}^n] \end{pmatrix} \leq K' c_n^r \begin{pmatrix} 1 \\ 1 \\ 1 \end{pmatrix}, \tag{A.102}$$

where all three conditional moments are finite for some $r > 2$, which can be readily verified with the Burkholder-Davis-Gundy inequality, and with finite r-th moment of $U_{n,i}^{(c)}$, i.e., $\mathbb{E}[|U_{n,i}^{(c)}|^r] = c_n^{-2r} \Delta_n^r \mathbb{E}[|\Pi_{n,1}^{(c)}|^r] < \infty$ by Lemma A.2 (ii). By Lemma A.5, we have

$$\mathbb{E}\left[\sum_{i=1}^{N_{n,t}^{(c)}+1} (\Delta H_{k,i}^n)^2 \mathbb{1}_{\{|\Delta H_{k,i}^n| > \varepsilon\}} \right] \leq K c_n^{r-2} = o(1), \tag{A.103}$$

which implies Eq. (A.100).

For Condition (ii), we have

$$\begin{aligned}
\mathbb{E}[\Delta H^n_{1,i} r^{(c)}_{n,i} | \mathcal{F}^n_{i-1}] &= c_n^{-1} \mathbb{E}[((r^{(c)}_{n,i})^2 - \Delta\tau^{(c)}_{n,i}) r^{(c)}_{n,i} | \mathcal{F}^n_{i-1}] = 0, \\
\mathbb{E}[\Delta H^n_{2,i} r^{(c)}_{n,i} | \mathcal{F}^n_{i-1}] &= c_n^{-1} \mathbb{E}[((\bar{r}^{(c)}_{n,i})^2 - \zeta_2^{-1}\Delta\tau^{(c)}_{n,i}) r^{(c)}_{n,i} | \mathcal{F}^n_{i-1}] = 0, \\
\mathbb{E}[\Delta H^n_{3,i} r^{(c)}_{n,i} | \mathcal{F}^n_{i-1}] &= c_n^{-1} \mathbb{E}[(c_n^2 - \zeta_3^{-1}\Delta\tau^{(c)}_{n,i}) r^{(c)}_{n,i} | \mathcal{F}^n_{i-1}] = 0,
\end{aligned} \tag{A.104}$$

by Lemma A.6 (iii) and (iv), and also $\mathbb{E}[(\bar{r}^{(c)}_{n,i})^2 r^{(c)}_{n,i}] = 0$.

For a generic martingale $Z \in \mathcal{M}_b$ starting from 0 and orthogonal to X, we define $\widetilde{Z}_{\tau(t)} = Z_t$ as the intrinsic-time counterpart of Z, where $\tau(t) = \langle X \rangle_t$. Then, Condition (iii) can be written into

$$\mathbb{E}\big[\Delta H^n_{k,i} \big(\widetilde{Z}_{\tau^{(c)}_{n,i}} - \widetilde{Z}_{\tau^{(c)}_{n,i-1}}\big) \big| \mathcal{F}^n_{i-1}\big] = 0, \tag{A.105}$$

and it suffices to show that

$$\mathbb{E}\big[\Delta H^n_{k,1} \widetilde{Z}_{\tau^{(c)}_{n,1}}\big] = 0. \tag{A.106}$$

As defined in Appendix A.1.1, the filtration $\widetilde{\mathbb{F}} = (\widetilde{\mathcal{F}}_\tau)_{\tau \geq 0}$ is generated by the Brownian motion $\widetilde{X}$. Since $\tau^{(c)}_{n,1}$ is a $\widetilde{\mathbb{F}}$-stopping time, the increments $\Delta H^n_{k,1}$ in Eq. (A.99) are measurable with respect to $\widetilde{\mathbb{F}}$ with zero mean and finite variance. Hence, by the martingale representation theorem, there exists a predictable process h_k which is adapted to $\widetilde{\mathbb{F}}$, such that

$$\Delta H^n_{k,1} = \int_0^\infty h_{k,s} d\widetilde{X}_s. \tag{A.107}$$

We also have the following integral representation for $\widetilde{Z}_{\tau^{(c)}_{n,1}}$:

$$\widetilde{Z}_{\tau^{(c)}_{n,1}} = \int_0^\infty \mathbb{1}_{\{s \leq \tau^{(c)}_{n,1}\}} d\widetilde{Z}_s. \tag{A.108}$$

Therefore, by the Kunita-Watanabe identity, we have

$$\mathbb{E}\big[\Delta H^n_{k,1} \widetilde{Z}_{\tau^{(c)}_{n,1}}\big] = \mathbb{E}\left[\int_0^\infty h_{k,s} \mathbb{1}_{\{s \leq \tau^{(c)}_{n,1}\}} d\langle \widetilde{X}, \widetilde{Z} \rangle_s\right] = 0, \tag{A.109}$$

since $\langle \widetilde{X}, \widetilde{Z} \rangle_{\tau(t)} = \langle X, Z \rangle_t \equiv 0$ as assumed. This result and an iterative conditioning argument lead to Eq. (A.105) and further implies Condition (iii) in Theorem A.1.

Finally, Condition (iv) translates to

$$\sum_{i=1}^{N^{(c)}_{n,t}+1} \mathbb{E}[\langle \Delta H^n_i \rangle | \mathcal{F}^n_{i-1}] \xrightarrow{\mathbb{P}} \frac{\tau(t)}{h_2(m)} \Sigma. \tag{A.110}$$

Note that $c_n^2 N_{n,t}^{(c)} \xrightarrow{\mathbb{P}} \tau(t)/h_2(m)$. We further calculate all cross moments $\mathbb{E}[\Delta H_{k,i}^n \Delta H_{k',i}^n | \mathcal{F}_{i-1}^n]$:

$$\mathbb{E}[(\Delta H_{1,i}^n)^2|\mathcal{F}_{i-1}^n] = c_n^{-2}\mathbb{E}[((r_{n,i}^{(c)})^2 - c_n^2 U_{n,i}^{(c)})^2|\mathcal{F}_{i-1}^n] = 2c_n^2(h_4(m) - \lambda(m)), \tag{A.111}$$

$$\begin{aligned}\mathbb{E}[(\Delta H_{2,i}^n)^2|\mathcal{F}_{i-1}^n] &= c_n^{-2}\mathbb{E}[((\overline{r}_{n,i}^{(c)})^2 - \zeta_2^{-1}c_n^2 U_{n,i}^{(c)})^2|\mathcal{F}_{i-1}^n] \\ &= c_n^2\left(\overline{h}_{4,\epsilon}(m) - \frac{2\overline{h}_{2,\epsilon}(m)\overline{\lambda}(m)}{h_2(m)} + \frac{\overline{h}_{4,\epsilon}(m)\overline{h}_{2,\epsilon}^2(m)}{h_2^2(m)}\right),\end{aligned} \tag{A.112}$$

$$\mathbb{E}[(\Delta H_{3,i}^n)^2|\mathcal{F}_{i-1}^n] = c_n^{-2}\mathbb{E}[(c_n^2 - \zeta_3^{-1}c_n^2 U_{n,i}^{(c)})^2|\mathcal{F}_{i-1}^n] = \frac{c_n^2(h_4(m) - h_2^2(m))}{h_2^2(m)}, \tag{A.113}$$

$$\begin{aligned}\mathbb{E}[\Delta H_{1,i}^n \Delta H_{2,i}^n|\mathcal{F}_{i-1}^n] &= c_n^{-2}\mathbb{E}[((r_{n,i}^{(c)})^2 - c_n^2 U_{n,i}^{(c)})((\overline{r}_{n,i}^{(c)})^2 - \zeta_2^{-1}c_n^2 U_{n,i}^{(c)})|\mathcal{F}_{i-1}^n] \\ &= c_n^2\left(\overline{\lambda}_r(m) - \frac{\overline{h}_{2,\epsilon}(m)\lambda(m)}{h_2(m)} - \overline{\lambda}(m) + \frac{h_4(m)\overline{h}_{2,\epsilon}(m)}{h_2(m)}\right),\end{aligned} \tag{A.114}$$

$$\mathbb{E}[\Delta H_{1,i}^n \Delta H_{3,i}^n|\mathcal{F}_{i-1}^n] = c_n^{-2}\mathbb{E}[((r_{n,i}^{(c)})^2 - c_n^2 U_{n,i}^{(c)})(c_n^2 - \zeta_3^{-1}c_n^2 U_{n,i}^{(c)})|\mathcal{F}_{i-1}^n] = \frac{c_n^2(h_4(m) - \lambda(m))}{h_2(m)}, \tag{A.115}$$

$$\begin{aligned}\mathbb{E}[\Delta H_{2,i}^n \Delta H_{3,i}^n|\mathcal{F}_{i-1}^n] &= c_n^{-2}\mathbb{E}[((\overline{r}_{n,i}^{(c)})^2 - \zeta_2^{-1}c_n^2 U_{n,i}^{(c)})(c_n^2 - \zeta_3^{-1}c_n^2 U_{n,i}^{(c)})|\mathcal{F}_{i-1}^n] \\ &= c_n^2\left(\frac{h_4(m)\overline{h}_{2,\epsilon}(m)}{h_2^2(m)} - \frac{\overline{\lambda}(m)}{h_2(m)}\right).\end{aligned} \tag{A.116}$$

The above calculations verify the result in Eq. (A.110). Therefore, the stable convergence in Eq. (A.92) follows from Theorem A.1 with all conditions satisfied, and it is safe to replace $N_{n,t}^{(c)} + 1$ with $N_{n,t}^{(c)}$ in Eq. (A.92) as the additional term of order $o_p(c_n)$ is asymptotic negligible.

Suppose that $(x_n, y_n, z_n)^\top - (x_0, y_0, z_0)^\top \xrightarrow{\mathcal{L}} \mathcal{MN}(0, \Sigma)$, where $\Sigma = (\sigma_{ij})_{1\le i,j\le 3}$. Consider the function $g(x, y, z) = (x/z, y/z)^\top$. The Jacobian matrix is given by

$$J_g(x, y, z) = \begin{pmatrix} 1/z & 0 & -x/z^2 \\ 0 & 1/z & -x/z^2 \end{pmatrix}. \tag{A.117}$$

By the multivariate delta method, we obtain

$$g(x_n, y_n, z_n)^\top - g(x_0, y_0, z_0)^\top \xrightarrow{\mathcal{L}} \mathcal{MN}(0, \widetilde{\Sigma}), \quad \text{where } \widetilde{\Sigma} = J_g(x_0, y_0, z_0)\Sigma J_g(x_0, y_0, z_0)^\top. \tag{A.118}$$

Explicitly, $\widetilde{\Sigma} = (\widetilde{\sigma}_{ij})_{1\le i,j\le 2}$ is given by

$$\begin{aligned}\widetilde{\sigma}_{11} &= \frac{\sigma_{11}}{z_0^2} - 2\frac{\sigma_{13}x_0}{z_0^3} + \frac{\sigma_{33}x_0^2}{z_0^4}, \\ \widetilde{\sigma}_{12} &= \frac{\sigma_{12}}{z_0^2} - \frac{\sigma_{23}x_0}{z_0^3} - \frac{\sigma_{13}y_0}{z_0^3} + \frac{\sigma_{33}x_0y_0}{z_0^4}, \\ \widetilde{\sigma}_{22} &= \frac{\sigma_{22}}{z_0^2} - 2\frac{\sigma_{23}y_0}{z_0^3} + \frac{\sigma_{33}y_0^2}{z_0^4}.\end{aligned} \tag{A.119}$$

Using the above result from the multivariate delta method and the joint stable CLT in Eq. (A.100),

we can derive the asymptotic distribution of the vector $\left(\sum_{i=1}^{N_{n,t}^{(c)}}(r_{n,i}^{(c)})^2/(c_n^2 N_{n,t}^{(c)}), \sum_{i=1}^{N_{n,t}^{(c)}}(\overline{r}_{n,i}^{(c)})^2/(c_n^2 N_{n,t}^{(c)})\right)^\top$. When $t=1$, it is the vector $(S_2, \overline{S}_{2,\epsilon})^\top$ defined in Eq. (11). We evaluate each term in Eq. (A.119) with $(x_0, y_0, z_0)^\top = \tau(t)(1, \overline{h}_{2,\epsilon}(m)/h_2(m), 1/h_2(m))^\top$:

$$\begin{aligned}\widetilde{\sigma}_{11} &= \frac{h_2(m)}{\tau(t)}(2(h_4(m)-\lambda(m)) - 2(h_4(m)-\lambda(m)) + h_4(m) - h_2^2(m)) \\ &= \frac{h_2(m)}{\tau(t)}(h_4(m) - h_2^2(m)),\end{aligned} \tag{A.120}$$

$$\begin{aligned}\widetilde{\sigma}_{21} = \frac{h_2(m)}{\tau(t)}&\left(\overline{\lambda}_r(m) - \frac{\overline{h}_{2,\epsilon}(m)\lambda(m)}{h_2(m)} - \overline{\lambda}(m) + \frac{h_4(m)\overline{h}_{2,\epsilon}(m)}{h_2(m)} - \left(\frac{h_4(m)\overline{h}_{2,\epsilon}(m)}{h_2(m)} - \overline{\lambda}(m)\right)\right. \\ &\left. - \frac{\overline{h}_{2,\epsilon}(m)}{h_2(m)}(h_4(m)-\lambda(m)) + \frac{\overline{h}_{2,\epsilon}(m)}{h_2(m)}(h_4(m)-h_2^2(m))\right) \\ &= \frac{h_2(m)}{\tau(t)}(\overline{\lambda}_r(m) - h_2(m)\overline{h}_{2,\epsilon}(m)),\end{aligned} \tag{A.121}$$

$$\begin{aligned}\widetilde{\sigma}_{22} = \frac{h_2(m)}{\tau(t)}&\left(\overline{h}_{4,\epsilon}(m) - \frac{2\overline{h}_{2,\epsilon}(m)\overline{\lambda}(m)}{h_2(m)} + \frac{\overline{h}_{4,\epsilon}(m)\overline{h}_{2,\epsilon}^2(m)}{h_2^2(m)} - 2\left(\frac{h_4(m)\overline{h}_{2,\epsilon}^2(m)}{h_2^2(m)} - \frac{\overline{h}_{2,\epsilon}(m)\overline{\lambda}(m)}{h_2(m)}\right)\right. \\ &\left. + \frac{\overline{h}_{2,\epsilon}^2(m)}{h_2^2(m)}(h_4(m)-h_2^2(m))\right) \\ &= \frac{h_2(m)}{\tau(t)}(\overline{h}_{4,\epsilon}(m) - \overline{h}_{2,\epsilon}^2(m)).\end{aligned} \tag{A.122}$$

By the u.c.p. result in Eq. (A.66), we have

$$\sqrt{N_{n,t}^{(c)}}\left(\begin{pmatrix}\sum_{i=1}^{N_{n,t}^{(c)}}(r_{n,i}^{(c)})^2/(c_n^2 N_{n,t}^{(c)}) \\ \sum_{i=1}^{N_{n,t}^{(c)}}(\overline{r}_{n,i}^{(c)})^2/(c_n^2 N_{n,t}^{(c)})\end{pmatrix} - \begin{pmatrix}h_2(m) \\ \overline{h}_{2,\epsilon}(m)\end{pmatrix}\right) \xrightarrow{\mathcal{L}} \mathcal{N}(0, \widetilde{\Sigma}), \tag{A.123}$$

where

$$\widetilde{\Sigma} = m^{-4}\begin{pmatrix}\mu_4(m) - \mu_2^2(m) & \overline{\rho}_{2,\epsilon}(m) - \mu_2(m)\overline{\mu}_{2,\epsilon}(m) \\ \overline{\rho}_{2,\epsilon}(m) - \mu_2(m)\overline{\mu}_{2,\epsilon}(m) & \overline{\mu}_{4,\epsilon}(m) - \overline{\mu}_{2,\epsilon}^2(m)\end{pmatrix}. \tag{A.124}$$

By the same u.c.p. result and Eq. (6), we have $N_t^n/N_{n,t}^{(c)} \xrightarrow{\mathbb{P}} \mu_2(m)$, and thus

$$\sqrt{N_t^n}\left(\begin{pmatrix}\sum_{i=1}^{N_{n,t}^{(c)}}(r_{n,i}^{(c)})^2/(c_n^2 N_{n,t}^{(c)}) \\ \sum_{i=1}^{N_{n,t}^{(c)}}(\overline{r}_{n,i}^{(c)})^2/(c_n^2 N_{n,t}^{(c)})\end{pmatrix} - \begin{pmatrix}h_2(m) \\ \overline{h}_{2,\epsilon}(m)\end{pmatrix}\right) \xrightarrow{\mathcal{L}} \mathcal{N}(0, \mu_2(m)\widetilde{\Sigma}). \tag{A.125}$$

Therefore, for the random vector

$$\begin{pmatrix} h_2^{-1}\big(\sum_{i=1}^{N_{n,t}^{(c)}}(r_{n,i}^{(c)})^2/(c_n^2 N_{n,t}^{(c)})\big) \\ \overline{h}_{2,\epsilon}^{-1}\big(\sum_{i=1}^{N_{n,t}^{(c)}}(\overline{r}_{n,i}^{(c)})^2/(c_n^2 N_{n,t}^{(c)})\big) \end{pmatrix}, \tag{A.126}$$

the multivariate delta method implies that

$$\sqrt{N_t^n}\left(\begin{pmatrix} h_2^{-1}(\sum_{i=1}^{N_{n,t}^{(c)}}(r_{n,i}^{(c)})^2/(c_n^2 N_{n,t}^{(c)})) \\ \overline{h}_{2,\epsilon}^{-1}(\sum_{i=1}^{N_{n,t}^{(c)}}(\overline{r}_{n,i}^{(c)})^2/(c_n^2 N_{n,t}^{(c)})) \end{pmatrix} - \begin{pmatrix} m \\ m \end{pmatrix}\right) \xrightarrow{\mathcal{L}} \mathcal{N}(0, \mu_2(m)\Lambda^\top \widetilde{\Sigma}\Lambda), \tag{A.127}$$

where

$$\Lambda = \left(\frac{1}{h_2'(h_2^{-1}(h_2^{-1}(m)))}, \frac{1}{\overline{h}_{2,\epsilon}'(\overline{h}_{2,\epsilon}^{-1}(\overline{h}_{2,\epsilon}^{-1}(\overline{h}_{2,\epsilon}(m))))}\right) = \left(\frac{1}{h_2'(m)}, \frac{1}{\overline{h}_{2,\epsilon}'(m)}\right). \tag{A.128}$$

This completes the proof.

A.5 Proof of Proposition 1

Proof. Firstly, we prove that the sequence of pre-averaged returns $(r_i^*)_{1\le i\le N'}$ converges in law to a centered stationary Gaussian process with desired variance under infill asymptotics for each i. We assume $k_n = 2k$ for simplicity, and expand r_i^* in terms of $\Delta_j^N X = X_j - X_{j-1}$ and ε_j:

$$\begin{aligned} r_i^* &= \frac{1}{k_n}\sum_{j=1}^{k}(X_{i+k+j} - X_{i+j}) + \frac{1}{k_n}\sum_{j=1}^{k}(\varepsilon_{i+k+j} - \varepsilon_{i+j}) \\ &= \underbrace{\sum_{j=1}^{k_n} g\Big(\frac{j}{2k}\Big)\Delta_{i+j}^N X}_{A_i} + \underbrace{\frac{1}{k_n}\sum_{j=1}^{k}(\varepsilon_{i+k+j} - \varepsilon_{i+j})}_{B_i}, \end{aligned} \tag{A.129}$$

where $g(s) = s \wedge (1-s)$ is the triangular kernel weighting function. Under Assumption 2 and by the strong approximation result in Eq. (A.21), we deduce that A_i converges in probability to $\sum_{j=1}^{k_n} g\big(\frac{j}{2k}\big)\breve{r}_{i+j}$, which is a linear combination of i.i.d. centered Gaussian random variables. The α-mixing ε with the conditions in Assumption 3 indidates a CLT under weak dependence (Theorem 1.7, Ibragimov, 1962; Theorem 8.3.7, Durrett, 2019), which implies the asymptotic Gaussianity of B_i. The independence between X and ε implies that r_i^* converges in distribution to a centered Gaussian random variable for all i.

We now identify the limiting law of (r_i^*) by calculating its variance kernel explicitly, which also establishes the stationarity of the limiting Gaussian process. With $\mathrm{Corr}(X_j, \varepsilon_{j'}) = 0$ for any $0 \le j, j' \le N$, we have $\mathrm{Var}(r_i^*) = \mathrm{Var}(A_i) + \mathrm{Var}(B_i)$ with

$$\mathrm{Var}(A_i) = \sum_{j=1}^{k_n} g^2\Big(\frac{j}{k_n}\Big)(\Delta_n + o(\Delta_n)) = \frac{k_n\Delta_n}{12} + o(\sqrt{\Delta_n}). \tag{A.130}$$

For the additive noise term, we define the partial sum of ε as

$$S_{n,h} = \sum_{i=1}^{h} \varepsilon_{n+i}, \tag{A.131}$$

and start with the following results for some $\lambda \geq h$:

$$\mathrm{Var}(S_{n,h}) = \sum_{m=1-h}^{h-1} (h - |m|)\Gamma_m = h \sum_{m=1-h}^{h-1} \Big(1 - \Big|\frac{m}{h}\Big|\Big)\Gamma_m, \tag{A.132}$$

$$\begin{aligned} \mathrm{Cov}(S_{n,h}, S_{n+\lambda,h}) = \mathbb{E}[S_{n,h}S_{n+\lambda,h}] &= \sum_{i=0}^{h-1}\sum_{j=0}^{h-1} \mathrm{Cov}(\varepsilon_{n+i}, \varepsilon_{n+\lambda+i+j}) \\ &= \sum_{m=1-h}^{h-1} (h - |m|)\Gamma_{m+\lambda} = h \sum_{m=1-h}^{h-1} \Big(1 - \Big|\frac{m}{h}\Big|\Big)\Gamma_{m+\lambda}, \end{aligned} \tag{A.133}$$

where the weight $1 - |m/h|$ is the Bartlett kernel. Therefore, we have

$$\begin{aligned} \mathrm{Var}(B_i) &= \frac{1}{4k^2}\mathrm{Var}(S_{i+k,k} - S_{i,k}) \\ &= \frac{1}{4k^2}\mathrm{Var}(S_{i+k,k}) + \frac{1}{4k^2}\mathrm{Var}(S_{i,k}) - 2\mathrm{Cov}(S_{i+k,k}, S_{i,k}) \\ &= \frac{1}{2k}\sum_{m=1-k}^{k-1} \Big(1 - \Big|\frac{m}{k}\Big|\Big)\Gamma_m - \frac{1}{2k}\sum_{m=1-k}^{k-1} \Big(1 - \Big|\frac{m}{k}\Big|\Big)\Gamma_{m+k} \end{aligned} \tag{A.134}$$

of the order $\sqrt{\Delta_n}$ by the absolute summability of Γ_m, which is implied by the α-mixing property of ε under Assumption 3 (Ibragimov and Linnik, 1971). Since $k_n \asymp \sqrt{N}$, both $\mathrm{Var}(A_i)$ and $\mathrm{Var}(B_i)$ are of the order $\sqrt{\Delta_n}$, such that we can ignore all terms with order smaller than $\sqrt{\Delta_n}$, which yields $\mathrm{Var}(r_i^*) = \mathrm{Var}(A_i) + \mathrm{Var}(B_i) \asymp \sqrt{\Delta_n}$.

With the time-invariant first moment and finite second moment of r_i^* for all time, in order to prove the weak stationarity of (r_i^*), we need to make sure that the autocovariance $\mathrm{Cov}(r_i^*, r_{i+\lambda}^*)$ does not vary with i. Here we firstly deal with the autocovariance of A_i. It suffices to examine the autocovariance for non-negative integer-valued lags λ, as the autocovariance function is always symmetric.

$$\mathrm{Cov}(A_i, A_{i+\lambda}) = \mathbb{E}[A_i A_{i+\lambda}] = \mathbb{E}\left[\sum_{j=1}^{k_n} g\Big(\frac{j}{k_n}\Big)\Delta_{i+j}^N X \sum_{\eta=1}^{k_n} g\Big(\frac{\eta}{k_n}\Big)\Delta_{i+\lambda+\eta}^N X\right]. \tag{A.135}$$

When $\lambda \geq k_n$, $\mathrm{Cov}(A_i, A_{i+\lambda}) = 0$. When $1 \leq \lambda \leq k_n - 1$, we have

$$\begin{aligned}\mathrm{Cov}(A_i, A_{i+\lambda}) &= \mathbb{E}\left[\sum_{j=1}^{k_n-\lambda} g\Big(\frac{j}{k_n}\Big) g\Big(\frac{j+\lambda}{k_n}\Big)(\Delta^N_{i+\lambda+j} X)^2\right] \\ &= \sum_{j=1}^{k_n-\lambda} g\Big(\frac{j}{k_n}\Big) g\Big(\frac{j+\lambda}{k_n}\Big)\mathbb{E}[(\Delta^N_{i+\lambda+j} X)^2] = O(\sqrt{\Delta_n}).\end{aligned} \tag{A.136}$$

For the noise term, we have the lag-λ autocovariance

$$\begin{aligned}&\mathrm{Cov}(B_i, B_{i+\lambda}) = \frac{1}{4k^2}\mathbb{E}[(S_{i+k,k} - S_{i,k})(S_{i+k+\lambda,k} - S_{i+\lambda,k})] \\ &= \frac{1}{4k^2}\left(\mathbb{E}[S_{i+k,k}S_{i+k+\lambda,k}] + \mathbb{E}[S_{i,k}S_{i+\lambda,k}] - \mathbb{E}[S_{i+k,k}S_{i+\lambda,k}] - \mathbb{E}[S_{i,k}S_{i+k+\lambda,k}]\right) \\ &= \frac{1}{2k}\sum_{m=1-k}^{k-1}\Big(1 - \Big|\frac{m}{k}\Big|\Big)\Gamma_{m+\lambda} - \frac{1}{4k}\sum_{m=1-k}^{k-1}\Big(1 - \Big|\frac{m}{k}\Big|\Big)\Gamma_{m+\lambda-k} - \frac{1}{4k}\sum_{m=1-k}^{k-1}\Big(1 - \Big|\frac{m}{k}\Big|\Big)\Gamma_{m+\lambda+k} \\ &= O(\sqrt{\Delta_n}),\end{aligned} \tag{A.137}$$

by the absolute summability of Γ_m. In the limit, both the covariances are finite and time-invariant (not depend on i) for all possible $\lambda \in \mathbb{N}$, which implies the weak stationarity of (r_i^*) in the limit, as desired.

For Step 2, we first demonstrate how the random sign flip eliminates serial correlations in (r_i^*). Let $F(x) = \mathbb{P}(r_i^* \leq x)$ denote the CDF of r_i^*. It is obvious that the product $\delta_i r_i^*$ is a Gaussian random variable with the same distribution:

$$\begin{aligned}\mathbb{P}(\delta_i r_i^* \leq x) &= \mathbb{P}(\delta_i = 1)\mathbb{P}(\delta_i r_i^* \leq x | \delta_i = 1) + \mathbb{P}(\delta_i = -1)\mathbb{P}(\delta_i r_i^* \leq x | \delta_i = -1) \\ &= \frac{1}{2}\mathbb{P}(r_i^* \leq x) + \frac{1}{2}\mathbb{P}(r_i^* \geq -x) = F(x),\end{aligned} \tag{A.138}$$

and the autocovariance function for any $i \in \{1, \ldots, N' - \lambda\}$ satisfies

$$\mathrm{Cov}(\delta_i r_i^*, \delta_{i+\lambda} r_{i+\lambda}^*) = \mathbb{E}[\delta_i \delta_{i+\lambda} r_i^* r_{i+\lambda}^*] = \mathbb{E}[\delta_i]\mathbb{E}[\delta_{i+\lambda}]\mathrm{Cov}(r_i^*, r_{i+\lambda}^*) = 0. \tag{A.139}$$

Next, we establish that, following the uniform random permutation $\pi : \{1, \ldots, N'\} \mapsto \{1, \ldots, N'\}$, any two variables in $(\tilde{r}_i)_{1 \leq i \leq N'}$ are independent when their indices are not sufficiently distant from each other each other in $\{1, \ldots, N'\}$ under infill asymptotics. We start with a formal definition of the local independence for a discrete-time stochastic process: The process $X = (X_i)_{1 \leq i \leq n}$ is said to be locally independent if

$$\begin{aligned}&\lim_{n\to\infty} \sup_{\substack{1\leq i,j\leq n \\ 1\leq |i-j|\leq \Lambda_n}} \mathbb{P}(X_i \text{ and } X_j \text{ are dependent}) = 0, \\ \text{or} \quad &\lim_{n\to\infty} \sup_{\substack{1\leq i,j\leq n \\ 1\leq |i-j|\leq \Lambda_n}} \{|\mathbb{P}(A \cap B) - \mathbb{P}(A)\mathbb{P}(B)| : A \in \sigma(X_i), B \in \sigma(X_j)\} = 0,\end{aligned} \tag{A.140}$$

where $\Lambda_n \asymp n^{\varpi}$ for some $\varpi \in (0,1)$, such that X_i is independent to other variables in X whose indices fall within the interval $[i-\Lambda_n, i+\Lambda_n]$. In our case, we need to verify

$$\lim_{n\to\infty} \sup_{\substack{1\le i,j\le N' \\ 1\le |i-j|\le \Lambda_n}} \mathbb{P}(\tilde{r}_i \text{ and } \tilde{r}_j \text{ are dependent}) = 0. \tag{A.141}$$

The fact that $(\varepsilon_i)_{0\le i\le N}$ is α-mixing implies that

$$\alpha(\Lambda_n) = \sup\{|\mathbb{P}(A\cap B) - \mathbb{P}(A)\mathbb{P}(B)| : A \in \sigma(\varepsilon_i), B \in \sigma(\varepsilon_{i+\Lambda_n})\} \to 0, \tag{A.142}$$

as $n\to\infty$, thus ε_i and ε_j are asymptotically independent if $|i-j| \ge \Lambda_n$.

With the uniform random permutation, we denote

$$\tilde{r}_i = r^*_{\pi(i)}\delta_{\pi(i)} \quad \text{and} \quad \tilde{r}_j = r^*_{\pi(j)}\delta_{\pi(j)} \tag{A.143}$$

where $\pi(i)$, $\pi(j)$ are the corresponding indices of the products before permutation. Therefore, for all $1\le i,j\le N'$ and $1\le |i-j|\le \Lambda_n$, $\tilde{r}_i$ and $\tilde{r}_j$ are independent if the corresponding indices $\pi(i)$ and $\pi(j)$ are sufficiently far apart from one another:

$$\begin{aligned}
\mathbb{P}(\tilde{r}_i \text{ and } \tilde{r}_j \text{ are dependent}) &= \mathbb{P}(r^*_{\pi(i)} \text{ and } r^*_{\pi(j)} \text{ are dependent}) \\
&= \mathbb{P}(\sigma(\{\varepsilon_{\pi(i)+\ell} : 0\le \ell \le k_n\}) \text{ and } \sigma(\{\varepsilon_{\pi(j)+\ell} : 0\le \ell\le k_n\}) \text{ are dependent}) \\
&\le 2\mathbb{P}(\pi(i)+1 \le \pi(j) \le \pi(i)+k_n+\Lambda_n) \\
&= \frac{2(k_n+\Lambda_n)}{N'-1} = O(\Delta_n^{\gamma}), \quad \text{where } \gamma = 1-\max\Big\{\frac{1}{2}, \varpi\Big\}.
\end{aligned} \tag{A.144}$$

For a sequence of N' variables, the uniform random permutation ensures that each of the $N'!$ possible permutations are equally likely and that each "ball" $r^*_{\pi(i)}\delta_{\pi(i)}$ has an equal chance of being placed into any "box" i, which has become a question of classical probability. As $n\to\infty$, $\tilde{r}_i$ and $\tilde{r}_j$ with $1\le |i-j|\le \Lambda_n$ are asymptotically independent. This completes the proof. □

Appendix B Supplementary Results

B.1 Parameter Choices for Other Tests

For other tests constructed in Sections 4 and 5, we clarify some specific parameter choices:

LM: For the local realized bipower variation, we consider the window size $K = \sqrt{252N}$, where N is the number of sampled observations.

ASJ: For the multipower variations constructed on two different sampling intervals δ and $k\delta$, we select $p = 4$ and $k = 2$, which satisfies the requirement.

CPR: For the auxiliary local variance estimator, we employ the nonparametric filter of length $2L + 1$ with $L = 25$ and a Gaussian kernel, which follows the recommendation in Appendix B of Corsi et al. (2010).

PZ: We employ the truncated realised power variation with $p = 4$ and the truncation threshold $cN^{-\varpi}$, where c and ϖ follow the recommendation in Section 5 of Podolskij and Ziggel (2010). For the noise-adjusted version, we select the pre-averaging window $k_n = 0.5\lfloor\sqrt{N}\rfloor$.

LM12: We select the pre-averaging window $k_n = 0.4\lfloor\sqrt{N}\rfloor$, which minimizes the absolute distance between the nominal size and the empirical size with the simulated tick-level noise-contaminated observations.

ASJL: We select the pre-averaging window $k_n = 0.9\lfloor\sqrt{N}\rfloor$ based on the simulated noise-contaminated data, and the truncation level $C = 5$.

B.2 Jump Detection

As detailed in Section 4.3, we consider the common jump filtering and detection method as a benchmark, which is based on the sequential detection approach of Andersen et al. (2007b) and the thresholding technique of Mancini (2009). Particularly, we adjust the threshold parameter k with two types of FWER corrections. Specifically, given N_{spl} tests of null hypotheses (N_{spl} sampled returns) and a family-wise significance level of α, we select the corresponding k for each individual return at α':

- Šidák correction: $\alpha' = 1 - (1 - \alpha)^{1/N_{\text{spl}}}$,
- Bonferroni correction: $\alpha' = \alpha/N_{\text{spl}}$.

Table B.1 presents the finite-sample size and size-adjusted power of the truncation-based filtering technique in the absence of market microstructure noise. The truncation thresholds are determined with (i) the latent true volatility, (ii) the localized tick-by-tick BV, and (iii) the localized pre-averaged BV of Podolskij and Vetter (2009). The threshold parameter k is adjusted with both FWER corrections, and we set $\varpi = 0.5$. Following the same procedure used for the noise case in Table 5, the spot volatility estimates are recursively obtained within a backward-looking tick-time window of 1,800 ticks. The pre-averaging window is chosen to be $\lceil 0.5\sqrt{1800}\rceil$ ticks.

Table B.1: Finite-sample size and power (%) of truncation-based filtering technique in the absence of market microstructure noise

Nominal size: 5%					
Panel A: Normalization with true spot volatility					
		No Jump (with FWER control)			
Ticks	N_{spl}	Šidák	Bonferroni	Moderate Jumps	Large Jumps
1	23400	4.92	4.83	93.13	96.80
5	4680	5.15	4.98	84.91	91.88
15	1560	5.38	5.25	75.12	87.18
30	780	4.96	4.80	67.55	82.46
60	390	5.13	4.99	57.84	76.16
120	195	5.22	5.08	46.50	69.19
180	130	4.93	4.81	40.92	64.71
300	78	5.03	4.90	31.98	56.20
Panel B: Normalization with localized tick-by-tick BV					
		No Jump (with FWER control)			
Ticks	N_{spl}	Šidák	Bonferroni	Moderate Jumps	Large Jumps
1	23400	5.95	5.74	91.21	95.92
5	4680	5.21	5.07	82.41	90.80
15	1560	5.31	5.23	72.45	85.60
30	780	5.06	4.87	64.37	81.08
60	390	5.13	5.01	53.72	74.08
120	195	5.15	5.02	42.28	66.33
180	130	4.89	4.75	36.51	61.57
300	78	4.98	4.89	27.52	52.92
Panel C: Normalization with localized pre-averaged BV					
		No Jump (with FWER control)			
Ticks	N_{spl}	Šidák	Bonferroni	Moderate Jumps	Large Jumps
1	23400	6.02	5.92	91.23	95.85
5	4680	5.87	5.73	82.44	90.72
15	1560	5.51	5.45	72.26	85.50
30	780	4.78	4.68	64.46	81.00
60	390	4.81	4.69	53.53	73.84
120	195	4.93	4.79	41.99	65.94
180	130	4.57	4.52	35.95	61.17
300	78	4.68	4.58	27.52	52.52

This table reports the finite-sample size and size-adjusted power (%) of 10,000 simulations of the truncation-based jump filtering technique in the absence of market microstructure noise. Observations are sampled at various multiples of ticks, where "N_{spl}" stands for the corresponding sampling frequencies. The truncation thresholds are constructed from (i) the latent true volatility, (ii) the localized tick-by-tick BV, and (iii) the localized pre-averaged BV. The threshold parameter k is adjusted with both the Šidák and Bonferroni corrections, and $\varpi = 0.5$.

In addition to the noise-case results in Table 5, we follow the empirical applications of Aït-Sahalia et al. (2025) to consider a broad range of fixed k from 3.5 to 9. Fig. B.1 illustrates the rejection rates under both the null and alternative hypotheses across various frequencies of tick-time sampling.

Furthermore, we extend the comparisons by examining returns sampled at equidistant calendar-time intervals. To estimate the spot volatility for each calendar-time interval and avoid the impact of tick irregularity, we construct the pre-averaged BV from all tick-level price observations within each day. We then adjust these daily volatility estimates to account for intraday volatility pattern for each calendar-time interval, where we follow Aleti et al. (2025) for the time-of-day adjustment

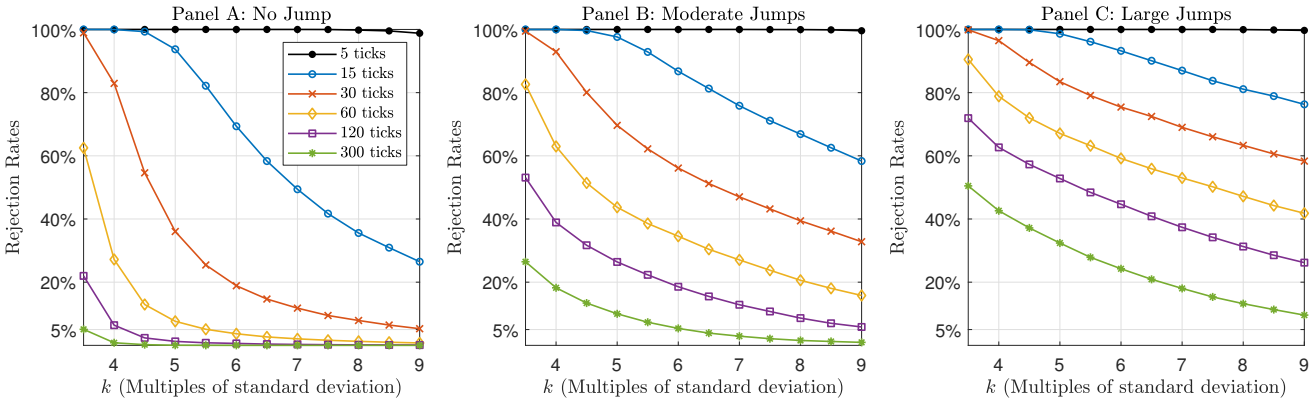

Figure B.1: Rejection rates of 10,000 simulations of the truncation-based jump filtering technique. Observations are sampled at various multiples of ticks. The truncation thresholds are constructed from the localized pre-averaged BV of Podolskij and Vetter (2009) computed within each backward-looking window of 1,800 ticks. The threshold parameter k is varied from 3.5 to 9, corresponding to progressively more stringent cutoffs, and $\varpi = 0.5$.

θ_j for the j-th calendar-time interval:

$$\theta_j = \left(\sum_{i=1}^{M} r_{i,j}^2 \right) \Big/ \left(\frac{1}{N_{\text{spl}}} \sum_{i=1}^{M} \sum_{j=1}^{N_{\text{spl}}} r_{i,j}^2 \right), \tag{B.1}$$

where $r_{i,j}$ is the return on the asset on day i at interval j, and θ_j is a simple ex ante measure of the fraction of daily RV that arrives at each time-of-day. Given a daily pre-averaged BV estimate BV_i, the spot volatility $\sigma_{i,j}$ is then estimated as $\hat{\sigma}_{i,j} = \sqrt{\text{BV}_i \theta_j}$. Table B.2 presents the finite-sample size and size-adjusted power of the truncation-based filtering technique applied to calendar-time sampled returns, with the threshold parameter k calibrated with both corrections to control a 5% FWER under the null.

Table B.2: Finite-sample size and power (%) of truncation-based filtering technique with calendar-time sampling

Nominal size: 5%					
		Panel A		Panel B	Panel C
		No Jump (with FWER control)			
Int. (sec)	N_{spl}	Šidák	Bonferroni	Moderate Jumps	Large Jumps
5	4680	100.00	100.00	15.58	39.79
15	1560	99.95	99.95	22.49	49.02
30	780	85.80	85.51	30.92	56.68
60	390	40.69	40.27	38.61	62.75
120	195	16.44	16.17	41.29	63.64
180	130	10.41	10.20	39.53	60.79
300	78	7.34	7.14	34.09	55.87

This table reports the finite-sample size and size-adjusted power (%) of 10,000 simulations of the truncation-based jump filtering technique. Observations are sampled at equidistant intervals in calendar time, where "N_{spl}" stands for the corresponding sampling frequencies. The truncation thresholds are constructed from the pre-averaged BV of Podolskij and Vetter (2009), with the intraday volatility seasonality incorporated, and the threshold parameter k is adjusted with both the Šidák and Bonferroni corrections, and $\varpi = 0.5$.

Similarly, we consider some fixed k varying from 3.5 to 9 for the truncation thresholds applied to calendar-time sampled returns. Fig. B.2 illustrates the rejection rates under both the null and alternative hypotheses across various frequencies of calendar-time sampling.

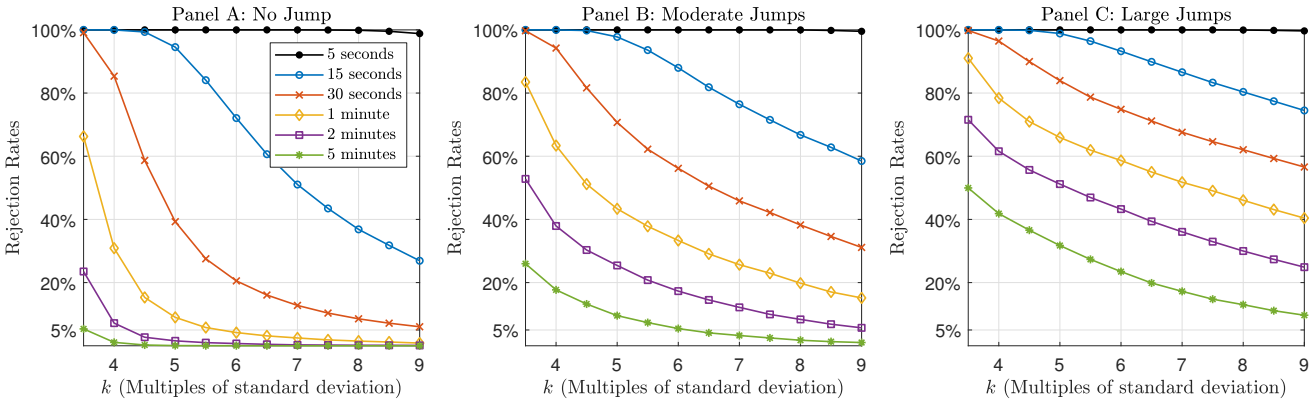

Figure B.2: Rejection rates of 10,000 simulations of the truncation-based jump filtering technique. Observations are sampled at equidistant intervals in calendar time. The truncation thresholds are constructed from the pre-averaged bipower variation of Podolskij and Vetter (2009), with the intraday volatility seasonality incorporated. The threshold parameter k is varied from 3.5 to 9, corresponding to progressively more stringent cutoffs, and $\varpi = 0.5$.

B.3 Simulation Results with Other Noise Specifications

In addition to the simulation results in Section 4, we consider three other specifications for the additive noise that follows Aït-Sahalia et al. (2012) as robustness checks:

(i) Gaussian noise:

$$\varepsilon_i = 2Z_i \sqrt{\frac{\sigma^2_{t_{n,i}}}{n}}, \tag{B.2}$$

where Z_i are i.i.d. draws from a standard normal distribution, see Tables B.3 to B.6.

(ii) Autocorrelated Gaussian noise:

$$\varepsilon_i = 2\omega^A_i \sqrt{\frac{\sigma^2_{t_{n,i}}}{n}}, \tag{B.3}$$

where ω^A_i is an autocorrelated Gaussian defined in Eq. (27), see Tables B.7 to B.10.

(iii) t-distributed noise:

$$\varepsilon_i = 2\omega^B_i \sqrt{\frac{\nu-2}{\nu}} \sqrt{\frac{\sigma^2_{t_{n,i}}}{n}}, \tag{B.4}$$

where ω^B_i are i.i.d. draws from a Student's t distribution with the degree of freedom ν, see Tables B.11 to B.14.

Table B.3: Finite-sample size and power (%) under Gaussian noise

Nominal size: 5%		$\theta = 0.3$				$\theta = 0.4$				$\theta = 0.5$			
			ϵ				ϵ				ϵ		
	$c/\sigma(\tilde{r}_i)$	$N^{(c)}$	0.05	0.07	0.10	$N^{(c)}$	0.05	0.07	0.10	$N^{(c)}$	0.05	0.07	0.10
Panel A No Jump	3	1785	4.90	5.21	5.35	1783	5.07	5.05	5.76	1783	5.01	5.07	5.70
	4	1099	5.33	5.03	5.49	1098	4.93	5.14	5.81	1098	5.24	5.21	5.62
	5	743	4.71	5.14	5.33	743	5.18	5.28	5.43	742	5.10	5.70	5.27
	6	535	5.26	5.01	5.49	535	4.63	4.89	5.53	535	4.82	5.47	5.13
	7	404	4.71	4.99	5.19	404	4.61	5.55	5.62	404	5.17	5.18	5.08
	8	316	4.83	4.79	5.59	315	4.83	5.23	5.73	315	5.08	5.12	5.30
	9	254	5.44	4.80	5.30	253	5.22	5.00	5.38	253	5.20	5.20	5.73
	10	208	4.93	5.31	5.71	208	4.98	5.41	5.68	208	5.18	5.28	5.75
Panel B Moderate Jump	3	1715	47.74	49.52	50.82	1716	44.73	47.04	49.52	1718	42.85	45.35	47.45
	4	1058	46.68	48.74	50.80	1059	43.38	46.51	48.46	1061	41.71	44.74	46.93
	5	717	45.27	47.51	50.26	718	43.27	45.29	48.09	720	41.23	43.10	45.95
	6	518	44.45	47.15	49.63	519	43.24	44.57	46.91	520	41.10	42.06	45.13
	7	392	44.91	46.79	49.45	393	42.51	43.70	46.51	394	40.31	41.96	44.21
	8	307	42.82	46.95	49.09	308	41.76	43.10	45.84	308	39.45	40.95	44.10
	9	247	42.13	45.59	48.45	248	40.81	42.65	46.06	248	38.43	40.97	43.46
	10	203	41.42	44.81	48.32	204	40.32	41.82	46.46	204	38.26	40.44	43.70
Panel C Large Jump	3	1587	69.98	71.41	73.31	1589	68.18	69.74	71.08	1594	67.26	68.39	69.95
	4	979	68.91	71.10	72.74	982	67.81	69.39	70.89	985	65.92	67.49	69.41
	5	665	68.80	70.14	72.20	668	66.75	69.09	70.32	670	65.28	66.87	69.25
	6	482	67.64	69.69	71.54	485	66.71	68.34	69.77	487	64.99	66.15	68.20
	7	365	67.61	69.10	71.27	368	65.47	66.78	69.89	370	63.94	65.80	67.99
	8	287	67.37	68.95	71.00	289	65.11	66.62	68.93	291	64.21	65.45	66.91
	9	232	65.90	69.22	70.84	234	64.78	66.60	68.88	235	63.87	64.83	67.73
	10	191	65.47	68.02	70.71	193	64.23	65.74	68.45	194	63.14	64.76	67.56

This table reports the finite-sample size and size-adjusted power (%) of 10,000 simulations of the test statistic $T_{c,\epsilon}$ at 5% nominal level. All simulated prices are contaminated by the additive Gaussian noise and rounding errors. We utilize the two-step noise reduction method in Section 3.2 to construct the sequence of pseudo-observations with three different pre-averaging windows, i.e., $k_n = \lceil \theta\sqrt{N} \rceil$ with $\theta \in \{0.3, 0.4, 0.5\}$. The observations are sampled with different PDS barrier widths $c = K\sigma(\tilde{r}_i)$, where K ranges from 3 to 10. Different censoring thresholds with $\epsilon \in \{0.05, 0.07, 0.1\}$ are considered. $N^{(c)}$ stands for the average sampling frequencies.

Table B.4: Finite-sample size and power (%) of other tests under Gaussian noise

Nominal size: 5%										
	Int. (sec)	N_{spl}	BNS	JO	LM	ASJ	CPR	PZ	MinRV	MedRV
Panel A No Jump	5	4680	0.23	1.06	14.02	100.00	0.37	5.59	0.00	0.00
	15	1560	4.93	3.70	22.26	93.73	5.43	9.91	0.91	2.89
	30	780	7.88	5.02	29.32	38.68	8.42	12.55	4.04	6.35
	60	390	7.69	6.23	27.86	13.10	8.26	14.47	5.37	7.14
	120	195	7.49	8.07	17.76	7.10	8.02	16.23	5.71	7.93
	180	130	7.91	9.05	15.11	5.36	8.70	16.12	5.78	8.78
	300	78	7.74	10.98	11.96	4.22	8.70	14.91	5.67	9.12
Panel B Moderate Jump	5	4680	44.28	51.82	69.09	99.76	47.13	66.49	40.11	45.46
	15	1560	40.43	44.90	60.35	92.97	43.88	61.13	37.19	41.85
	30	780	36.17	38.30	51.11	65.25	39.14	52.79	33.48	36.97
	60	390	29.52	30.92	42.23	37.60	32.97	43.63	27.36	31.32
	120	195	21.55	22.20	36.06	22.08	24.92	32.72	21.00	24.32
	180	130	17.48	17.40	30.52	14.55	20.17	26.98	17.02	20.84
	300	78	15.27	11.91	21.62	11.67	17.54	19.96	14.36	16.51
Panel C Large Jump	5	4680	68.50	74.10	84.55	99.83	70.65	82.69	64.96	68.91
	15	1560	65.66	69.37	79.03	95.72	68.29	79.36	62.52	66.47
	30	780	61.28	64.47	73.60	78.16	64.28	74.79	58.50	62.36
	60	390	55.16	57.63	67.45	57.04	58.50	68.70	52.97	57.53
	120	195	46.02	48.22	61.94	36.07	50.16	59.34	44.72	49.98
	180	130	41.61	42.27	56.76	26.63	45.35	53.82	40.37	44.59
	300	78	35.12	33.77	46.86	17.83	39.24	45.27	34.30	38.21

This table reports the finite-sample size and size-adjusted power (%) of 10,000 simulations of 8 classical tests at 5% nominal level: BNS (Barndorff-Nielsen and Shephard, 2006), JO (Jiang and Oomen, 2008), LM (Lee and Mykland, 2008), ASJ (Aït-Sahalia and Jacod, 2009b), CPR (Corsi et al., 2010), PZ (Podolskij and Ziggel, 2010), MinRV and MedRV (Andersen et al., 2012). All simulated prices are contaminated by the additive Gaussian noise and rounding errors. All these tests are constructed on observations equidistantly sampled with various intervals in calendar time: 5, 15, 30, 60, 120, 180 and 300 seconds, and "N_{spl}" stands for the sampling frequencies.

Table B.5: Finite-sample size and power (%) of other noise-robust tests under Gaussian noise

Nominal size: 5%					
	Int. (sec)	N_{spl}	PZ*	LM12	ASJL
Panel A: No Jump	tick	23400	5.10	3.27	5.12
	5	4680	4.93	8.59	8.79
Panel B: Moderate Jump	tick	23400	39.34	24.12	38.06
	5	4680	29.96	18.97	16.88
Panel C: Large Jump	tick	23400	64.18	39.18	62.90
	5	7680	56.03	32.23	41.41

This table reports the finite-sample size and size-adjusted power (%) of 10,000 simulations of 3 noise-robust tests at 5% nominal level: noise-adjusted PZ (Podolskij and Ziggel, 2010), LM12 (Lee and Mykland, 2012), and ASJL (Aït-Sahalia et al., 2012). All simulated prices are contaminated by the additive Gaussian noise and rounding errors. All these tests are constructed on tick-level and 5-second-sampled observations. The tuning parameters for those tests are selected by minimizing the absolute distance between the nominal size and the empirical size with the simulated tick-level noise-contaminated observations.

Table B.6: Finite-sample size and power (%) of truncation-based filtering technique under Gaussian noise

Nominal size: 5%					
		Panel A			
		No Jump (with FWER control)		Panel B	Panel C
Ticks	N_{spl}	Šidák	Bonferroni	Moderate Jumps	Large Jumps
1	23400	100.00	100.00	74.84	86.80
5	4680	100.00	100.00	72.45	85.36
15	1560	73.56	73.04	66.19	82.02
30	780	28.77	28.23	59.89	78.41
60	390	12.97	12.69	51.74	73.25
120	195	7.89	7.72	40.75	64.72
180	130	6.25	6.12	35.06	59.93
300	78	5.77	5.61	27.01	53.77

This table reports the finite-sample size and size-adjusted power (%) of 10,000 simulations of the truncation-based jump filtering technique. All simulated prices are contaminated by the additive autocorrelated Gaussian noise and rounding errors. Observations are sampled at various multiples of ticks, where "N_{spl}" stands for the corresponding sampling frequencies. The truncation thresholds are constructed from the localized pre-averaged BV of Podolskij and Vetter (2009) computed within each backward-looking window of 1,800 ticks. The threshold parameter k is adjusted with both the Šidák and Bonferroni corrections, and $\varpi = 0.5$.

Table B.7: Finite-sample size and power (%) under autocorrelated Gaussian noise

Nominal size: 5%		$\theta = 0.3$				$\theta = 0.4$				$\theta = 0.5$			
			ϵ				ϵ				ϵ		
	$c/\sigma(\tilde{r}_i)$	$N^{(c)}$	0.05	0.07	0.10	$N^{(c)}$	0.05	0.07	0.10	$N^{(c)}$	0.05	0.07	0.10
Panel A No Jump	3	1785	4.85	5.28	5.39	1784	5.14	5.34	5.69	1783	5.38	5.70	5.84
	4	1099	5.02	5.36	5.34	1099	5.05	4.94	5.32	1097	5.23	5.62	5.69
	5	743	4.84	5.45	4.96	743	4.82	5.58	5.37	743	5.41	5.64	6.07
	6	536	4.71	5.14	5.30	536	4.87	5.32	5.23	535	4.73	5.33	5.63
	7	404	5.21	5.36	5.44	404	5.11	4.91	5.60	404	5.20	5.02	5.45
	8	316	4.74	5.21	5.50	316	4.91	4.79	5.74	316	4.75	5.17	5.41
	9	253	4.56	5.05	5.37	254	4.92	5.16	5.35	253	4.86	5.36	5.32
	10	208	4.87	5.45	5.33	208	5.01	5.48	5.77	208	5.36	5.42	5.75
Panel B Moderate Jump	3	1715	47.02	49.41	52.39	1717	45.14	47.22	49.69	1719	43.27	45.53	48.29
	4	1058	46.22	48.63	51.34	1059	43.97	46.88	48.80	1061	42.70	44.28	47.16
	5	717	45.80	47.83	51.35	719	43.38	45.64	48.35	720	40.70	43.64	45.82
	6	518	45.25	46.85	49.59	519	41.62	45.13	47.71	520	40.83	42.25	45.93
	7	392	43.53	46.57	48.48	393	41.06	44.33	46.80	394	39.47	42.48	45.30
	8	307	43.39	45.85	49.41	308	41.95	43.80	46.44	309	39.25	41.64	44.64
	9	247	43.28	45.83	48.46	248	40.78	43.20	46.57	248	39.04	40.64	45.10
	10	203	42.70	44.97	48.27	204	40.26	41.86	45.96	204	38.51	40.48	43.28
Panel C Large Jump	3	1587	69.39	70.70	72.91	1590	67.87	69.33	71.27	1594	66.82	68.17	70.24
	4	979	68.87	70.46	72.68	983	66.80	69.17	70.63	985	65.84	67.74	69.17
	5	665	67.98	70.11	72.16	668	66.93	68.16	70.27	671	65.21	66.26	68.55
	6	482	68.20	69.38	71.78	485	65.87	67.95	69.81	487	64.66	66.04	67.63
	7	366	66.57	68.81	71.08	368	65.20	67.12	68.95	370	64.53	66.31	67.93
	8	287	67.04	69.14	71.08	289	64.39	66.85	69.28	291	63.97	65.09	67.34
	9	232	66.01	68.47	70.40	234	64.17	66.33	69.04	235	63.15	64.93	67.69
	10	191	66.15	67.95	70.27	193	63.67	65.80	68.23	194	62.39	64.69	67.11

This table reports the finite-sample size and size-adjusted power (%) of 10,000 simulations of the test statistic $T_{c,\epsilon}$ at 5% nominal level. All simulated prices are contaminated by the additive autocorrelated Gaussian noise and rounding errors. We utilize the two-step noise reduction method in Section 3.2 to construct the sequence of pseudo-observations with three different pre-averaging windows, i.e., $k_n = \lceil \theta\sqrt{N} \rceil$ with $\theta \in \{0.3, 0.4, 0.5\}$. The observations are sampled with different PDS barrier widths $c = K\sigma(\tilde{r}_i)$, where K ranges from 3 to 10. Different censoring thresholds with $\epsilon \in \{0.05, 0.07, 0.1\}$ are considered. $N^{(c)}$ stands for the average sampling frequencies.

Table B.8: Finite-sample size and power (%) of other tests under autocorrelated Gaussian noise

Nominal size: 5%										
	Int. (sec)	N_{spl}	BNS	JO	LM	ASJ	CPR	PZ	MinRV	MedRV
Panel A No Jump	5	4680	0.00	0.72	10.46	100.00	0.00	5.19	0.00	0.00
	15	1560	2.48	2.79	19.26	97.34	2.84	8.11	0.40	1.59
	30	780	5.59	4.27	26.71	47.36	6.32	11.46	2.93	4.99
	60	390	6.84	5.87	26.53	14.89	7.32	13.67	4.93	6.60
	120	195	7.08	7.43	17.00	8.51	7.64	15.53	5.55	7.50
	180	130	7.33	8.53	14.31	5.60	8.09	15.63	5.56	7.98
	300	78	7.92	10.90	12.15	4.35	9.20	15.09	5.73	9.55
Panel B Moderate Jump	5	4680	42.34	49.60	68.05	99.81	45.64	64.41	37.27	42.66
	15	1560	39.11	43.61	59.86	93.84	42.79	60.18	36.30	40.82
	30	780	36.35	37.43	50.10	66.10	40.00	52.66	32.51	37.08
	60	390	28.49	29.46	41.52	39.38	32.06	43.30	26.18	30.62
	120	195	22.16	21.09	34.90	21.09	25.48	32.18	20.48	23.39
	180	130	17.80	16.58	29.83	15.66	20.78	25.61	17.18	19.83
	300	78	13.36	11.19	19.64	10.68	14.91	18.07	12.98	14.99
Panel C Large Jump	5	4680	66.02	71.75	83.05	99.73	68.49	80.74	61.79	66.31
	15	1560	63.75	67.48	78.59	95.40	66.49	78.52	61.00	64.90
	30	780	60.36	62.07	72.40	78.66	63.52	73.58	57.06	61.05
	60	390	53.77	55.08	65.78	56.45	57.05	67.04	51.59	55.26
	120	195	46.55	46.82	60.23	35.58	49.80	57.96	44.44	48.75
	180	130	40.73	41.31	55.31	24.87	44.99	51.75	39.56	44.64
	300	78	33.58	32.74	44.99	16.57	37.28	42.89	32.71	36.46

This table reports the finite-sample size and size-adjusted power (%) of 10,000 simulations of 8 classical tests at 5% nominal level: BNS (Barndorff-Nielsen and Shephard, 2006), JO (Jiang and Oomen, 2008), LM (Lee and Mykland, 2008), ASJ (Aït-Sahalia and Jacod, 2009b), CPR (Corsi et al., 2010), PZ (Podolskij and Ziggel, 2010), MinRV and MedRV (Andersen et al., 2012). All simulated prices are contaminated by the additive autocorrelated Gaussian noise and rounding errors. All these tests are constructed on observations equidistantly sampled with various intervals in calendar time: 5, 15, 30, 60, 120, 180 and 300 seconds, and "N_{spl}" stands for the sampling frequencies.

Table B.9: Finite-sample size and power (%) of other noise-robust tests under autocorrelated Gaussian noise

Nominal size: 5%					
	Int. (sec)	N_{spl}	PZ*	LM12	ASJL
Panel A: No Jump	tick	23400	5.06	2.91	5.19
	5	4680	4.98	8.10	8.92
Panel B: Moderate Jump	tick	23400	38.51	21.87	37.46
	5	4680	29.10	18.91	17.09
Panel C: Large Jump	tick	23400	65.58	39.64	63.69
	5	7680	55.98	32.62	41.88

This table reports the finite-sample size and size-adjusted power (%) of 10,000 simulations of 3 noise-robust tests at 5% nominal level: noise-adjusted PZ (Podolskij and Ziggel, 2010), LM12 (Lee and Mykland, 2012), and ASJL (Aït-Sahalia et al., 2012). All simulated prices are contaminated by the additive autocorrelated Gaussian noise and rounding errors. All these tests are constructed on tick-level and 5-second-sampled observations. The tuning parameters for those tests are selected by minimizing the absolute distance between the nominal size and the empirical size with the simulated tick-level noise-contaminated observations.

Table B.10: Finite-sample size and power (%) of truncation-based detection under autocorrelated Gaussian noise

Nominal size: 5%					
		Panel A			
		No Jump (with FWER control)		Panel B	Panel C
Ticks	N_{spl}	Šidák	Bonferroni	Moderate Jumps	Large Jumps
1	23400	100.00	100.00	72.29	85.15
5	4680	100.00	100.00	70.59	85.03
15	1560	85.80	85.44	65.00	81.64
30	780	36.99	36.46	58.82	77.33
60	390	15.62	15.28	51.05	72.25
120	195	8.96	8.74	41.05	64.41
180	130	7.06	6.86	34.71	59.46
300	78	5.83	5.73	27.36	52.70

This table reports the finite-sample size and size-adjusted power (%) of 10,000 simulations of the truncation-based jump filtering technique. All simulated prices are contaminated by the additive autocorrelated Gaussian noise and rounding errors. Observations are sampled at various multiples of ticks, where "N_{spl}" stands for the corresponding sampling frequencies. The truncation thresholds are constructed from the localized pre-averaged BV of Podolskij and Vetter (2009) computed within each backward-looking window of 1,800 ticks. The threshold parameter k is adjusted with both the Šidák and Bonferroni corrections, and $\varpi = 0.5$.

Table B.11: Finite-sample size and power (%) under t-distributed noise

Nominal size: 5%		$\theta = 0.3$				$\theta = 0.4$				$\theta = 0.5$			
			ϵ				ϵ				ϵ		
	$c/\sigma(\tilde{r}_i)$	$N^{(c)}$	0.05	0.07	0.10	$N^{(c)}$	0.05	0.07	0.10	$N^{(c)}$	0.05	0.07	0.10
Panel A No Jump	3	1785	4.74	5.28	5.54	1784	5.25	5.01	5.79	1783	5.04	5.38	5.73
	4	1100	5.01	5.04	5.40	1098	5.05	5.00	5.78	1098	5.05	5.10	5.61
	5	743	4.62	4.85	5.29	743	4.77	5.04	5.51	743	4.60	5.31	5.82
	6	536	4.93	5.01	5.35	535	4.67	5.01	5.42	535	4.81	5.44	5.81
	7	404	4.83	5.08	5.22	404	4.81	5.04	5.48	403	5.24	5.58	5.67
	8	316	4.86	5.34	5.27	316	4.91	5.22	5.67	316	4.88	5.15	5.70
	9	254	4.77	5.42	5.24	253	5.13	5.41	5.39	253	4.83	5.01	5.72
	10	208	5.12	5.37	5.64	208	5.27	5.56	5.77	208	4.93	5.62	5.84
Panel B Moderate Jump	3	1716	46.47	48.75	50.70	1718	44.29	46.93	48.39	1718	42.42	45.03	46.94
	4	1058	45.56	48.39	50.84	1060	43.27	45.47	47.73	1061	41.57	43.20	45.28
	5	717	45.09	47.07	50.32	719	42.73	45.48	47.82	720	40.67	42.31	45.21
	6	519	44.78	46.46	48.26	519	41.76	44.18	46.61	521	40.50	42.15	44.40
	7	392	44.00	45.75	48.66	393	40.80	43.60	46.14	394	39.99	41.48	43.88
	8	307	42.56	44.26	48.15	308	40.08	42.59	45.58	308	39.08	41.55	43.25
	9	247	42.79	44.68	48.11	248	39.44	41.88	45.47	248	38.55	41.12	42.51
	10	203	41.21	44.19	46.88	204	39.69	41.62	44.87	204	37.62	39.87	42.92
Panel C Large Jump	3	1585	70.44	71.21	73.23	1589	68.58	70.69	72.01	1592	66.90	68.86	70.80
	4	978	69.91	71.37	73.07	981	68.25	69.64	71.07	985	66.59	68.75	69.66
	5	664	69.36	71.15	72.79	668	67.65	69.30	71.08	670	66.09	67.79	69.56
	6	481	68.75	70.43	72.67	484	66.82	68.64	70.50	487	65.24	66.70	68.72
	7	365	68.08	69.77	71.74	368	65.70	67.87	69.97	370	64.57	66.43	68.83
	8	287	67.67	68.95	70.93	289	65.10	68.12	69.69	291	63.77	66.09	67.83
	9	232	66.89	68.86	71.66	234	64.52	66.96	69.63	235	63.39	66.10	67.81
	10	191	66.21	68.25	70.90	192	64.24	66.28	69.49	194	62.52	64.96	67.43

This table reports the finite-sample size and size-adjusted power (%) of 10,000 simulations of the test statistic $T_{c,\epsilon}$ at 5% nominal level. All simulated prices are contaminated by the additive t-distributed noise and rounding errors. We utilize the two-step noise reduction method in Section 3.2 to construct the sequence of pseudo-observations with three different pre-averaging windows, i.e., $k_n = \lceil \theta\sqrt{N} \rceil$ with $\theta \in \{0.3, 0.4, 0.5\}$. The observations are sampled with different PDS barrier widths $c = K\sigma(\tilde{r}_i)$, where K ranges from 3 to 10. Different censoring thresholds with $\epsilon \in \{0.05, 0.07, 0.1\}$ are considered. $N^{(c)}$ stands for the average sampling frequencies.

Table B.12: Finite-sample size and power (%) of other tests under t-distributed noise

	Int. (sec)	N_{spl}	BNS	JO	LM	ASJ	CPR	PZ	MinRV	MedRV
Panel A No Jump	5	4680	58.90	15.85	100.00	99.92	99.87	99.70	0.12	0.02
	15	1560	12.76	10.10	89.87	92.05	56.23	72.27	0.71	2.19
	30	780	8.89	7.81	62.42	44.91	24.70	40.96	3.06	5.18
	60	390	7.25	7.38	38.66	16.35	11.91	24.07	4.49	7.09
	120	195	7.23	8.22	20.16	7.68	8.87	18.31	5.11	7.38
	180	130	7.37	8.99	16.35	5.38	8.42	17.48	5.30	8.46
	300	78	7.34	10.83	11.47	4.33	8.64	14.86	5.22	8.55
Panel B Moderate Jump	5	4680	37.49	37.05	17.64	99.97	11.25	13.71	39.54	41.12
	15	1560	40.61	38.20	25.74	97.85	21.65	20.95	34.45	37.18
	30	780	36.25	35.77	31.96	70.97	30.82	27.51	31.47	35.67
	60	390	30.11	29.45	36.41	40.48	30.72	35.36	27.12	31.05
	120	195	22.54	21.73	34.11	21.92	24.58	30.89	20.59	23.94
	180	130	17.55	17.67	29.39	14.43	20.16	25.77	16.98	20.66
	300	78	14.49	12.22	22.25	10.45	16.11	20.07	13.74	17.01
Panel C Large Jump	5	4680	62.75	63.82	45.20	99.98	31.59	38.22	63.94	65.60
	15	1560	65.71	64.24	53.45	98.79	47.84	47.73	59.14	61.94
	30	780	61.92	62.02	59.38	81.94	56.98	54.91	56.36	60.86
	60	390	55.55	55.88	63.00	57.74	56.36	62.26	52.38	56.60
	120	195	47.62	47.85	60.48	37.89	51.29	57.77	45.42	50.37
	180	130	41.65	43.02	55.53	25.61	45.02	52.02	40.67	45.06
	300	78	35.10	34.13	47.57	16.34	39.19	45.37	34.32	39.24

This table reports the finite-sample size and size-adjusted power (%) of 10,000 simulations of 8 classical tests at 5% nominal level: BNS (Barndorff-Nielsen and Shephard, 2006), JO (Jiang and Oomen, 2008), LM (Lee and Mykland, 2008), ASJ (Aït-Sahalia and Jacod, 2009b), CPR (Corsi et al., 2010), PZ (Podolskij and Ziggel, 2010), MinRV and MedRV (Andersen et al., 2012). All simulated prices are contaminated by the additive t-distributed noise and rounding errors. All these tests are constructed on observations equidistantly sampled with various intervals in calendar time: 5, 15, 30, 60, 120, 180 and 300 seconds, and "N_{spl}" stands for the sampling frequencies.

Table B.13: Finite-sample size and power (%) of other noise-robust tests under t-distributed noise

Nominal size: 5%					
	Int. (sec)	N_{spl}	PZ*	LM12	ASJL
Panel A: No Jump	tick	23400	5.07	5.46	6.18
	5	4680	4.64	9.24	8.74
Panel B: Moderate Jump	tick	23400	39.40	25.31	37.68
	5	4680	29.26	18.76	17.19
Panel C: Large Jump	tick	23400	65.11	41.81	62.48
	5	7680	55.60	31.85	41.42

This table reports the finite-sample size and size-adjusted power (%) of 10,000 simulations of 3 noise-robust tests at 5% nominal level: noise-adjusted PZ (Podolskij and Ziggel, 2010), LM12 (Lee and Mykland, 2012), and ASJL (Aït-Sahalia et al., 2012). All simulated prices are contaminated by the additive t-distributed noise and rounding errors. All these tests are constructed on tick-level and 5-second-sampled observations. The tuning parameters for those tests are selected by minimizing the absolute distance between the nominal size and the empirical size with the simulated tick-level noise-contaminated observations.

Table B.14: Finite-sample size and power (%) of truncation-based detection under t-distributed noise

Nominal size: 5%					
		Panel A		Panel B	Panel C
		No Jump (with FWER control)			
Ticks	N_{spl}	Šidák	Bonferroni	Moderate Jumps	Large Jumps
1	23400	100.00	100.00	9.95	29.93
5	4680	100.00	100.00	15.54	39.25
15	1560	97.71	97.63	23.69	50.02
30	780	63.20	62.93	29.69	56.28
60	390	26.47	26.23	36.40	61.59
120	195	11.41	11.26	38.29	62.58
180	130	8.19	7.99	32.68	58.53
300	78	5.73	5.48	26.31	52.13

This table reports the finite-sample size and size-adjusted power (%) of 10,000 simulations of the truncation-based jump filtering technique. All simulated prices are contaminated by the additive t-distributed noise and rounding errors. Observations are sampled at various multiples of ticks, where "N_{spl}" stands for the corresponding sampling frequencies. The truncation thresholds are constructed from the localized pre-averaged BV of Podolskij and Vetter (2009) computed within each backward-looking window of 1,800 ticks. The threshold parameter k is adjusted with both the Šidák and Bonferroni corrections, and $\varpi = 0.5$.

B.4 Supplementary Empirical Results

Table B.15 reports the empirical results for 8 other tests. Based on the simulation results in Tables 3 and 4, we select four calendar-time-sampling-based tests: BNS, CPR, MinRV and MedRV, with different sampling intervals: 30, 60, 120, and 300 seconds, and we also construct the noise-robust tests PZ*, LM12 and ASJL from tick-by-tick and 5-second data. Moreover, we consider the truncation-based filtering technique on calendar-time-sampled returns, with the truncation parameter k calibrated with the Šidák correction. For most of the selected stocks, the noise-robust ASJL constructed from tick-level observations obtains comparable results to our PDS-based test.

Table B.15: Empirical rejection rates (%) of other tests for selected NYSE stocks

Test	Int. (sec)	AXP	BA	DIS	IBM	JNJ	JPM	MRK	MCD	PG	WMT
BNS	30	32.02	20.55	20.95	28.46	36.36	32.81	49.80	25.69	43.08	32.41
	60	20.16	11.07	19.37	25.69	28.06	24.51	37.55	26.09	31.23	26.88
	120	17.00	16.21	16.21	22.53	27.67	25.30	25.69	23.32	27.27	27.67
	300	18.58	18.58	15.42	19.76	20.16	17.00	23.32	22.13	22.13	22.13
CPR	30	38.34	32.02	35.57	39.13	47.83	38.34	59.29	33.20	52.57	41.11
	60	28.46	16.60	26.88	33.99	40.32	32.41	45.85	29.25	40.32	35.57
	120	25.30	20.16	21.74	30.83	34.78	32.02	33.99	28.85	32.81	33.60
	300	23.32	23.72	21.34	27.67	29.64	22.13	32.81	28.46	30.43	30.83
MinRV	30	22.53	17.39	15.42	18.18	22.92	21.74	27.67	19.76	26.48	21.34
	60	14.23	9.88	15.42	19.76	21.74	16.21	22.92	20.95	22.13	22.13
	120	14.23	12.65	12.65	18.58	18.18	17.79	18.58	19.76	19.76	21.74
	300	13.04	14.62	13.83	17.39	13.04	11.07	15.81	15.42	16.21	14.23
MedRV	30	30.83	23.72	28.46	31.62	37.15	29.64	40.71	29.64	37.94	32.02
	60	20.55	15.81	22.92	28.46	37.15	27.67	33.60	28.85	32.81	30.04
	120	20.55	18.58	18.58	26.48	29.64	26.48	27.27	26.88	28.85	34.78
	300	18.97	17.00	16.60	24.11	21.74	20.55	23.72	24.90	28.06	25.30
PZ*	tick	7.51	6.32	6.32	5.93	6.32	6.72	7.51	5.14	7.51	4.74
	5	31.23	22.92	19.76	26.09	22.13	23.32	23.72	24.90	30.04	31.62
LM12	tick	12.65	4.35	7.51	9.49	12.65	11.46	12.65	9.49	18.58	11.86
	5	32.02	21.34	30.04	37.55	29.25	27.27	38.74	27.67	40.32	35.18
ASJL	tick	15.81	20.16	13.04	13.83	13.83	13.44	15.02	20.55	13.83	15.02
	5	32.02	20.95	29.25	21.34	26.48	21.74	22.92	26.09	30.04	32.41
Truncation-based Detection	30	69.96	67.98	70.75	63.64	77.87	64.43	80.63	74.31	80.63	75.10
	60	52.96	44.27	49.80	45.45	59.29	45.45	64.43	58.50	65.22	56.13
	120	32.41	36.36	33.99	32.81	40.32	34.78	43.87	36.36	42.69	36.36
	300	21.34	22.92	19.37	20.55	22.53	16.60	21.34	24.11	24.90	24.51

This table reports the proportions of days with jumps for 10 NYSE stocks in 2020, as identified by the following procedures: BNS (Barndorff-Nielsen and Shephard, 2006), CPR (Corsi et al., 2010), PZ (Podolskij and Ziggel, 2010), MinRV and MedRV (Andersen et al., 2012), PZ* (Podolskij and Ziggel, 2010), LM12 (Lee and Mykland, 2012), ASJL (Aït-Sahalia et al., 2012), and the truncation-based filtering technique in the spirit of Andersen et al. (2007b) and Mancini (2009). The first four tests, together with the truncation-based filtering, employ observations sampled equidistantly in calendar time (with the last tick interpolation): 30, 60, 120 and 300 seconds. The noise-adjusted PZ*, LM12, and ASJL are constructed from tick-by-tick and 5-second-sampled data. The total number of trading days is 253.

Table B.16 reports the empirical results for other tests constructed from calendar-time-sampled data, with the control of spurious detections using the thresholding methods in Bajgrowicz et al. (2016): (i) the universal threshold $\sqrt{2\ln 253}$, and (ii) the FDR threshold. We only consider one-sided tests whose limiting distribution is $\mathcal{N}(0,1)$ under the null, which includes the upper-tailed BNS,

CPR, MinRV, MedRV, PZ*, and the lower-tailed ASJL, but excludes the Gumbel-distributed LM12.

Table B.16: Adjusted empirical rejection rate (%) of other tests for selected NYSE stocks

	Test	Int. (sec)	AXP	BA	DIS	IBM	JNJ	JPM	MRK	MCD	PG	WMT
Panel A Universal threshold	BNS	30	24.11	18.18	17.79	23.32	27.67	25.69	33.99	20.95	30.83	22.92
		60	15.81	9.09	15.42	19.37	18.58	18.97	29.25	20.55	24.11	20.16
		120	13.44	13.83	15.02	20.55	22.92	22.13	21.74	17.79	19.37	20.55
		300	15.02	16.21	13.04	15.42	16.21	14.62	19.76	17.79	17.00	20.55
	CPR	30	27.67	27.27	29.64	27.67	31.23	26.88	36.76	23.32	33.99	26.48
		60	22.92	13.83	20.55	25.69	27.67	22.92	31.23	20.95	27.67	24.11
		120	21.34	17.00	19.76	24.90	24.11	27.27	25.69	23.32	23.72	24.51
		300	18.18	20.55	16.60	22.53	23.72	18.18	25.69	22.13	21.74	26.09
	MinRV	30	17.79	16.21	13.44	16.21	19.37	18.18	23.32	16.60	20.55	16.60
		60	11.86	8.30	14.23	15.81	17.79	14.62	20.55	18.97	20.16	18.97
		120	12.25	12.25	12.25	18.18	17.39	17.39	15.02	17.79	16.21	18.97
		300	12.25	13.44	13.44	16.21	12.25	11.07	15.42	13.44	15.02	13.83
	MedRV	30	24.51	21.74	26.09	25.30	26.09	21.74	30.04	22.92	28.46	26.09
		60	17.00	14.23	19.76	23.32	29.64	21.34	24.90	25.69	24.11	22.53
		120	17.39	16.21	17.39	21.34	24.11	24.11	22.53	22.13	22.13	29.64
		300	16.21	15.42	15.02	20.55	18.97	18.97	18.18	20.95	24.51	22.13
	PZ*	tick	5.53	5.53	6.32	3.56	3.56	5.93	5.93	3.95	5.14	3.16
		5	2.77	4.35	1.58	3.95	3.16	2.77	2.77	3.16	3.56	4.74
	ASJL	tick	14.23	18.58	13.04	13.04	13.44	12.25	12.25	19.37	13.44	14.62
		5	26.09	17.39	26.09	18.18	21.34	17.00	18.58	22.53	25.30	24.11
Panel B FDR threshold	BNS	30	14.23	15.02	16.21	14.23	12.25	15.02	9.09	14.62	11.46	11.07
		60	13.04	7.11	12.25	12.65	10.28	14.23	15.02	13.04	14.23	9.09
		120	9.88	13.44	14.62	14.62	13.83	17.39	12.25	15.02	13.83	10.28
		300	13.04	13.04	9.88	12.25	13.83	11.46	12.65	13.44	9.09	16.21
	CPR	30	9.09	15.42	19.37	13.04	11.86	9.09	7.51	12.25	8.30	10.28
		60	14.62	10.67	15.02	15.02	13.04	15.02	12.25	11.46	11.07	9.88
		120	13.83	16.21	16.21	13.04	14.62	16.21	13.04	13.44	13.04	10.67
		300	13.04	16.21	11.46	17.00	13.04	10.28	17.79	15.02	13.44	15.42
	MinRV	30	15.81	14.23	12.65	16.21	12.65	17.39	11.07	14.23	15.02	13.83
		60	10.67	7.51	11.07	12.65	12.65	11.86	13.44	18.58	13.44	14.62
		120	10.67	12.25	12.65	18.18	13.83	16.21	14.23	16.21	14.62	16.21
		300	12.65	11.86	13.44	15.81	12.25	11.07	13.04	13.44	15.02	13.83
	MedRV	30	15.02	19.37	19.76	10.28	16.60	16.60	10.67	16.21	17.39	13.44
		60	13.04	13.04	13.44	11.86	19.76	13.04	13.83	18.18	16.60	11.07
		120	15.42	15.02	13.83	15.42	18.58	21.74	16.21	18.97	12.25	18.58
		300	11.07	13.83	9.49	16.60	13.83	16.60	13.04	13.04	16.60	18.97
	PZ*	tick	5.53	5.53	6.32	3.56	3.56	5.93	5.93	3.95	5.14	3.16
		5	2.77	4.35	1.58	3.95	3.16	2.77	2.77	3.16	3.56	4.74
	ASJL	tick	13.04	16.21	13.04	10.28	13.44	12.25	11.07	17.39	13.44	14.62
		5	15.02	13.44	18.58	15.42	15.42	14.23	12.65	18.58	17.39	14.62

This table reports the proportions of days with jumps for 10 NYSE stocks in 2020, as identified by the following procedures: BNS (Barndorff-Nielsen and Shephard, 2006), CPR (Corsi et al., 2010), PZ (Podolskij and Ziggel, 2010), MinRV and MedRV (Andersen et al., 2012), PZ* (Podolskij and Ziggel, 2010), and ASJL (Aït-Sahalia et al., 2012), with the control of spurious detections using the thresholding methods in Bajgrowicz et al. (2016). The first 4 tests are constructed from observations equidistantly sampled in calendar time (with the last tick interpolation): 30, 60, 120 and 300 seconds. The noise-adjusted PZ* and ASJL are constructed from tick-by-tick and 5-second-sampled data. The total number of trading days is 253.